RADC-TDR-64-381

RADAR CROSS SECTION TARGET SUPPORTS - PLASTIC MATERIALS

TECHNICAL DOCUMENTARY REPORT NO. RADC-TDR-64-381
June 1964

136p

Space Surveillance and Instrumentation Branch
Rome Air Development Center
Research and Technology Division
Air Force Systems Command
Griffiss Air Force Base, New York

Project No. 6503

(Prepared by General Dynamics/Fort Worth,
A Division of General Dynamics Corporation
under Contract No. AF30(602)-2831)

NOTICES

Copies available at Office of Technical Services.

Qualified requesters may obtain copies from Defense Documentation Center.

When US Government drawings, specifications, or other data are used for any purpose other than a definitely related government procurement operation, the government thereby incurs no responsibility nor any obligation whatsoever, and the fact that the government may have formulated, furnished, or in any way supplied the said drawings, specifications, or other data is not to be regarded by implication or otherwise, as in any manner licensing the holder or any other person or corporation, or conveying any rights or permission to manufacture, use, or sell any patented invention that may in any way be related thereto.

Do not return this copy. Retain or destroy.

BLANK PAGES
IN THIS
DOCUMENT
WERE NOT
FILMED

F O R E W O R D

In order to meet the need for a National Radar Reflectivity Range, Rome Air Development Center (RADC) awarded a development contract on 29 June 1962 to General Dynamics/Fort Worth (GD/FW) to design, fabricate, and develop the Radar Target Scatter Site (Project RAT SCAT) on the Alkali Flats, Holloman AFB, New Mexico, (Contract AF30(602)-2831). The operational RAT SCAT Site was delivered to the Air Force on 30 June 1964.

The RAT SCAT facility was developed for full-scale radar cross section measurements. In the pursuit of this development, an R&D Program was undertaken to provide for the specific needs of Project RAT SCAT as requirements appeared in the implementation of the function of the Site. A significant portion of this work was subcontracted. Emphasis was placed on those areas thought to be most promising in achieving measurement objectives. The presentation of the results of the R&D Program is covered in eight reports which were prepared as RADC Technical Documentary Reports.

This report (General Dynamics/Fort Worth Report No. FZE-222-6) is No. 6 in the series. It contains a description of the results of studies by The University of Michigan Radiation Laboratory and General Dynamics/Fort Worth into the scattering properties of cellular plastic materials. Also contained in this report are discussions of (1) the structural considerations in the use of Styrofoam as a target support material, (2) methods for achieving low cross section bonds between pieces of Styrofoam, and (3) results of a limited study of the feasibility of air inflated structures as target supports. The material in this report was written by C. H. Smith and C. C. Freeny with the exception of Section 2 which was prepared by E. F. Knott and T. B. A. Senior of The University of Michigan, under subcontract to General Dynamics/Fort Worth.

The contents of this report and the abstract are unclassified.

RADC-TDR-64-381
June 1964

A B S T R A C T

The results of studies by The University of Michigan Radiation Laboratory and General Dynamics/Fort Worth into the scattering properties of cellular plastic materials are presented. A mathematical model for scattering from cellular plastics, developed by The University of Michigan and extended by General Dynamics/Fort Worth, to provide a method of determining the optimum low cross section target support for a given application is also presented. The results of investigations of field perturbations near a Styrofoam surface are described along with cross section measurements made at the RAT SCAT Site using theoretical minimum cross section formula for circular target supports. Structural considerations in the use of Styrofoam as target support material are discussed. Methods for achieving low cross section bonds between pieces of Styrofoam are also discussed.

The results of a limited study of the feasibility of air inflated structures as target supports at the RAT SCAT Site are also presented.

This is Report No. 6 of a series of eight RAT SCAT Research and Development Program reports.

PUBLICATION REVIEW

This report has been reviewed and is approved. For further technical information on this project, contact

Approved: DONALD M. MONTANA
Program Directors' Office
Space Surveillance and
Instrumentation Branch

Approved: JOSEPH FALLIK
Chief, Space Surveillance and
Instrumentation Branch
Surveillance and Control Division

TABLE OF CONTENTS

L I S T O F F I G U R E S

L I S T O F T A B L E S

SECTION 1

INTRODUCTION

One of the more important considerations in the static measurement of radar cross section of Aerospace Vehicles is the target support mechanism. It is imperative, for accurate measurement, that the selected vehicle support device produce a negligible effect on both the incident and reflected electromagnetic fields. Two basic approaches to the solution of the support problem are commonly employed on present radar cross section ranges. The first approach is to use materials in the construction of support devices whose impedance is closely matched to that of air and thereby produce a negligible effect on the electromagnetic field. Such supports are commonly fabricated from plastic materials. The second approach is to construct support devices which are, for the most part, outside of the electromagnetic field and/or designed so as to divert both the incident and reflected energy in such a manner as to not significantly disturb the target field. Target supports constructed using this latter approach are commonly fabricated from heavy nylon cables or from metals and have the capability of supporting extra heavy targets.

At the initiation of the RAT SCAT R&D program, both approaches to the solution of the target support problem were considered worthy of investigation. Accordingly, in the first phase of these two investigations, subcontracts were awarded for theoretical and limited experimental studies covering both approaches to the solution of the target support problem.

A subcontract was awarded to Cornell Aeronautical Laboratory to study suspension target supports. The results obtained from this study and studies by General Dynamics/Fort Worth on the application of shielded metal columns to the support of radar cross section targets may be found in Technical Documentary Report No. RADC-TDR-64-382.

A subcontract was awarded to The University of Michigan to study the scattering properties of cellular plastic materials. The results obtained from this study and studies made by General Dynamics/Fort Worth are contained in the following report.

This report contains, except for format changes necessary for proper presentation of the combined results, the final

subcontract report from The University of Michigan entitled, "Studies of Scattering by Cellular Plastic Materials". An extension by GD/FW of the mathematical scattering model developed by The University of Michigan to provide a method of determining the optimum low cross section for a given application is herein presented. Correlation of this model with measurements made at the RAT SCAT Site is shown.

It will be noted in reading this report that a documentation is presented of initial efforts in the investigation of (1) Styrofoam structural properties, (2) low cross section structural bonds, and (3) the feasibility of air-inflated target supports. These investigations were not completed due to diversion of contract funds to more promising R&D areas. However, documentation has been included to provide a base from which a continuation and completion of these investigations may be initiated.

SECTION 2

STUDIES OF SCATTERING BY CELLULAR PLASTIC MATERIALS

GENERAL

This section of the Report was prepared by The University of Michigan for General Dynamics/Fort Worth between 17 June 1963 and 31 March 1964.

The overall purpose of this task was to investigate matters pertaining to the use of cellular plastic materials as target supports for radar scattering ranges. Five specific tasks were enumerated in the work statement. These may be paraphrased as follows:

1. Survey and analyze the results of relevant past work on cellular plastic supports

2. Study the scattering properties of these materials to establish mathematical models with which to predict observed effects and define the controlling parameters

3. Investigate their electrical, physical and mechanical properties

4. Consider in brief the effects of size, shape, surface treatment and internal joints on radar cross section

5. Define the relations between support strength, size, and radar cross section with a view to possible trade-offs.

The time available for the study precluded an exhaustive treatment. In several cases topics which were outgrowths of the above and which appeared to have some theoretical promise were ignored in order to provide at least a partial coverage of the five basic tasks. One such topic, for example, is the use of variable density materials. This would have been a major investigation in itself, and the lack of sufficient control in existing manufacturing processes gave little confidence in our ability to fabricate one-piece columns of this type at the moment. Attention was therefore confined to materials which are presumed homogeneous in the large.

As the study progressed other problems suggested themselves and some of these were judged to be of sufficient importance to take priority. In particular, the near field effects of a Styrofoam beam were investigated in some detail and the discovery that cellular materials can produce a considerable incident field perturbation near to their surface could have a decisive bearing on the design of target supports. In many cases the resulting target-support interaction may be a more critical factor than the cross section of the support per se.

This additional investigation necessarily entailed a reduction of effort on the five basic tasks, and though each of these was studied in some degree, the program that actually evolved can be summarized under the following five headings:

1. A survey of the types, manufacturers, manufacturing processes, and physical and mechanical properties of available cellular plastic materials

2. A survey of existing theoretical and experimental work on the use of such materials for target supports

3. A theoretical study of scattering by inhomogeneous media as it applies to cellular materials

4. A theoretical and experimental investigation of the back scattering from shaped blocks of this material as a function of frequency

5. A theoretical and experimental investigation of surface wave effects near a Styrofoam beam.

A complete description of this work is contained in the papers, reports and memoranda which have emanated from the sub-contract. These are listed in the Appendix and this section of the report is intended only as an expanded summary of the main lines of investigation.

MATERIAL CONSIDERATIONS

Definition and Application as Target Supports

A foam is simply a collection of bubbles or cells, each of which is bounded by thin walls of more or less irregular shape. The cell walls enclose a gas, which need not be air, and the foam structure is called unicellular if every cell, save those on the very boundary of the mass, shares all its walls with neighboring cells. An open-cell structure is one in which the gas is not partitioned in separate pockets; in this kind of foam, the cells are interconnected. The degree of interconnection is usually specified as "percentage open cell structure". A multicellular foam is composed of relatively large cells, each of which houses an independent colony of finer cells, usually of unicellular structure.

Cell walls are planar, rigid and a typical thickness is 0.0002 inch for a typical cell diameter of 0.02 inch. Cell diameters vary from material to material and from cell to cell within a given material. Distribution of cell diameter has apparently not been studied in detail, but it seems that the most common size is the geometric mean of the largest and smallest sizes that can be found in a given block of foam. Cells may be as small as 0.002 inch in the urethanes to as large as 0.06 inch in the (useful) polystyrene foams. There are foams which have cells as large as 0.5 inch, but these are decorative materials ill-suited for target support applications.

Of the unicellular foams, Styrofoam[+] was probably the best known and most widely used for early target support requirements. It was practically invisible to the radar, was rigid enough and strong enough to support most of the models, and was easily worked. Its density was very low: it weighed from 1.5 to 2.0 pounds per cubic foot (pcf) since its volume was nearly 98 per cent gas. It has become the classical support material and even now is probably more widely used than any other. The advent of low cross section shapes of large physical dimensions caused people to look into other model support schemes since Styrofoam, while virtually invisible, was not invisible enough. An early competitor for the job was the string which could easily be made a magnitude or more smaller (in radar cross section) then the

[+]This is the registered trade mark for an expanded polystyrene foam produced by the Dow Chemical Company, Midland, Michigan.

best foam, but which was not without its disadvantages. More recently, several exotic support schemes have attracted attention. Spin dropping, air jets, magnetic fields, and air bags are among the latest ideas. In spite of these schemes, rigid foam materials remain the most widely used. In those cases for which foam is the only feasible support method, techniques have been developed which remove or compensate for target support effects (Hiatt et al, 1963).

Types of Rigid Foam and How They are Made

There are nine commercially recognized types of foam, of which seven may be classed as rigid

cellulose acetates
epoxies
polystyrenes
silicones
urea-formaldehydes
urethanes
vinyls

Of these, the polystyrene foams, and perhaps the urethanes, are the most familiar to the target support designer. The styrene foams are available in two forms, expanded and expandable bead. The former is an extruded foam while the latter is molded.

Styrofoam is produced by dissolving polystyrene in a solvent such as methyl chloride and subjecting the resulting gel to heat and pressure. The gel is permitted to escape through an orifice and the sharp drop in pressure causes the heated solvent to flash into vapor, creating bubbles. A "take-away" table removes the frothing mass at the proper speed. A cooling period follows during which the outermost cells harden first and the interior cells last. The final cell size and density is determined by several variables, among them the raw materials, take-away speed, pressure, etc. The differential cooling rate (from surface to interior) produces a variation in cell size which can be as great as 5:1 or 10:1, the interior cells being the larger. Better uniformity than this is possible if thinner cross sections are extruded. The material near the surface hardens first, hence the cells there have little chance to grow while those in the core may expand considerably before enough heat is removed from the mass. Presumably the fire-retardent properties and colors (Styrofoam can be made blue or green as well as white) are imparted with the necessary additives prior to extrusion. The cell structure tends to be elongated in the direction of extrusion and

ratios in dimensions of 2:1 are not uncommon. The anisotropy causes physical properties to vary with the direction of the applied stresses. Occasionally one finds a sizable chip or sliver of wood embedded in the log; the presence of foreign matter such as this, as well as other inhomogeneities, is not usually detectable until exposed by a fresh cut through the log.

The molded foams first appeared in 1954 (Randolph, 1960). These are expandable bead foams and the process begins with small beads which contain not only the polymer but the expanding agent ("blowing" agent is the name used in the trade) as well. The pinhead-size beads require a two-state expansion, the first of which is called pre-foaming. This step is accomplished by exposing the beads to any form of heat, ranging from infra-red lamps to live steam, and is halted when the bulk density of the pre-foamed beads matches that of the volume desired to be fabricated. The pre-foamed beads are typically 1/8 to 1/4 inch in diameter and must be stored for a period of 1 to 14 days prior to the final foaming process.

Final foaming is done in a steam heated mold which must be constructed to withstand typical steam pressures of 20 to 35 psig. Large volumes must be produced by the insertion of perforated steam pipes into the mold cavity; after foaming, the pipes are quickly withdrawn and the residual heat in the mass causes the beads to fill the voids left by the pipes. This may produce some local variations in density which cannot be avoided in large volumes. When molding small volumes, a convenient heating arrangement is a steam jacket encasing the mold. Another scheme provides a perforated jacket, which permits the steam to seep through the volume. Expandable bead foams can be produced with densities as low[+] as 1.1 pcf, while 1.5 pcf is more common for Styrofoam.

Urethane foams do not depend on the application of heat for the foaming process, but upon the evolution of gases formed by an isocynate-fluorocarbon reaction. In commercial production, elaborate mixing fixtures bring together the reacting compounds and deposit them in a suitable mold. The molds may be open at the top and thus need not be as strong as those required for the pre-foamed polystyrene beads. The reaction is accompanied by the evolution of heat, which may become a problem if very large volumes are desired, and takes place in a matter of minutes.

[+]Recently, a representative of The Armstrong Cork Co., Lancaster, Pennsylvania, stated that densities as low as 0.5 pcf have been achieved.

The foam is permitted to rise and the material near the bottom will be more dense than that near the top. Generally, a few inches of the material can be removed from the surfaces of the volume after withdrawal, leaving a substantially uniform density core. As with polystyrene foams, urethane foams may be anisotropic because of the direction of rise. Densities as low as 1.5 pcf are attainable (Stengard, 1963).

Other foams are known to be produced, such as epoxy foams and polyvinyl chloride foams, but little has been done with these as regards target support applications. It is probable that they are no better, perhaps worse, than the classic Styrofoam, since the dielectric constant of the base polymer may be 35 per cent greater than that of polystyrene while the strength may be 20 per cent less.

Description and Comparison of Foams

Expanded polystyrene, of which Styrofoam is probably the widest known, first appeared commercially in the United States in 1944 (Randolph, 1960). It is presently available in billet or board form and is sold for insulation, toys, novelties and construction. The larger billets, known in the trade as "logs", may come in several sizes. The largest, and usually the most difficult to obtain, is about 2 feet by 3 feet in cross section and 9 feet or 15 feet long. The surface is heavily corrugated and cracked, which is an unfortunate consequence accompanying the extrusion of large cross sections. These cracks make it impossible to fabricate a circular column much greater than 19 inches in diameter. The next size log is 12 by 29 inches in cross section, 9 feet long and has a smooth, tough skin. The skin is under stress and if it is sliced off, the core of the log will immediately shrink about an inch along the 9-foot dimension. This property renders fabrication processes difficult and unless care is taken, a column fashioned from this log is likely to be deformed.

Expandable bead polystyrenes are familiar to practically everyone. These are the foams that may be found in low-cost ice chests, floats, toys, and uncountable other items. While not of importance for radar purposes, it can be dyed and beads of different colors may be mixed for decorative effects. The foams are multicellular and are available in logs as large as 16 inches by 48 inches in cross section and 9 feet long. The material is cut easily and cleanly by hot-wire techniques and has low density. The density can be controlled to a much greater degree than the extruded styrene foams due to the ease of control during the pre-foaming operation. Logs of expandable bead foam

lack the skin found on extruded polystyrene. It is conceivable that they can be manufactured in circular as well as rectangular cross sections.

Urethane foams have strikingly uniform cell size distributions compared with those of the polystyrene foams. They can be unicellular and generally can be had with relatively small cells. Common colors are white, yellow and tan. Urethanes are considerably weaker than the polystyrenes when compared on an equal density basis. Construction of large volumes is possible but there is a danger of damage by the heat of reaction if the core cannot be sufficiently cooled.

Of the remaining foams previously listed, no attempt has been made to determine sizes available or to describe them further, except as summarized in Table 2-1. It is felt that these materials are not important in the light of target support requirements and do not warrant any further attention here.

Foam properties are usually presented as functions of density, which is an easily measured parameter, and since strength and dielectric constant are two important properties to consider in target support design, it is useful to relate column radar cross section to density. A convenient shape for discussion is the right circular cylinder: if it is illuminated with a wave polarized parallel to the cylinder axis, and if $d >> \lambda$, the cross section will be periodic with frequency and will reach maximum values[+]

$$\sigma = \frac{1}{8} kd \ell^2 \left(\frac{\epsilon}{\epsilon_o} - 1\right)^2$$

in which

d = cylinder diameter
ℓ = cylinder length
ϵ = dielectric constant for material
k = propagation constant of free space

The assumption has been made that the column will be used for several frequencies so that one cannot select a diameter favoring the cancellation of front and rear surface returns.

[+]It is here assumed that the dominant return is the coherent one produced by the exterior surfaces.

The presence of d in the expression suggests that the smallest diameter possible should be used, which in turn suggests the column will be a slender one. Hence the column is expected to fail by buckling rather than by excessive compression under load. The critical load at which the column will fail is (Timoshenko and MacCullough, 1949)

$$P = \frac{\pi^3}{256} \frac{Ed^4}{\ell^2}$$

where E is the modulus of elasticity of the material. The worst case (i.e., most conservative) has been assumed, namely that one end of the column is fixed, being capable of sustaining moment, and the other end free. Thus, the minimum diameter required for a given load P has been established and can be used in the expression for cross section.

Considering now the dielectric constant, a simple approximation in terms of density can be written

$$\epsilon \simeq \epsilon_o (1 + \alpha \rho),$$

where α is a constant depending upon the density and dielectric constant of the base polymer and ρ is the foam density. The approximation yields somewhat larger values of ϵ than measured data indicates (Cuming and Andress, 1958; Myshkin, 1958), but is adequate for this discussion. If the above values for d and ϵ are used in the expression for cross section, there results

$$\sigma = \frac{k\ell^{5/2} p^{1/4}}{2\pi^{3/4}} \frac{\alpha^2 \rho^2}{E^{1/4}} .$$

Thus the best foam, given a frequency, load, and column length, is the one which has the smallest value for $\alpha^2\rho^2/E^{1/4}$.

It is tempting to try to further improve the expression by finding the relation between E and density but this leads to many complications. The primary objection is due to manufacturers' listed data, which rarely specify properties but instead present ranges in values that bracket the expected foam properties. Another is that the modulus of elasticity generally varies inversely with cell size, requiring one more piece of information for a materials comparison. In addition, the foam becomes plastic for relatively small loadings and the description "modulus of elasticity" seems inappropriate.

Fortunately, the cross section is in terms of the square of density but only the fourth root of E. This means that variations in E will have a much smaller effect than variations in ρ. Hence a very rough judgment of the relative radar performance of foams can be made by inspection of their densities. Generally, the lowest density foams make the best target support columns. The presence of α^2 in the expression suggests that for a fine comparison of materials, the properties of the base polymers must be studied as well as foam density and elastic modulus. Table 2-1 summarizes some of the properties that can be expected of commercial foams (Hodgman, 1958; McCann, 1962).

Table 2-1 SOME PROPERTIES OF COMMERCIAL FOAMS

Foam Type	Density, pfc	Tensile Strength, psi	α of base polymer
Urethane	1.5 - 3.0	15 - 70	---
Polyvinyl chloride	3 and up	10 - 200	3 - 4
Cellulose acetate	6 - 8	170	3.2 - 7.0
Urea-formaldehyde	0.8 - 1.2	poor	6.7 - 6.9
Polystyrene (bead)	1.0	33	2.50 - 2.65
Polystyrene (extruded)	1.8	55	2.50 - 2.65
Epoxy	5 - 20	55 - 500	3.5 - 5.0

Foam Manufacturers

Table 2-2 is a list of some foam manufacturers in the United States. The list is by no means a complete one, but it does include some of the larger and better known producers. Those which are marked by an asterisk (*) have been solicited by this laboratory for product information.

Survey

Several organizations and individuals were contacted, either in person or by letter, in an attempt to survey previous work on foam materials. None had information for foams other than polystyrenes or urethanes. The survey results are presented below.

MIT Lincoln Laboratory (Peter Fritsch)

Fritsch measured a Styrofoam cylinder at K_a-band frequencies using diameter-to-wavelength ratios from 7.6 to 8.7. The measurements verified the periodic nature of the return with frequency and showed the maximum cross section to be about $4\lambda^2$. The

Table 2-2 PARTIAL LIST OF FOAM PRODUCERS

Manufacturer	Product	Trade Name
*Dow Chemical Co. Midland, Michigan	Expanded polystyrene (extruded)	Styrofoam
	Expandable bead polystyrene	Pelaspan
	Urethane	Thurane
Armstrong Cork Co. Lancaster, Pennsylvania	Expandable bead polystyrene	-------
Emerson and Cuming, Inc Canton, Massachusetts	Expandable bead polystyrene	Eccofoam PS
Koppers Company, Inc Pittsburgh, Pennsylvania	Expandable bead polystyrene	Dylite
*Atlas Chemical Co. Wilmington, Delaware	Urethane	-------
*Wyandotte Chemical Co Wyandotte, Michigan	Urethane	-------
Nopco Chemical Co. Newark, New Jersey	Urethane	-------
*Ciba Products Co. (Div. Ciba Corp.) Fair Lawn, New Jersey	Epoxy	-------
*Shell Chemical Co. (Plastics and Resins Div.) New York, New York	Epoxy	-------

periodicity agreed with that expected of a dielectric sphere of dielectric constant 1.05.

Lockheed Missiles and Space Company (N. J. Gamara)

Lockheed had no helpful data available.

GM Defense Research Laboratories (W. P. Melling)

Melling reported he had no organized data although some measurements had been made of foam columns of various diameters. He said that DRTE had measured the returns from Styrofoam and Eccofoam, and the periodic nature was observed. They (at DRTE) had found shaping to be unsuccessful and that no foam was superior to Styrofoam.

Canadian Defense Research Telecommunications Establishment (John Keys)

Keys confirmed that DRTE had concluded grooving or fluting a column offers little advantage over a smooth one. He had no organized data to present, but noted that Emerson and Cuming's foam was a little better than Styrofoam. He reported that an aged column is somewhat better than a virgin one; they expose their columns to direct sunlight to speed up the aging process.

Radiation Incorporated (J. E. Landfried)

This organization has compared the return of several foams and found no improvement was gained by shaping or serrating the columns. No foam was better than Styrofoam but there were inhomogeneities whose effects were more severe at the higher (K_a-band) frequencies. Scattering from sample to sample was not consistent.

B. F. Goodrich Company

Goodrich, in its evaluation of the anechoic chamber it built for Sperry, conducted measurements of several kinds of columns, varied in both shape and materials. The data presented in the report suggests low density foams are the best and that tapering is helpful. Serrations or grooves seem to be beneficial if the resulting edges are orthogonal to the incident radiation.

University of Michigan (Harold Borkin, Architect)

Mr. Borkin is qualified to discuss foams since he studied them in connection with low cost housing. He feels that urethane

foams may be worthy materials since they are available in large volumes and can be tailored to yield densities from 1 to 20 pcf. The high dielectric constant expected of high densities may be offset by their superior strengths.

Conductron Corporation (Howard Brooks)

Conductron has found the expandable bead foam, Pelaspan, superior to Styrofoam, although their data is not organized. The material is easily cut by hot-wire techniques and is available in logs of respectable size.

Ohio State University (E. M. Kennaugh)

Some of the O.S.U. efforts are contained in their reports. Generally, Styrofoam is found to be the best material for support of models and antennas. One of the reports deals with the effects of interfaces, for example, while others discuss scattering from dielectric bodies. O.S.U. has not made a study of foams, per se.

It can be seen that among those surveyed there is a difference of opinion. Most assert that shaping or serrating the columns makes little difference, yet one source suggests shaping is advantageous if the incident polarization is in the right direction. Most of those surveyed indicate there is nothing better than Styrofoam, yet there are two who have found something they consider better. Note that those who found something better have studied the expandable bead polystyrene foams.

SCATTERING BY CELLULAR MATERIALS

The most obvious characteristic of any cellular plastic material is its cellular structure. A material such as Tyrilfoam where the cell sizes are quite large (of order 1 cm) appears almost as a honeycomb with the air pockets separated by only thin membranes, and is in marked contrast to the denser materials such as Styrofoam FR where the air pockets can be no more than pin pricks. In both cases, however, the structure is not entirely regular within the sample. The sizes, shapes and separation vary from point to point in a manner which, for a well chosen sample, is more or less random, and though it is possible that these variations could be reduced by greater care in manufacturing (the irregularities are of no concern for most applications of the materials), some lack of uniformity would seem inseparable from an extrusion (or similar) process of fabrication.

Since the material is almost transparent at radar frequencies, an incident field will penetrate to all depths and will be scattered by the individual cells. If these scatterers were substantially independent and if the material were uniform in the large, the net back scattering from within the medium would be zero, and the entire return would be a coherent one contributed by the bounding faces of the sample. But as we have seen, structural variations do exist, and in this respect the material can be likened to a diffuse but inhomogeneous medium. The individual contributions from the cells will not now add up to zero, but will leave a residual return whose statistical properties are related to those of the inhomogeneities, and if the structural variations are effectively random, the return will be incoherent in the sense that, from sample to sample, the phase is random.

Theoretically at least the coherent signal provided by the exterior surfaces can be reduced to an arbitrarily small amount by shaping and/or cancellation. Not so, however, with the incoherent or 'volume' contribution. On an independent scattering theory, the power in the incoherent signal is proportional to the sum of the powers from the individual scatterers, and is therefore proportional to the volume. There is a limit to which the volume of a support pedestal can be reduced consistent with the support of targets of a specified weight at a chosen height and this in turn gives a lower bound for the incoherent scattering. Quite obviously such scattering is affected by shaping only to the extent that the volume is, and is in principle immune to any cancellation technique. If its phase is truly random from sample to sample or from aspect to aspect with a given sample, no preprogrammed subtraction of the signal in phase and amplitude could

succeed, and though in practice there may be sufficient correlation between neighboring aspects to allow some of this return to be removed by cancellation, the magnitude of the 'incoherent' contribution will still be indicative of the minimum to which the cross section of a column could be reduced. The importance of estimating its magnitude for different cellular materials is now apparent.

A general discussion of scattering from cellular materials has been given by Plonus (1963), starting with the concept of an assembly of particles all scattering independently. It has been suggested (Van de Hulst, 1957) that a sufficient condition for independence is that the separation between particles exceed three times their radius, and it will be appreciated that the assumption of single scattering is a gross approximation when applied to the present type of materials where the cells are closely packed. Nevertheless, it has the overwhelming advantage that it enables us to study the scattering by one particle without reference to the others.

Consider first of all a one-dimensional distribution of scatterers whose particle density is given by n(r). For a plane wave incidence along the line, the back scattered field of a single particle can be written as

$$E^s = E_o \frac{p}{\sqrt{4\pi}} \frac{e^{-2ik(R+r)}}{R+2r}$$

where R is the distance to the point of observation and p is a constant of proportionality, and hence, for the entire assembly the far zone field is

$$E^s = E_o \frac{p}{\sqrt{4\pi}} \frac{e^{-2ikR}}{R} \int n(r) e^{-2ikr} dr.$$

The scattering cross section is therefore

$$\sigma = |p|^2 \iint n(r)n(r') \; e^{-2ik(r-r')} drdr'. \qquad (1)$$

In practice n(r) will be known only in a statistical sense, and if the resulting processes are stationary, the averages obtained in the time and ensemble domains will be identical. For definiteness, let us assume that n(r) is a function of time. The expression for the scattering cross section is now

$$\sigma = |p|^2 \iint \overline{n(r,t)n(r',t)}\; e^{-2ik(r-r')}\, dr\, dr'$$

where the bar denotes a time average, and by subtracting the fluctuating portion of the integrand from its mean, we have

$$\sigma = |p|^2 \left| \int \bar{n}(r) e^{-2ikr}\, dr \right|^2 + |p|^2 \iint \overline{(n(r,t)n(r',t)} - \bar{n}(r)\bar{n}(r')\; e^{-2ik(r-r')}\, dr\, dr', \tag{2}$$

where $\bar{n}(r)$ is the time average of the distribution.

The first term in (2) is proportional to the square of the number of particles and is the coherent part of the scattering. The second arises solely from the fluctuations in the density of the particles about its time average and is therefore zero for a purely static distribution. Moreover,

$$\overline{n(r,t)n(r',t)} - \bar{n}(r)\bar{n}(r') = \overline{(n(r,t) - n(r))(n(r',t) - n(r'))}$$

and hence (Kerr, 1951)

$$\sigma = |p|^2 \left| \int \bar{n}(r) e^{-2ikr}\, dr \right|^2 + |p|^2 \int \bar{n}(r)\, dr \tag{3}$$

where the second term represents the incoherent contribution produced by the average distribution.

All back scattering is ultimately attributable to deviations from uniformity in the particle distribution. If the particles are arranged in a fixed uniform arrary of infinite extent so that $n(r,t)$ is independent of both t and r, even the coherent part of σ will vanish. This can be seen by partial integration of the first term in (3), and if the density is arbitrarily taken as zero at the origin and infinity, we have

$$\int_0^\infty \bar{n}(r) e^{-2ikr}\, dr = \frac{1}{2ik} \int_0^\infty \frac{d\bar{n}(r)}{dr}\; e^{-2ikr}\, dr$$

which shows explicitly the dependence of the coherent scattering on variation of density. Such a variation can come about either by internal variations in the density or by the boundaries which define the particle system in any practical case.

Even if $\bar{n}(r)$ is uniform within the sample, so that the only contributions to the first term of (3) are provided by the boundaries, the density can still exhibit statistical fluctuations about the average. These fluctuations will result in a further scattering which is proportional to the number of scatterers (second term in equation 3) and which is incoherent.

For a distribution which is three dimensional rather than one, the preceding formulae are unchanged, and it is now a simple matter to obtain the return from a specified distribution of known scatterers. We shall begin by examining the return from the bounding surfaces of the sample and then go on to look at the contribution from the interior.

Consider a rigid uniform distribution of small spheres of radius a forming a rectangular lattice so that in each of the three planes of symmetry the distance between the centers of adjacent spheres is ℓ. The numbers of spheres in the three directions are m, n and n, with $m,n \gg 1$. The lattice therefore constitutes a rectangular parallelepiped of length $L = m\ell + a \simeq m\ell$ and cross sectional area $(n\ell + a)^2 \simeq (n\ell)^2$. If this is illuminated by a plane wave incident in the direction of the length L, the only back scattered return is a coherent one produced by the front and rear faces, and from the first term of (3) we have

$$\sigma = \sigma_i \left| \int_0^\infty n(r) e^{-2ikr}\, dr \right|^2$$

$$= \sigma_i N^2 \left| \frac{1 - e^{-2ikL}}{2kL} \right|^2 \qquad (4)$$

where σ_i is the scattering cross section of each sphere, and N is the number of spheres in the block.

Two particular cases of this formula are of special interest. If the individual scatterer is a dielectric sphere whose radius is so small that the Rayleigh approximation is appropriate,

$$\sigma_i = 4\pi a^2 (ka)^4 \left| \frac{\epsilon - 1}{\epsilon - 2} \right|^2 , \qquad (5)$$

where ϵ is the relative permittivity, and the resulting expression for σ is

$$\sigma = 4\pi a^2 (ka)^4 \left| \frac{\epsilon - 1}{\epsilon - 2} \right|^2 N^2 \left| \frac{1 - e^{-2ikL}}{2kL} \right|^2 . \qquad (6)$$

Comparison with the standard physical optics cross section for a homogeneous dielectric whose voltage reflection coefficient R is such that $1 - R \ll 1$ now gives

$$|R| = \pi (a/\ell)^3 \left| \frac{\epsilon - 1}{\epsilon - 2} \right| , \qquad (7)$$

and the implications of this relation can be seen by taking Styrofoam as an example. The relative permittivity of polystyrene, the constitutive material, is 2.55, and the bulk permittivity ϵ_s of Styrofoam is approximately 1.04. Using the Fresnel reflection coefficient formula we therefore have

$$|R| \simeq 0.01$$

and when this is substituted into (7) with ϵ put equal to 2.55 we obtain a value for the packing factor a/ℓ, viz

$$a/\ell = 0.104.$$

Note that the packing factor deduced from the expansion ratio of polystyrene is approximately 0.285.

Conversely, by postulating a packing factor 0.285 and inserting this into (7), the reflection coefficient obtained exceeds the Fresnel value by a factor 2, whereas for maximum possible packing (touching spheres: $a/\ell = 0.5$), (7) with $\epsilon = \epsilon_s$ gives a reflection coefficient smaller than the Fresnel value by a factor 2. Thus, the above formula for the reflection coefficient based on a lattice of Rayleigh scatterers compares favorably with the usual definition.

An aggregate of solid dielectric spheres is hardly a

convincing model for plastic foams. Spherical shells (or ping-pong balls) would almost certainly be a better choice, and would seem to give a reasonable representation of the cell structure when closely spaced. The Rayleigh cross section of such a shell is

$$\sigma_i = 4\pi t^2 (ka)^4 \left| \epsilon - 1 \right|^2 , \qquad (8)$$

where t and a are the thickness and outer radius respectively of the shell, and ϵ is the relative permittivity of the shell material. The shell is assumed thin, such that $t/a \ll 1$. Substituting (8) into (4), the equivalent reflection coefficient is found to be

$$|R| = \pi (t/\ell)(a/\ell)^2 \left| \epsilon - 1 \right| , \qquad (9)$$

which reduces to

$$|R| = \frac{\pi t}{8a} \left| \epsilon - 1 \right| \qquad (10)$$

for shells that are touching.

The appropriate value of t/a for any particular cellular material (e.g., Styrofoam) can be determined from its density. If ρ_p, ρ_s and ρ_o are the densities of polystyrene, Styrofoam and air respectively, the volume ratio of air to polystyrene is

$$v = \frac{\rho_p - \rho_s}{\rho_s - \rho_o} , \qquad (11)$$

and for a typical Styrofoam ($\rho_p = 66.5$ lbs/ft^3, $\rho_s = 1.6$ lbs/ft^3 and $\rho_o = 0.08$ lbs/ft^3) equation (11) gives

$$v = 43.$$

Knowing the volume ratio we can now calculate the effective dielectric constant from the equation

$$\epsilon_s = \frac{v + \epsilon_p}{v+1} \qquad (12)$$

and with the above value of v and $\epsilon_p = 2.55$,

$$\epsilon_s = 1.037.$$

We can also determine t/a directly from v by regarding it as the ratio of air to material for each shell. Hence

$$t/a = 1/3v , \tag{13}$$

giving

$$t = 0.0082a,$$

and although (13) is not exact since it ignores the volume between the shells, the results obtained are close to the experimental values (Baer, 1964). The equivalent reflection coefficient computed from (10) is

$$R = 0.005.$$

Thus, the boundaries of a rigid uniform particle system give rise to a coherent scattered signal which is in reasonable agreement with the physical optics prediction. Since its magnitude is proportional to the square of the number of particles it will usually be the dominant contribution, but it is also susceptible to shaping effects and to cancellation techniques. Under these conditions, it is conceivable that its effective magnitude will be no greater (and perhaps even less) than the incoherent return generated by inhomogeneities within the system, and it is therefore necessary to consider now the contribution from the interior.

If the particle distribution is not uniform but has a specified behavior as a function of position, coherent scattering from the interior will result. On the other hand, the scattering is incoherent if the irregularities vary from sample to sample (or as a function of time) in a manner which can only be described statistically, and this is the case of most interest in studies of cellular materials. The magnitude of the resulting contribution can be estimated in any one of several ways.

In the first of these we postulate a medium specified only by its permittivity (or refractive index) and imagine the inhomogeneities to consist of irregularly spaced spherical 'blobs'. Each blob could represent a typical cell, and within it we assume a Gaussian distribution of refractive index μ of the form

$$\mu - \mu_o = \mu_1 e^{-\pi(r/a)^2} \tag{14}$$

where a is a measure of the size of the cell and r is the radial distance from the center. The cross section of each blob is then

$$\sigma = \frac{1}{\pi} \mu_1^2 a^2 (ka)^4 \, e^{-\frac{2}{\pi}(ka)^2},$$

The separate inhomogeneities scatter incoherently with respect to one another and consequently the cross section of the complete sample is

$$\sigma = \frac{N}{\pi} \mu_1^2 a^2 (ka)^4 \, e^{-\frac{2}{\pi}(ka)^2},$$

where N is the number of inhomogeneities. If the cells are 'touching' (i.e., spaced 2a apart) the volume V is simply

$$V = 8Na^3$$

and hence

$$\sigma = \frac{V}{8\pi} \mu_1^2 a^2 (ka)^4 \, e^{-\frac{2}{\pi}(ka)^2}. \qquad (15)$$

Even such an elementary formula as this has many interesting properties. We note that the incoherent cross section is proportional to the volume and to the square of the refractive index fluctuations. The expression has a maximum when $a = \lambda/2\sqrt{3/2\pi}$, so that cell size plays a vital role in the magnitude of the scattering. In general, however, the cell size will be less than $\lambda/4$ and minimum scattering now corresponds to the smallest possible value of a. Nevertheless, if the refractive index did not show any fluctuation about its average, the incoherent return would be identically zero.

Perhaps a more general approach is to assume that the index of refraction varies from point to point in a random manner, and the analysis is then comparable to that employed in many ionospheric and tropospheric investigations. The magnitude of the cross section for incoherent scattering in the backwards direction is proportional to an integral over the autocorrelation function of the irregularities, and it is a trivial matter to evaluate the integral for any particular choice of correlation function. Inherent in the analysis, however, is the assumption that the relative variations of refractive index are small, and this is certainly hard to justify for a cellular plastic material. Indeed, the permittivity jumps from unity within a cell to a typical value

of 2.55 in the cell wall, and this is the main objection to the application of most analyses of scattering by inhomogeneous media to materials such as we are concerned with here.

Under these circumstances it seems most realistic to return to the concept of closely spaced spherical shells as a model for the cell structure. If these are randomly arranged with mean radius and shell thickness a and t respectively, the cross section of each shell is as shown in equation (8). The incoherent return is then

$$\sigma = 4\pi t^2 (ka)^4 \left| \epsilon - 1 \right|^2 N \ , \qquad (16)$$

where N is the number of shells, and for a dense distribution (16) reduces to

$$\sigma = \frac{\pi}{2} t^2 k^4 a \left| \epsilon - 1 \right|^2 V \ , \qquad (17)$$

where V is the volume. Typical values can be had by inserting the values of t/a and ϵ previously employed, and with an average cell radius 0.05 cm the incoherent cross section at a wavelength of 3 cm is 6.10×10^{-5} m^2 per m^3. Increasing the cell radius to 0.08 cm increases the return to 2.50×10^{-4} m^2 per m^3, and conversely decreasing the radius to 0.04 cm decreases the return to 3.12×10^{-5} m^2 per m^3.

There is as yet no experimental evidence to confirm these estimates, but since a mean cell radius of 0.05 cm is characteristic of one of the more widely used materials (Styrofoam DB), it is of interest to examine the consequences of the corresponding incoherent return on the minimum scattering cross section of three column supports. If these columns have to support weights of 1000, 5000, and 10,000 lbs. at a height of 5 feet, the end areas of the columns must exceed 40, 200, and 400 square inches respectively, where these are based on a compressive strength of 25 p.s.i. (yield) and a uniformly distributed load. The resulting incoherent cross sections at a wavelength of 3 cm are 56.2, 49.2 and 46.2 db < m^2, and these are irreducible in the sense that they are immune to shaping and (formally at least) cancellation.

MEASURED CROSS SECTIONS OF STYROFOAM CYLINDERS

At the request of General Dynamics/Fort Worth, an experimental study of the back scattering cross sections of nine Styrofoam cylinders was undertaken. It is obvious that such data is desirable for checking the available methods for calculating the cross section when the dielectric constant is close to unity (we note in passing that data of a similar character has recently been published by Blore, 1964), but since the full motivation of this work is discussed elsewhere[+], the present account will concentrate on the experimental techniques employed. Only two samples of the data are included (a complete listing is given in Memorandum 5849-512-M) and the theoretical remarks are limited to those necessary for an understanding of the results.

Requirements

The nine right circular cylinders represented all combinations of the three diameters 16, 15 and 14 inches and the three lengths 20, 15 and 10 inches. The back scattering cross section was to be determined as a function of frequency at the broadside aspect, with the cylinder in a horizontal position illuminated by a horizontally polarized wave. The test frequencies were to be X-band, and were specified only to the extent that they should span at least two maxima and two minima in the cross section against frequency plots. In practice they were limited to the range 8.5 to 9.3 gigacycles and this was sufficient to satisfy the above criterion.

Because of the large forward scatter from the cylinders, the measurements were made at a range of 226 inches to the cylinder axis. This is short of the far field distance for the 20 and 15 inch models and in order that the data could be corrected for near-field effects, the phase and amplitude of the incident field was mapped out in the region normally occupied by the models. A string suspension was used (the return from the available support pedestals was of the same order as that of the model under test), and though it was verified that the suspension was invisible, it did result in some loss of azimuth control.

Separation of Room Effects

In the conventional CW bridge arrangement, the reflections

[+]General Dynamics/Fort Worth Report No. FZE-335, dated 29 August 1964.

from the empty chamber are balanced out with a sample of transmitted signal and then the test object is installed in the balanced room. Generally the forward scatter from the model alters the room return and the room is no longer balanced, but for most objects this effect is small. However, for some bodies, such as the Styrofoam cylinders under consideration, the effect is significant, and the cross section displayed at the output of the receiving system is therefore composed of two signals, one arising from the model and the other from background effects. The total cross section can be shown to be

$$\sigma = \sigma_m + \sigma_b + 2\sqrt{\sigma_m}\sqrt{\sigma_b}\cos 2kR,$$

where

σ_m = true model cross section,
σ_b = effective cross section of background effects,
R = range to the model, assumed to be variable by a few wavelengths.

The background "cross section" is in turn due to two signals, one of which arises from room return, σ_r, and the other from the coupling signal $\sqrt{\sigma_c}\, e^{j\phi}$ which is deliberately added for balancing purposes:

$$\sqrt{\sigma_b} = \sqrt{\sigma_r} + \sqrt{\sigma_c}\, e^{j\phi} .$$

If the model is rocked a few wavelengths (or permitted to swing like a pendulum as in the present measurements) the display cross section will attain the maximum and minimum values

$$\sigma_{max} = \sigma_m \left[1 + \frac{\sqrt{\sigma_b}}{\sqrt{\sigma_m}}\right]^2, \quad \sigma_{min} = \sigma_m \left[1 - \frac{\sqrt{\sigma_b}}{\sqrt{\sigma_m}}\right]^2 .$$

The "rock" ρ is defined as $\rho = \sigma_{max}/\sigma_{min}$ and in theory can be made as large or as small as desired through control of $\sqrt{\sigma_c}\, e^{j\phi}$, which thereby controls σ_b. The form of the equations suggests that the quantity σ_b/σ_m is an error term. If the bracketed terms are plotted as a function of σ_b/σ_m as shown in Figure 2-1, the background effects can be accounted for and a correction applied, provided it is known which half of the plot is the proper one (i.e., if σ_b/σ_m is greater or less than unity). For example, a 2 db rock may lie either at σ_b/σ_m = -19 db or σ_b/σ_m = + 19 db. But if σ_b is changed slightly, the rock will change; if this

change in rock is accompanied by a change in level ("level" is represented by the dashed lines in Figure 2-1) the left side of the figure must be used for the correction process and if there is no change in level, the right side must be used. In either case, Figure 2-1 provides the necessary correction for room effects, but it must be established which region is appropriate. The two regions have been labelled "over-riding" and "dynamic nulling", following the suggestion of others who have investigated these techniques.+

The Test Cylinders

The cylinders were fabricated from a rough Styrofoam log whose dimensions were about 28 inches by 33 inches by 108 inches long. The log was first reduced to four rectangular parallelepipeds, of which three were used to obtain the cylinders. Each was mounted in a lathe and cut to approximately the correct diameter with hot-wire techniques. The final size was produced by making several passes parallel to the axis with a high speed machine cutter. The surfaces produced by the cutter were smooth and no further preparation (i.e., sanding) was required. The cylinder dimensions were maintained to a tolerance of ± 0.032 inch. The ends of each were all within 0.5 degree of being perpendicular to the cylinder axis.

The three longest cylinders were measured first and since these were destroyed in the course of fabricating their successors, the data was plotted to ensure that it was sufficient. The cylinders were then cut down to the second required length, and the measurements repeated and plotted. Similarly for the third length. After each cut the cylinders were weighed so that their densities (and hence their dielectric constants) could be determined. Table 2-3 lists these values, with the dielectric constants (or permittivities) ϵ computed from the equation

$$\epsilon = 0.99834 + 0.2334\,\delta,$$

where δ is the sample density in pounds per cubic foot.

+"Dynamic nulling" is appropriate since the rock is tuned to a small value (in db) while the test object is in motion. "Over-riding" describes the condition of a σ_b being much larger than σ_m.

Table 2-3 PROPERTIES OF THE TEST CYLINDERS

Cylinder diameter, inches	Cylinder length, inches	Density, pcf	Dielectric constant
	10	1.531	1.0341
14	15	1.529	1.0340
	20	1.537	1.0342
	10	1.532	1.0341
15	15	1.534	1.0342
	20	1.526	1.0340
	10	1.548	1.0345
16	15	1.566	1.0349
	20	1.551	1.0345

Measurement Technique

The cylinder measurements were made by one of the two described methods: depending on the magnitude of the cross section to be determined, σ_b was made either large or small by varying $\sqrt{\sigma_c}\, e^{j\phi}$ while the cylinder was swung. It was not convenient to slip the cylinder into or out of the string harness, so an absorbent barrier was installed near the test location to hide the model. When an empty room was desired for balancing purposes, the test model was lowered behind the barrier and when a measurement was desired, it was hoisted into position. The steps in the experimental operation were as follows:

1. The empty room was balanced out

2. The test cylinder was run up and made to swing through a few wavelengths, usually about 2 inches

3. The recording pen was turned on and observed to oscillate between σ_{max} and σ_{min}

4. The waveguide tuners in the RF system were adjusted slightly in in attempt to reduce the rock ρ

5a. If step 4 was successful (i.e., the rock was reduced to 2 db or less) the rock was recorded

6a. The tuners were readjusted to produce a slightly different rock but having the same level as the first. This was recorded

7a. Step 6a was repeated

5b. If step 4 was unsuccessful, the tuners were adjusted to produce a relatively large σ_b yielding a 3 to 8 db rock which was recorded

6b. The tuners were readjusted to produce a slightly different rock accompanied by a significant change in level. This was recorded

7b. Step 6b was repeated

8. The test cylinder was lowered behind the barrier

9. The empty room was balanced

10. A calibration sphere was lowered (the sphere was also suspended by string; its hiding place was in the ceiling) and its cross section recorded.

Observe that the steps labelled "a" required that the right side of Figure 2-1 be used to correct for the room effects while those labelled "b" demanded the use of the left side. Several times, as a check of the measurement technique, a cross section was measured both ways and found to agree within a fraction of a db. The above sequence was repeated three times for each frequency for each cylinder, yielding nine values which were averaged to produce a single datum point on the σ vs. frequency curves. The averaging was done graphically, as was the correction process, in order to save time: over 2300 individual values were recorded.

The error is estimated to be $\pm$ 0.2 db for most of the higher cross sections (-30 dbm^2) but inspection of the plotted data suggests that the error for a few points is greater than this. The accuracy of the lower values (-50 dbm^2) is probably no better than one or two db. Use of the over-riding technique was the only way the lower cross sections could be measured and the dynamic nulling procedure was useful only for cross sections greater than about -36 dbm^2. The cross-over point occurs when the changes in rock become excessively sensitive to slight mechanical adjustment of the RF tuners.

Bifilar suspension of the models by means of the vertical lines attached near the ends resulted in a loss of azimuth

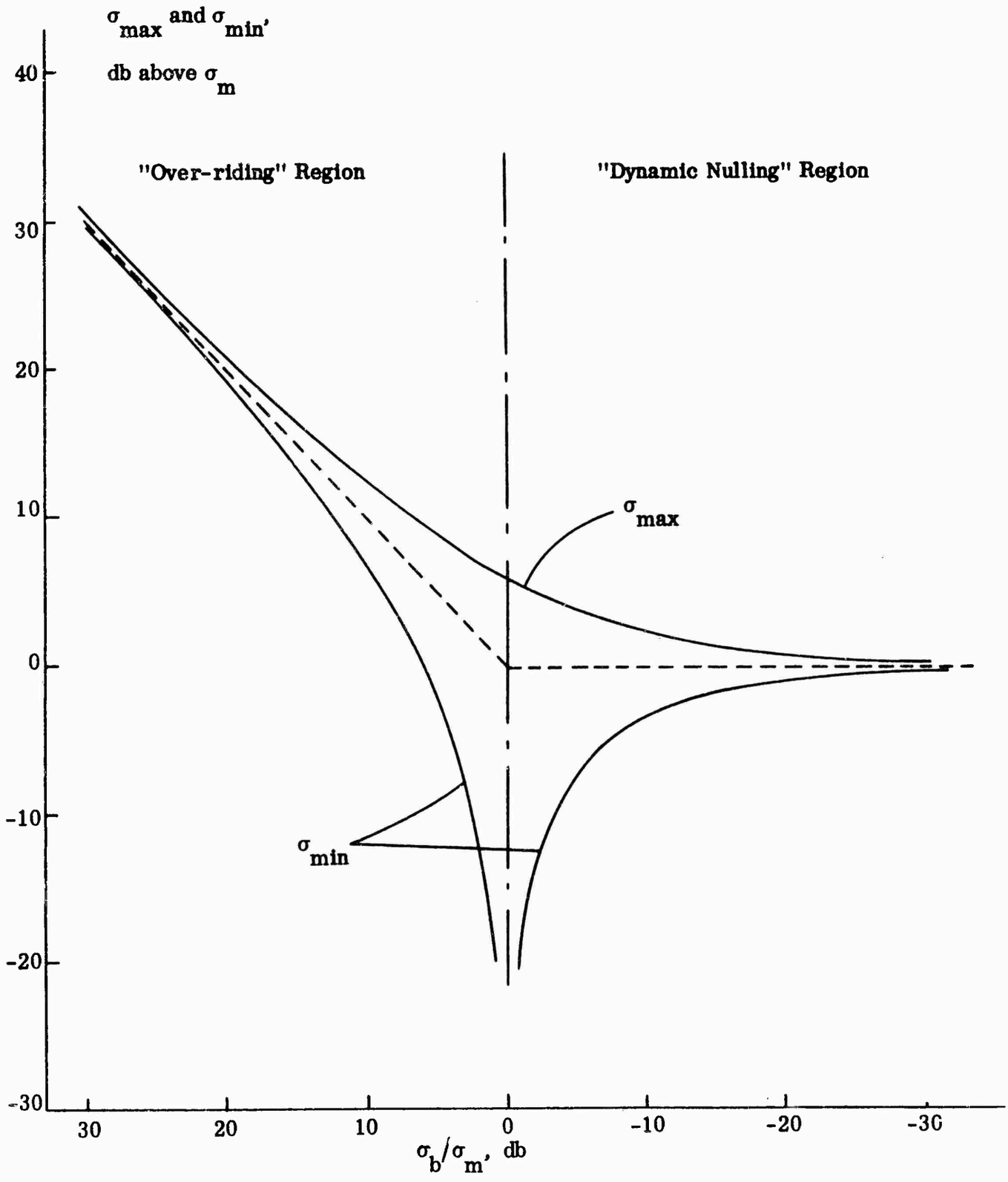

Fig. 2-1 CORRECTION CURVES TO ACCOUNT FOR ROOM EFFECTS

control. Broadside alignment of the cylinders was accomplished with a "naked eye" approach. An observer would station himself so that his line of sight lay in the plane of one of the ends and he would note where the transmitter appeared to be located with respect to this plane. He would then repeat the process with the other end and by quick, alternate sightings, he could judge which way the body should be adjusted. The alignment was checked electrically by fastening a thin copper wire along the surface and by observing the signal variation as the cylinder was made to oscillate in a horizontal plane. The oscillation caused the wire scattering lobes to sweep past the transmitter and the maximum observed response agreed with that when the cylinder was stationary.

Another check of the alignment accuracy was accidentally encountered when the first set of data was plotted. The cross section was apparently falling off faster than it should down the reverse side of one of the maxima and some sleuthing revealed that a knot in one of the support lines had slipped. Further checking showed that the misalignment could easily be detected by the "naked eye" method described above. The operators of the range soon acquired considerable experience and confidence in the alignment of the models and it is felt that the error is less than 0.5 degree for all the measurements. This corresponds to an azimuth error of 2 inches at a range of 226 inches, which was found to be easily detectable.

Data

To illustrate the type of results obtained, the data for the largest and smallest cylinders is shown in Figures 2-2 and 2-3. Note that the solid lines do not represent theory but are merely graphical "smoothing" curves intended to lead the eye from point to point. They are also valuable in indicating the frequencies at which the minima fell and were sketched to be as symmetrical about the minima as the datum points would permit. Near each minimum peak of the curves will be found a number which gives the apparent frequency of that minimum in gigacycles. Such numbers for all nine cylinders are listed in Table 2-4. Since the maxima are broad and the minima deep, no attempt was made to determine the frequencies associated with the maxima or cross sections of the minima.

Included in Table 2-4 are the theoretical predictions for the inter-null spacing and peak cross sections computed for the formulae in the section on Remarks. It will be observed that the periodicity is predictable with an accuracy of 2 per cent or better,

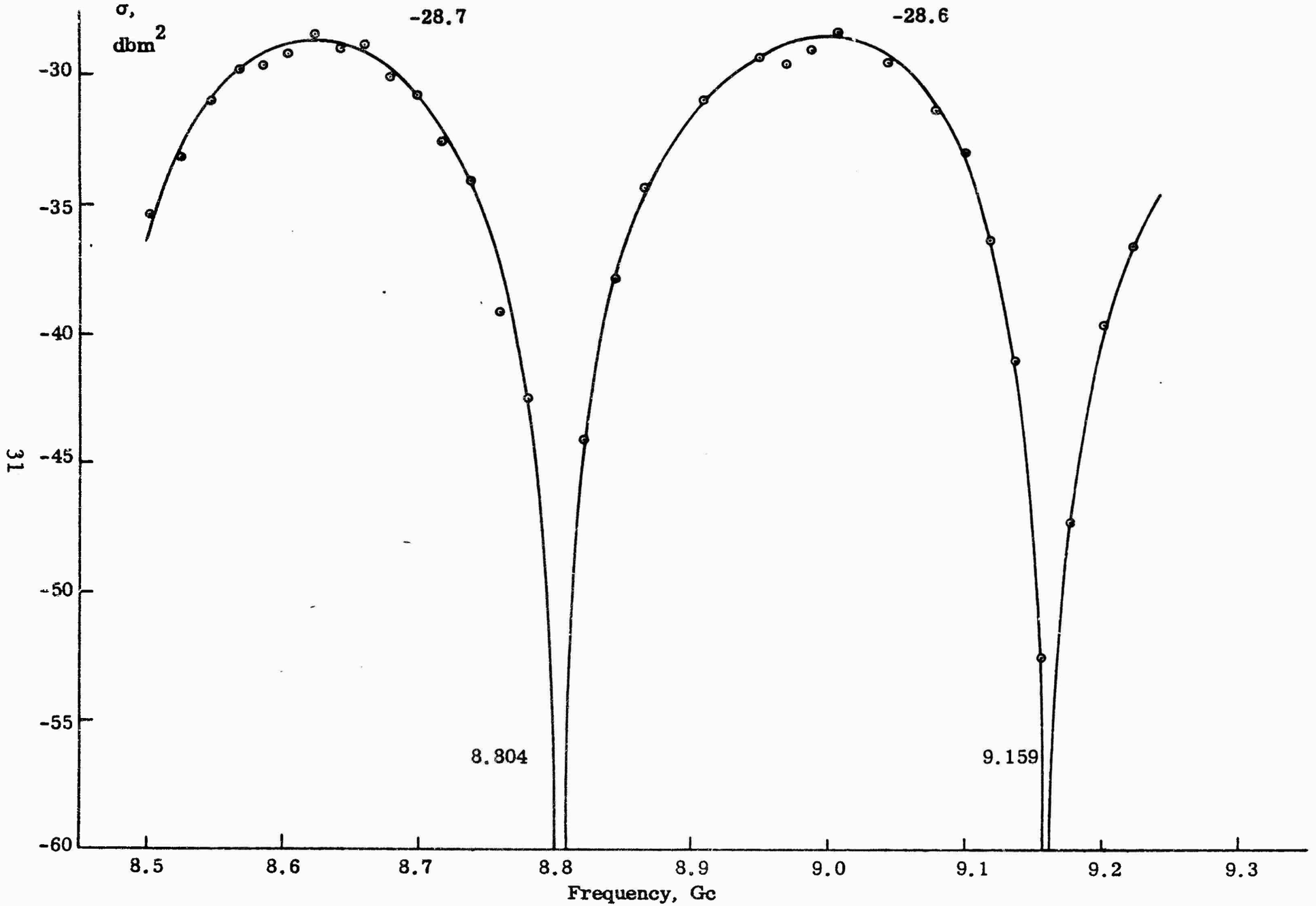

Fig. 2-2 CROSS SECTION VS. FREQUENCY OF 16" DIAMETER, 20" LONG STYROFOAM CYLINDER

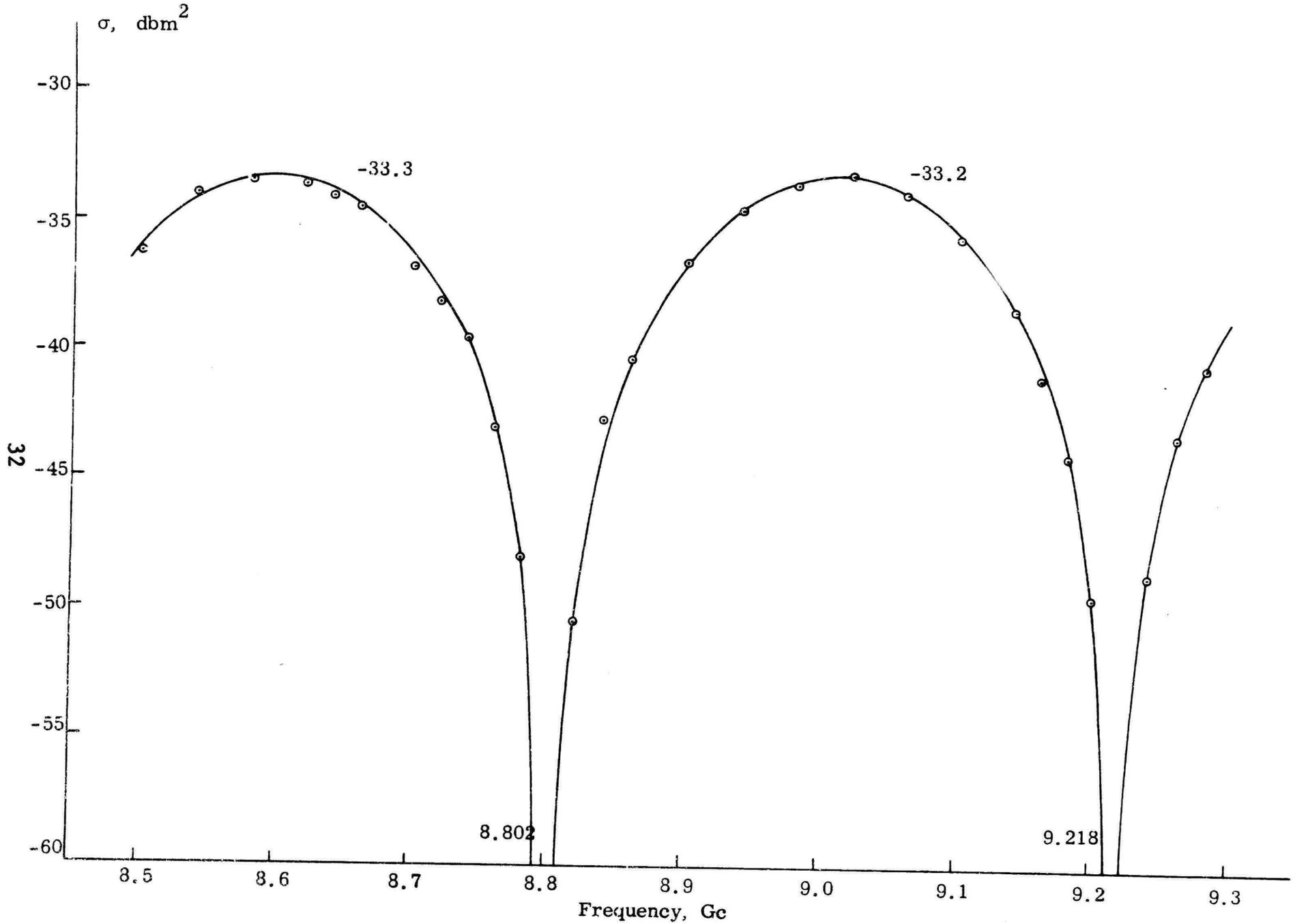

Fig. 2-3 CROSS SECTION VS. FREQUENCY OF 14" DIAMETER, 10" LONG STYROFOAM CYLINDER

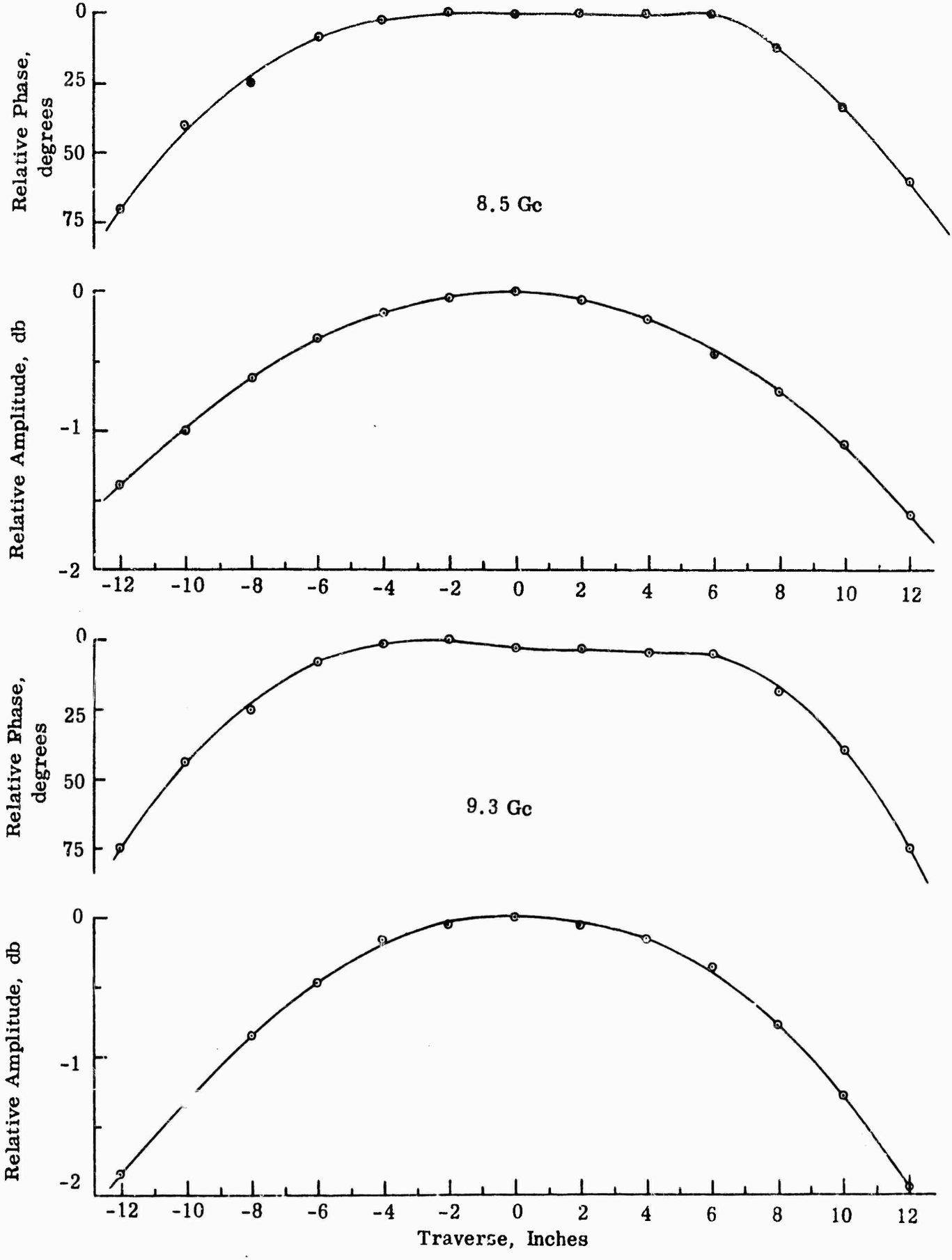

Fig. 2-4 PHASE AND AMPLITUDE OF INCIDENT FIELD AT RANGE = 226 INCHES

and though the peak cross sections disagree by as much as 4.2 db, this is probably due to near-field effects. If attention is confined to the 10 inch long models which were in the far field at a range of 226 inches, the disagreement is much less, being of order 1.4 db.

The correction of the measured data to account for the near field effects is beyond the scope of this summary, but it may be of interest to present the results of the incident field mapping carried out in the region of the test object. The measurements were made using the techniques described in the subsection on Surface Wave Effects Near a Styrofoam Cylinder and both amplitude and phase were determined at 8.5 and 9.3 gigacycles. The data is shown in Figure 2-4.

Remarks

Several analyses of the scattering behavior of an almost transparent cylinder have been published and the results are in complete agreement in spite of the diverse methods of approach, but because of the notational confusion which has recently crept into the literature, it may be appropriate to quote the formulae.

One of the most complete analyses is that of Wait (1955) who considers an infinite right circular cylinder of radius a composed of a homogeneous isotropic material whose (complex) permittivity and permeability are ϵ and μ respectively. For plane wave illumination at an arbitrary angle the exact modal expansion of the far-zone scattered field is determined, and this is then approximated in several specific cases including the low contrast one in which $|\epsilon - 1| \ll \epsilon_o$, where ϵ_o is the permittivity of free space. In particular, for normal incidence the back scattering cross section σ' per unit length defined as

$$\sigma' = \lim_{r \longrightarrow \infty} 2\pi r \left| \frac{E^s}{E^i} \right|^2 ,$$

(r is the radial distance) is found to be

$$\sigma' = \frac{\pi}{8} \lambda (ka)^2 \left| \frac{\mu}{\mu_o} \right|^2 \left| \frac{\epsilon}{\epsilon_o} - 1 \right|^2 J_1^2(2ka) , \quad (18)$$

where $k = 2\pi/\lambda$ is the propagation constant for free space and J_1 is the Bessel function of order unity. The above expression for σ' is tantamount to that of the "echo width" W_e obtained by Rhodes (1953) using a somewhat different approach.

TABLE 2-4 SUMMARY OF THE MEASUREMENTS AND COMPARISON WITH THEORY

Diameter, inches	Length, inches	$2\ell^2/\lambda$, feet	Min.No.1, Gc	Min.No.2, Gc	Δf Gc	Δf, Gc theory	$\sigma_{max}^{\#1}$, dbm^2	$\sigma_{max}^{\#2}$, dbm^2	σ_{max} theory
14	10	13.1	8.802	9.218	0.416	0.414	-33.3	-33.2	-31.9
14	15	29.5	8.807	9.225	0.418	0.414	-30.4	-30.5	-28.4
14	20	52.5	8.808	9.224	0.416	0.414	-29.5	-30.1	-25.9
15	10	13.1	8.631	9.027	0.396	0.387	-33.0	-32.9	-31.7
15	15	29.5	8.633	9.026	0.393	0.387	-30.4	-30.3	-28.2
15	20	52.5	8.617	9.012	0.395	0.387	-29.4	-29.3	-25.7
16	10	13.1	8.809	9.169	0.360	0.363	-32.7	-32.3	-31.3
16	15	29.5	8.800	9.159	0.359	0.363	-29.9	-29.5	-27.8
16	20	52.5	8.804	9.159	0.355	0.363	-28.7	-28.6	-25.3

Still another method was adopted by Albini and Nagelberg (1962), who used the Born approximation to treat an infinite inhomogeneous dielectric cylinder. When specialized to the low contrast homogeneous problem, the results are the same as those of Wait, but the scattering cross section q which they define is, in fact $\frac{1}{2\pi}\sigma'$.

If it is now assumed that at the surface of a cylinder of large but finite length ℓ the field is the same as it would have been had the cylinder been infinite in length, the determination of the scattering cross section σ is reduced to quadratures. In terms of the scattering cross section σ' in the two dimensional case, we have

$$\sigma = \frac{2\ell^2}{\lambda}\,\sigma' \tag{19}$$

(Mentzer, 1955; Rhodes, 1953) and hence from equation (18)

$$\sigma = \pi \left| \frac{ka\ell}{2}\,\frac{\mu}{\mu_o}\left(\frac{\epsilon}{\epsilon_o} - 1\right) J_1(2ka) \right|^2 . \tag{20}$$

For $ka \gg 1$ the Bessel function can be replaced by the leading term of its asymptotic expansion for large argument to give

$$\sigma = \frac{ka\ell^2}{8} \left| \frac{\epsilon}{\epsilon_o} - 1 \right|^2 (1 + \sin 4ka) , \tag{21}$$

where, for brevity, we have put $\mu = \mu_o$. The oscillatory character of the cross section is now obvious. The frequency spacing between successive results is

$$\Delta f = \frac{c}{4a}\sqrt{\frac{\epsilon_o}{\epsilon}} , \tag{22}$$

where c is the velocity of light in vacuo, and this is the formula used in the computation of the seventh column in Table 2-4. The maximum cross section is

$$\sigma_{max} = \frac{ka\ell^2}{4} \left| \frac{\epsilon}{\epsilon_o} - 1 \right|^2 \tag{23}$$

and numerical values are given in the last column of Table 2-4.

Note that the maximum is proportional to the radius, the square of the length and the square of the departure of the relative dielectric constant from unity. Such dependences are clearly evident in the measured data and Blore (1964) has recently presented results for cylinders of four different cellular materials as functions of the radii in wavelengths. He also quotes a formula for σ which is in disagreement with that in equation (21), and even when the typographical errors are corrected a more fundamental error still remains: Blore gives the expression for q obtained by Albini and Nagelberg, but labels it W, and then proceeds to use equation (19) with σ' replaced by W instead of the equation

$$\sigma = \frac{4\pi\ell^2}{\lambda} q$$

required by the relationship between W (or σ') and q.

BACK SCATTERING FROM CELLULAR PLASTIC SHAPES

Soon after the commencement of the contract a series of experiments was undertaken aimed at furthering our knowledge of the scattering behavior of cellular materials. Our initial conception was that the scattering could be broken down into two components, one arising from the interfaces and the other from irregularities within the materials. The first of these is essentially a coherent return and for a volume of relatively simple shape it can be calculated with a reasonable degree of accuracy. But even for a well chosen sample of material which has no large cavities or cracks, a close inspection shows that the size, shape and separation of the individual cells vary from point to point in a manner which appears random and such irregularities could be expected to generate a return which is fundamentally incoherent.

An analysis of the scattering from this type of medium was described in the subsection on Scattering by Cellular Materials and when the values appropriate to a typical Styrofoam material are inserted into the formulae, the resulting scattering cross section is of order 10^{-5} m^2 per m^3. A return of this magnitude would be observable only if the coherent face returns had been suppressed almost entirely, but by suitable choice of sample shape it seemed feasible that a sufficient reduction of the coherent contributions could be achieved. Under these conditions the resulting return should have some statistical distribution (e.g., Rayleigh), and to obtain a reliable experimental estimate of its magnitude it would be necessary to pursue a lengthy measurement program. Ideally, one should construct a large number of superficially identical samples and examine the statistical properties of the measured returns from these, but the cost of so doing would be almost prohibitive, apart from the difficulty of cutting "identical" pieces of a cellular material. It was therefore essential to find an alternative way of changing the phase relationships between the individual scatterers using only a minimum number of samples. If the chosen sample shape were symmetrical about an axis perpendicular to the direction of incidence, a rotation about this axis would be sufficient, but such shapes were not regarded as compatible with the desired reduction of the face returns. Nevertheless, this did suggest that a similar effect could be achieved by shifting frequencies within a narrow band. Providing the band was small enough for us to ignore the change in scattering from each irregularity, a frequency shift would be similar to an aspect change in effecting the phases of the elementary returns from the inhomogeneities, and a program based on this procedure would enable us to get by with only one sample of the material.

Two contrasting types of shape were selected for investigations. The first was a rectangular block whose front and rear faces were cut successively, leading to a family of shapes whose back scattering cross sections were dominated by two, one and zero specular contributions respectively. In the last case it was hoped that the residual return would be the incoherent one whose determination was the objective of the experiment. The results are summarized below. The second shape was an ogive formed by the rotation of an arc of a circle about a chord. Simple optics theory predicts a zero back scattering cross section for on-axis incidence, which suggests that any return observed in practice will be substantially the incoherent one. This investigation is described in the discussion on Scattering from Ogives.

Scattering from Blocks

Given a large rectangular block of almost transparent material, the back scattering cross section for incidence normal to one of the faces should be dominated by returns from the front and rear faces, and if the cross section is measured at a series of closely spaced frequencies, an analysis of the resulting interference curve should enable the magnitude of the two contributors to be determined. For a block of sufficiently large size, it is presumed that these will be simply specular returns whose magnitude can be estimated by physical optics, and from a comparison with the measured values the electromagnetic parameters of the material can then be deduced. If, now, the rear face is cut at such an angle as to suppress the corresponding contribution, the cross section $\sigma\lambda^2$ (where the λ^2 factor is introduced to remove the wavelength dependence characteristic of a flat plate reflection) should be independent of frequency and arise from the front face only, and if the front face is then slanted also, it is feasible (on a physical optics basis at least) that the net cross section could be reduced to an arbitrarily small value by appropriate choice of angle at which the cuts are made. Hopefully, therefore, the incoherent return would then be dominant.

The results of an initial series of experiments (see Memorandum No. 5849-502-M) seemed to hold sufficient promise to warrant a comprehensive set of measurements. These were carried out at X-band using vertical polarization with the blocks mounted on a pedestal such that their front faces were 160 inches from the aperture of the horn. A parent block was cut from a Dow Chemical Company buoyancy billet, and this was trimmed to give a rectangular parallelepiped (G) of dimensions 5 x 11 x 30 inches. In all cases, incidence was in the direction of the long dimension.

Block G was the first in a sequence of three basic shapes. Each was obtained by cutting one new face, either slanted or upright, in its predecessor, and this process yielded a series of blocks of ever decreasing volume whose shapes followed the sequence a - b - c - b - a (Figure 2-5). Each block was therefore destroyed in the course of fabricating its successor. The various blocks were identified by letters G through T and their physical properties are listed in Table 2-5.

With the exception of block 1, which appeared to show edge effects and was immediately modified to give J, all of the blocks G through T were examined at a variety of frequencies in the X-band range. Providing the angle of cut is such as to suppress the corresponding face return, the cross sections for blocks of shape c should be of generally noisy appearance, and the average of the data for any one block as a function of frequency would then be a measure of the incoherent contribution. If this is indeed true, the averages for successive shape c blocks should decrease in proportion to their volume.

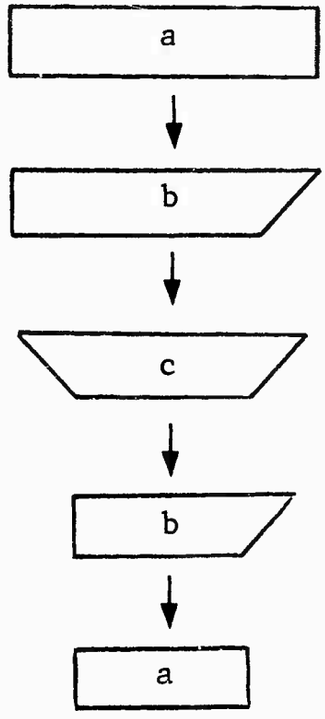

Fig. 2-5 FABRICATION SEQUENCE FOR SHAPED BLOCKS

Two factors governed the choice of angle for the slanted faces: the requirement that the angle be sufficiently large to supress any specular return and keep the side lobes to an acceptable level over the frequency range of interest, yet not so large as to remove too much of the volume at each step in the block sequence. From an examination of an experimental scattering pattern for a 5 x 12 inch metal plate it appeared that a reasonable compromise could be achieved by choosing an angle of cut of about 23 degrees to the vertical, corresponding to the third minimum in the pattern at approximately the center frequency of the band. An angle of 23 degrees was therefore selected, and for an effective permittivity of 1.037 the frequency at which the null occurs is 8.90 gigacycles. For the frequency range 9.6 to 9.9 gigacycles, the reduction in the normal incidence specular return is 23 db or more.

Table 2-5 PHYSICAL CHARACTERISTICS OF BLOCKS

Block	Shape	Median Length (in.)	Volume ($in^3 \times 10^{-2}$)	Weight (lb.)
G	a	30.00	18.00	1.664
H	b	29.00	17.40	1.603
J	c	27.25	16.35	1.510
K	b	25.56	15.34	1.407
L	a	23.62	14.17	1.296
M	b	22.19	13.31	1.217
N	c	20.81	12.49	1.146
O	b	19.56	11.74	1.071
P	a	18.25	10.95	0.9987
Q	b	17.12	10.27	0.9392
R	c	16.03	9.618	0.8796
S	b	14.88	8.928	0.8157
T	a	13.75	8.250	0.7540

Blocks of shapes b and c were placed on the support pedestal with the longest side uppermost and in the case of shape b the slanted face was the rear one furthest from the antenna. For the entire experiment over 100 different frequencies were used, with an average of almost 30 for any one block. A minimum of three determinations of the scattering cross section were made at each frequency, and these were averaged to give the values of $\sigma\lambda^2$ included in Memorandum 5849-511-M.

A complete description of the experimental data and of the analysis that was performed is given in the above reference, and

we shall here content ourselves with a summary of the main conclusions.

For the four blocks G, H, P and T of shape a the measured values are quite similar, and in Figure 2-6 the data for block G is shown. The oscillation is typical of the interference between two contributors whose phase centers are a fixed distance apart in the direction of propagation. The period of oscillation is then proportional to the electrical separation of the phase centers, and since the measured period decreases with decreasing length of block, it is natural to expect that in the present case the front and rear faces are the sources of the contributions.

Given two scatters $\frac{A_1}{\lambda} e^{i\phi_1}$ and $\frac{A_2}{\lambda} e^{i\phi_2}$ a distance ℓ apart in a medium of propagation constant k, the net scattering cross section is

$$\sigma\lambda^2 = A_1^2 + A_2^2 + 2A_1A_2\cos\left\{4\pi\frac{k}{k_o}\frac{\ell}{c} f + \phi_1 - \phi_2\right\}, \qquad (24)$$

where k_o is the free space propagation constant ($= 2\pi/\lambda$), c is the velocity of propagation and f is the frequency. Assuming A_1 and A_2 are relatively independent of frequency, $\sigma\lambda^2$ will oscillate at a rate proportional to the coefficient of f, and an expression of the general form (24) was fitted to the data for the four blocks by the least squares method using an IBM 7090 computer. The resulting values of A_1, A_2, and $\phi = \phi_1 - \phi_2$ are listed in Table 2-6 along with the number of data points on which the analysis is based and the rms error associated with the fit. Note that the values of k/k_o are based on the assumption of a physical separation equal to the block length.

Table 2-6 SCATTERER PARAMETERS

Block	A_1 (x $10^3 m^2$)	A_2 (x $10^3 m^2$)	ϕ	k/k_o	No. of Points	rms Error
G	1.973	1.247	-0.0052	1.004	49	0.540
L	1.493	1.378	0.7339	0.9948	36	0.428
P	1.549	1.092	0.7993	0.9891	26	0.262
T	1.238	1.118	1.147	1.024	33	0.0779

the analysis is based and the rms error associated with the fit. Note that the values of k/k_o are based on the assumption of a physical separation equal to the block length.

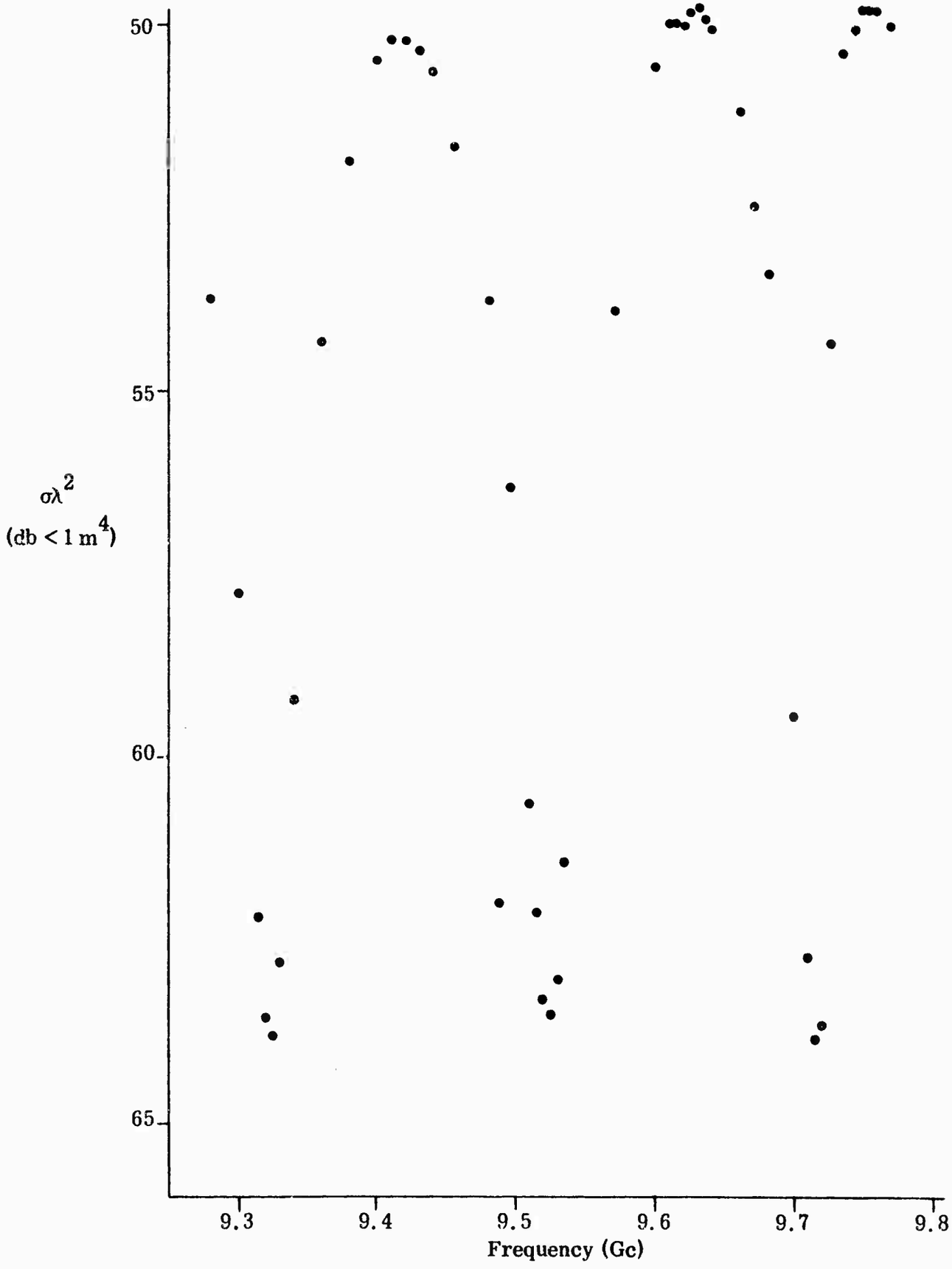

Fig. 2-6 SCATTERING BEHAVIOR OF BLOCK G

There are several intriguing features of these results but perhaps the most surprising of all are the values of the phase difference ϕ. From the simple theory of the effective reflection coefficient of a dielectric slab, we have for the back scattering cross section of the block

$$\sigma\lambda^2 = 4\pi S^2 \left| \frac{k-k_o}{k+k_o} \left\{ 1 - \frac{4kk_o}{(k+k_o)^2} e^{2ik\ell} \right\} \right|^2 , \qquad (25)$$

where S is the area of the front (or rear) face and, for simplicity, we have put $\mu = \mu_o$. The above expression is identical to what would have been obtained by considering a single reflection at the front face of the block, together with a transmission through this face with subsequent reflection at the rear. This interpretation enables us to correct equation (25) to account for the relative closeness of the transmitting and receiving antenna used in this experiment. If the distance of the antenna from the front face is L the ratio of the incident field amplitudes at the front and rear faces is nominally

$$\frac{1}{\gamma} = \frac{L+\ell}{L}$$

and because of the transparency of the Styrofoam it is expected that the same ratio will obtain even in the presence of the block. This factor must now be squared to account for the two way transmission and the modified version of equation (25) is therefore

$$\sigma = 4\pi \frac{S^2}{\lambda^2} \left| \frac{k-k_o}{k+k_o} \left\{ 1 - \gamma^2 \frac{4kk_o}{(k+k_o)^2} e^{2ik\ell} \right\} \right|^2 . \qquad (26)$$

The final simplification is to note that the effective permittivity of Styrofoam is primarily real, so that if $\epsilon = \epsilon' + i\epsilon''$, $\epsilon'' \ll \epsilon'$. Hence

$$k \sim k'(1 + \tfrac{1}{2} ip) ,$$

where $k' = \sqrt{\mu_o \epsilon'}$ is the real propagation constant and $p = \epsilon''/\epsilon'$ is the power factor, and if the latter is retained only in the exponential portion of (26),

$$\sigma = 4\pi \frac{S^2}{\lambda^2} \left| \frac{k'-k_o}{k'+k_o} \left\{ 1 - \gamma^2 \frac{4k'k_o}{(k'+k_o)^2} e^{-2k'p\ell} e^{2ik'\ell} \right\} \right|^2 . \qquad (27)$$

With the notation previously employed we now have

$$A_1 = 2\sqrt{\pi} \quad S \frac{k'-k_o}{k'+k_o}$$

$$A_2 = 2\sqrt{\pi} \quad S \frac{k'-k_o}{k'+k_o} \quad \gamma^2 \quad \frac{4k'k_o}{(k'+k_o)^2} \; e^{-2ik'p}$$

and $\phi_1 - \phi_2 = \pm\pi$, where we have again identified A_1 with the larger of the two scatterers, and in consequence A_1 should be the same for all the blocks, with A_2 increasing as ℓ decreases. This would account for the observed decrease in the minima with ℓ, but the above trends of A_1 and A_2 are in no sense matched in Table 2-6, and this is even more true of the phase. In fact, it would appear that there is an additional contributor to the cross section whose phase center coincides with one of the faces, and evidence to support this conclusion is provided by the data for blocks of shape b.

The initial expectation was that for the six blocks H, K, M, O, Q and S with slanted rear faces the return would be independent of frequency corresponding to a front face return only. The frequencies selected for experiment were therefore grouped in small regions of the X-band range and only with block K was a reasonably uniform coverage obtained. The results for this sample are shown in Figure 2-7. It will be seen that there is still evidence of an oscillation and this was originally attributed to the failure of the slanting to remove all reflections from the rear face. In theory at least, however, the angle of cut should reduce the specular return from the rear by 23 db or more throughout the entire frequency range, and a more likely source of the interference is some form of travelling wave on the longitudinal surfaces of the block. That there must be a contributor over and above the two faces is confirmed by the fact that for blocks of shape b the maximum cross section is 7 or 8 db lower than for the corresponding block of shape a. With a simple theory in which the larger contribution is provided by the front face, even the complete suppression of the rear face return could only decrease the maxima by something less than 6 db.

For the later blocks of shape b the oscillation is by no means as well defined as it is at the lower end of the frequency range with block K, and it is therefore feasible to obtain some information about the length dependence of the contributors by

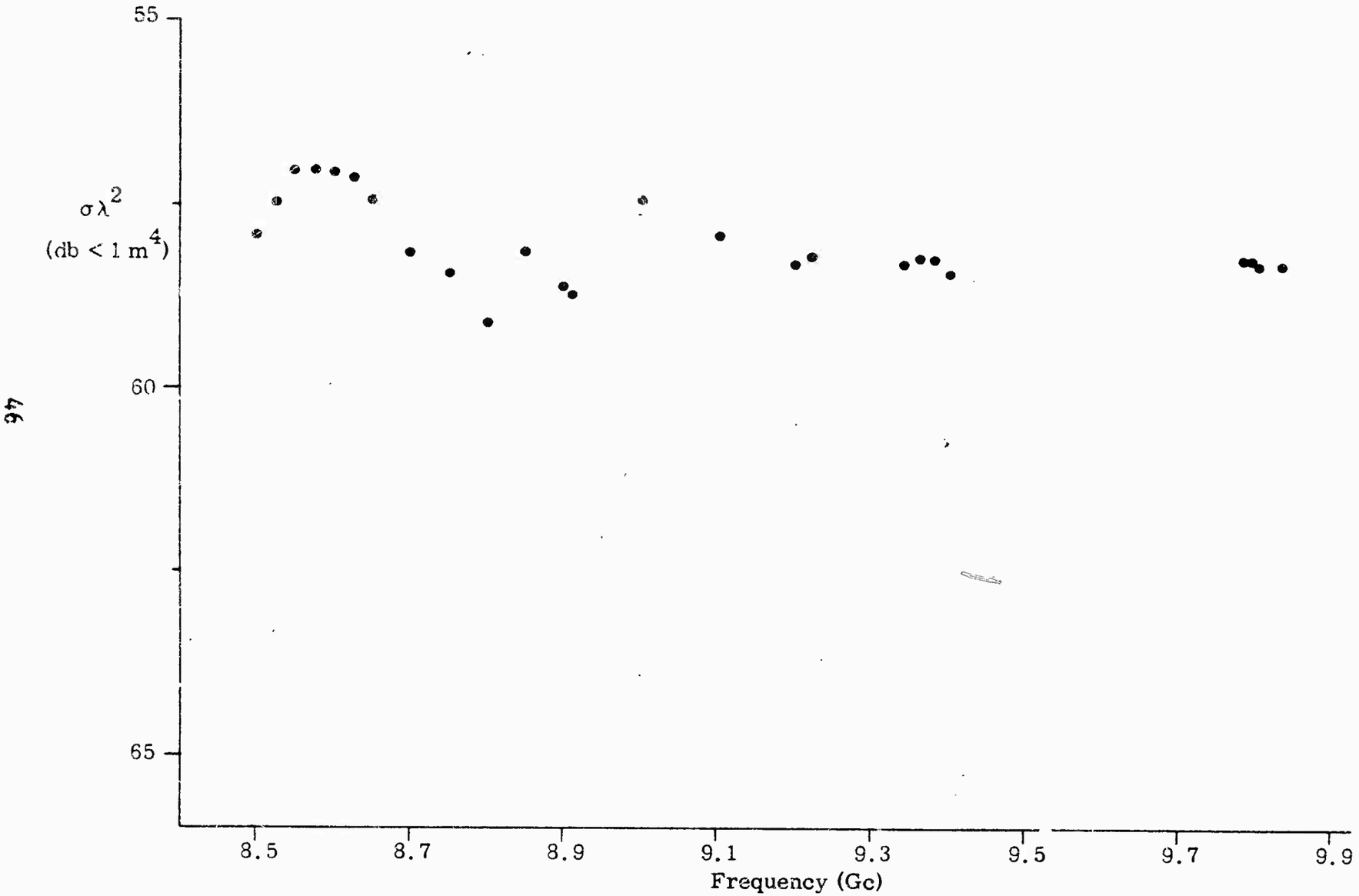

Fig. 2-7 SCATTERING BEHAVIOR OF BLOCK K

averaging the cross sections for each sample. The average values listed in Table 2-7 increase more or less proportionally to ℓ, and when fitted to the formula

$$\sigma\lambda^2 = c_1 + c_2\ell \qquad (28)$$

by the method of least squares, the best fit corresponds to

$$c_1 = 1.184 \times 10^{-6} m^4$$
$$c_2 = 5.929 \times 10^{-7} m^3$$

with ℓ measured in meters. The second term in (28) is not inappropriate to a travelling wave contribution and certainly must be associated with a rear end return: although a volume contribution would be an alternative explanation (since c_2 is proportional to V), the resulting magnitude is three orders greater than the expected one. The first term in (28) is therefore attributable to the front face. The implied value of k'/k_o is 1.0160, which is close to that obtained by identifying the <u>smaller</u> of the coefficients A (i.e., A_2) in Table 2-6 with a front face reflection.

Table 2-7 AVERAGE VALUES FOR SHAPE b BLOCKS

Block	Average $\sigma\lambda^2 x 10^3$	No. of Readings	St. Dev. x 10^3
H	1.612	10	0.061
K	1.580	26	0.207
M	1.520	16	0.158
O	1.480	13	0.124
Q	1.474	12	0.120
S	1.364	25	0.162

When the front face of the blocks was also slanted the back scattering cross section decreased considerably, and returns as low as $10^{-8} m^2$ were now common. Of the three samples examined, the first (block J) showed a completely anomalous behavior with the cross section increasing rapidly as the frequency was raised from 9.58 to 9.64 gigacycles (the highest frequency used). This was believed due to the poor edge condition which had required the abandoning of block I, and the data will therefore be ignored. The measured values for the remaining blocks of shape c, namely, N and R, are presented in Figure 2-8. There is some slight indication of an oscillation with a period of about 0.4 gigacycle which may be due to surface wave effects but which could also be

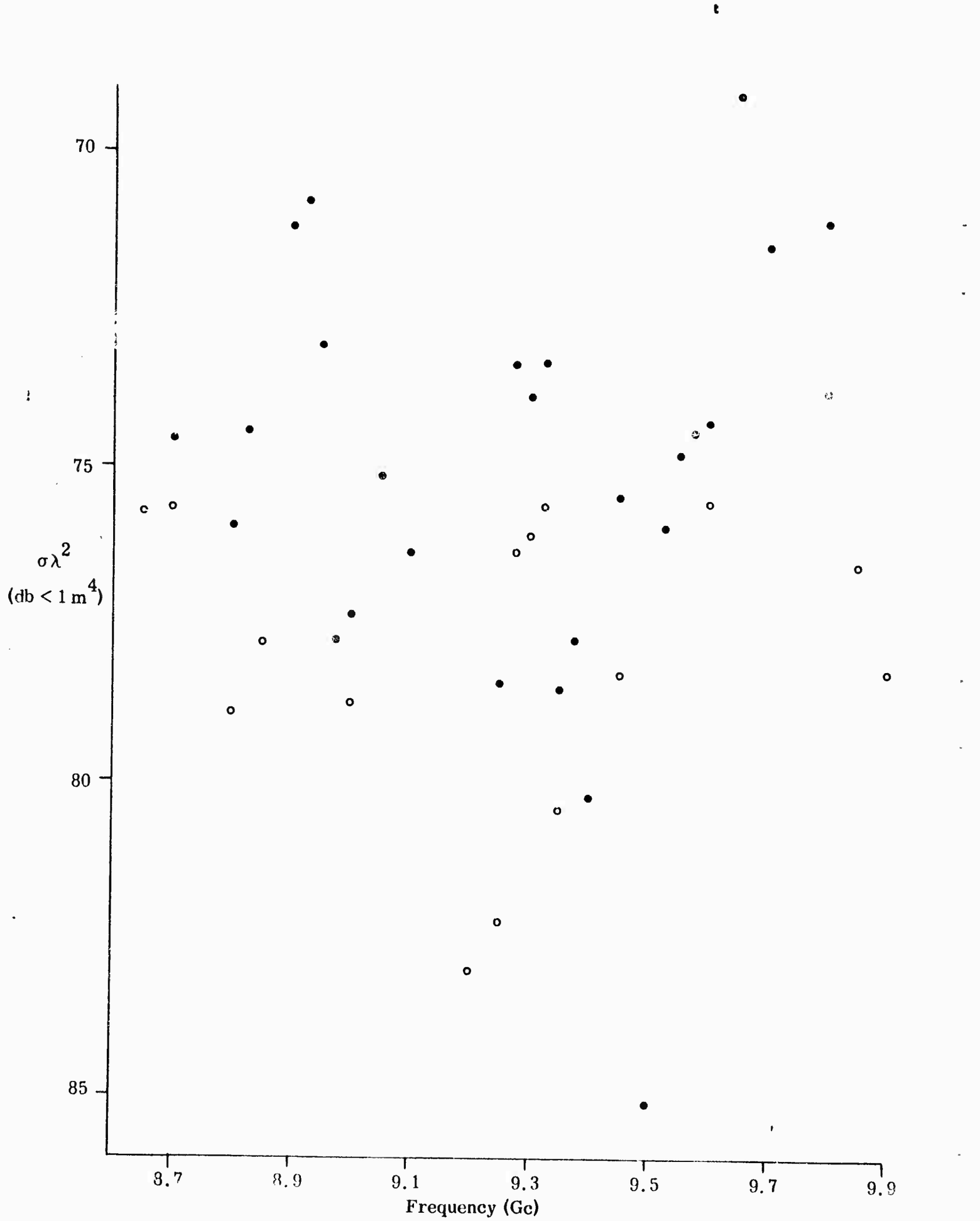

Fig. 2-8 SCATTERING BEHAVIOR OF BLOCKS N (•••) AND R (ooo)

a consequence of the experimental errors which are liable in measurements of cross sections as low as this. Certainly the source(s) of the return cannot be identified with certainty and though it was originally hoped that the incoherent contribution would be dominant, it is apparent that this is not true for blocks of the shape used here.

Scattering from Ogives

In the early stages of the Contract, samples of six kinds of foams which are representative of those presently available were acquired. The intention was to use these to estimate the variation of scattering properties as a function of the material characteristics. If the study of the shaped blocks had been successful in isolating the volume or incoherent scattering, similar measurements would have been made for each of these samples. When it was found that even with both front and rear faces of the blocks slanted the volume contribution was still not dominant, a new approach was adopted.

At that time the study of the near field characteristics of Styrofoam cylinders (see subsection on Surface Wave Effects Near a Styrofoam Cylinder) had not yet been performed, and the interfering signals which masked the volume effects for the shape c blocks were attributed to the failure of the slanting to reduce the specular contributions to sufficiently low level. In theory at least, however, an ogive (arc of a circle rotated about its chord) at end-on incidence would have no specular return and the tip contributions could be made negligible by choosing a small enough apex angle. Moreover, the elementary theory of travelling waves leads to an on-axis null, and in principle, therefore, the only nose-on contributor should be the volume return. If the six ogives were of the same size, the effect of volume per se should disappear from the comparison, and likewise the wavelength dependence would be of no consequence if the measurements were confined to a narrow band.

To this end, ogives about 18-3/4 inches long and 3-5/8 inches in diameter were fashioned from each of the six kinds of foam. Based on the measured weights and densities, the volumes were between 100 and 107 cubic inches. To minimize the return from the support, the ogives were suspended with fine cotton threads, and their nose-on back scattering cross sections measured at X-band from 8.5 to 9.9 gigacycles at intervals of 0.1 gigacycle. To decrease the room background the range from the transmitter to the midpoints of the ogives was held constant at 20-1/2 inches. This is uncomfortably close, but the effect is

not too serious inasmuch as the range was the same for each ogive. Cross sections can therefore be compared, although they cannot be regarded a priori as accurate in the absolute sense. Polarization was horizontal (because of the vertical threads) and calibration was with respect to a 0.94 inch diameter sphere.

The measured data for two of the materials - Pelaspan and Thurane - is presented in Figure 2-9, and the corresponding data for the other four materials (Tyrilfoam, Styrofoam FB, Styrofoam DB and Styrofoam FR) can be found in Memorandum 5849-513-M.

On the basis that the volume return was the dominant contribution, the 15 cross sections per ogive, one for each frequency used, were reduced to square meter values and then averaged. These numbers were now expressed in db and are listed in Table 2-8. Also shown is cell size information obtained from a study of the foam structure under a stereomicroscope. Magnifications of from 30 to 60 diameters were used, and the cells were measured by comparison with several copper wire probes whose diameters ranged from 0.006 to 0.028 inches. Two of the foams were multicellular; they had a cell-within-a-cell structure, and one of these (Tyrilfoam) even had two distinct sizes of subcells.

Table 2-8 DENSITY, CELL SIZE, AND CROSS SECTION OF THE SIX FOAMS

Material	Density (pcf)	Structure	Cell Size (in.)	σ, dbm^2
Tyrilfoam	0.70	Multi-cellular	.461	-58.7
Pelaspan	1.15	Multi-cellular	.125	-70.2
Styrofoam FB	1.76	Simple	.025	-68.9
Styrofoam DB	1.80	Simple	.057	-69.6
Styrofoam FR	1.97	Simple	.011	-72.3
Thurane	2.04	Simple	.019	-72.4

According to the theory in the subsection on Scattering by Cellular Materials, the incoherent cross section should vary as the fourth power of the average cell size. The values in the above table do not confirm this behavior, and though there is a general tendency for the returns to decrease with decreasing cell size, the variation is only qualitative. It would therefore seem that either the theory is in error or the return is still being masked by a coherent contribution. Of the two alternatives, the latter is the more probable. The data in Figure 2-9 does not have the noisy appearance expected of an incoherent signal and with some of the materials (particularly Tyrilfoam) the cross

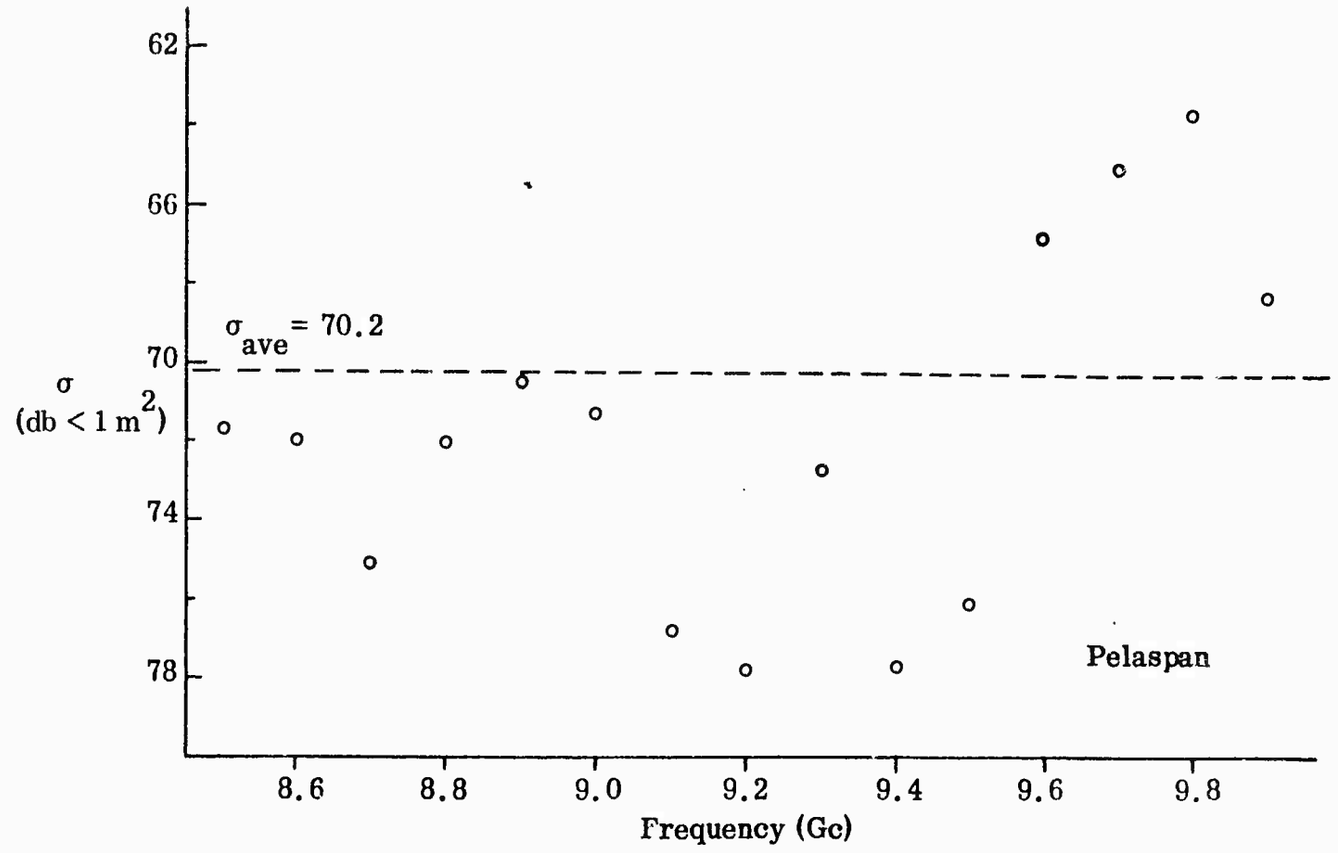

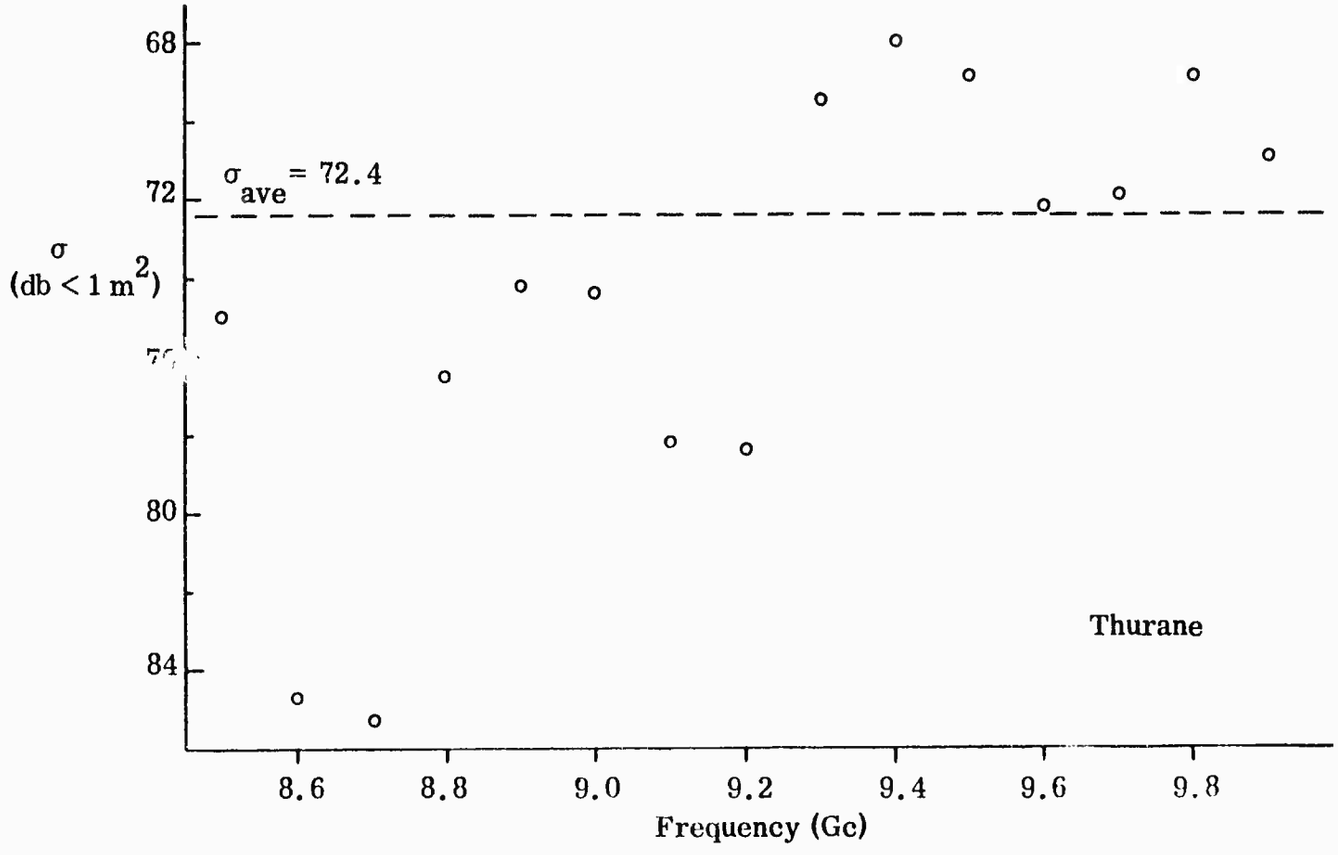

Fig. 2-9 CROSS SECTIONS OF PELASPAN AND THURANE OGIVES

sections displayed a marked and regular cyclical variation with frequency whose period is consistent with a traveling wave effect. The experiment described in the subsection on Surface Wave Effects Near A Styrofoam Cylinder clearly revealed the sizable surface wave which can be supported by materials such as these, and it is believed that part of the return is attributable to this wave notwithstanding the fact that the elementary theory of the traveling wave antenna would predict an on-axis null. Accordingly, the cross section values in Table 2-8 are in all probability not truly representative of the incoherent return alone. They do, however, provide upper bounds on the incoherent contribution, varying from 8 x $10^{-4}m^2$ per m^3 for Tyrilfoam down to 3 x $10^{-4}m^2$ per m^3 for Thurane, and on any interpretation of the sources of the data the fact that they were obtained from like samples of different materials enables us to use the values as a basis for selecting the most promising material for target supports.

From the data in Table 2-8 alone, Tyrilfoam might appear the worst material and Styrofoam FR and Thurane the equal best, but this does not take into account the differences in their load bearing properties. In the subsection on Material Considerations a formula was obtained for the peak (coherent) surface return from a cylindrical column of length ℓ at broadside whose diameter is the minimum to support a loading P. The peak is proportional to $\rho^2/E^{1/4}$, where ρ is the foam density and E is the Young's modulus, which factor should be as small as possible to achieve a minimum coherent contribution.

Unfortunately, the selection of materials on this basis is not quite so simple since there appears to be no standardization of the physical strength characteristics presented by foam manufacturers. The compressive strength is sometimes rated at 10 per cent deflection, at other times 5 per cent, and still other times at the yield point. For some materials the stress-strain curve is nearly linear until the foam suddenly yields, while others seem to be in a state of constant yield (plastic deformation) from almost the instant of loading. In view of this inconsistency in manufacturers' data, it was decided to obtain our own stress-strain curves for the six materials using machines in the Engineering Mechanics Laboratory of The University of Michigan.

Since a buckling column fails by rupture of the cells on the convex side and, perhaps, by cell compression on the concave side, the Young's modulus required may be that determined by a tensile load rather than a compressive one. In general, however, the tensile strength exceeds the compressive one by a factor two or more, so that column failure may be a complicated process, and the stress-strain data obtained for the six materials should therefore by interpreted in a relative sense.

A comparison of the six foams is given in Table 2-9. The elastic modulus E was found from the initial (linear) portion of the curve for deflections under 1 per cent and since the variation of ρ^2 tends to outweigh that of $E^{-1/4}$, a Tyrilfoam column would produce the smallest coherent scattering and Thurane the largest. To illustrate the load bearing properties, the minimum column diameter for a 5 foot column to support a 1000 pound target has been calculated and, with a safety factor of 2 added, the diameters (in inches) are shown in Table 2-9. The values of the peak coherent cross sections then follow immediately from the formulae in the subsection on Material Considerations.

Table 2-9 FURTHER COMPARISON OF THE SIX MATERIALS

Material	ρ, pcf	E, psi	$\rho^2/E^{1/4}$	d_{min}, in.	σ, dbm^2
Tyrilfoam	0.70	207	.129	38.9	-17.9
Pelaspan	1.15	733	.256	28.6	-14.9
Styrofoam FB	1.76	2061	.460	21.9	-12.2
Styrofoam DB	1.80	1692	.505	23.0	-12.0
Styrofoam FR	1.97	3000	.524	19.9	-11.8
Thurane	2.04	710	.806	28.6	- 9.9

Thus, from the standpoint of the coherent returns, Tyrilfoam appears the best material for target support columns, but the data in Table 2-8 shows that this material gives a "volume" return at least an order of magnitude greater than the other foams. Presumably this is due to the large size of its cells, which are of order $\lambda/2$ at X-band, and it could be expected that the return from a Tyrilfoam column would vary with azimuth. The next choice based on Table 2-9 is Pelaspan[+], which is nearly twice as good as its nearest competitor, and faced with the selection of a material, we would advocate this.

[+]It is not intended that Pelaspan be construed as better than other expandable bead foams, such as those produced by Emerson and Cuming, Inc. Probably all foams of this kind, embracing several trade names, would perform equally well.

SURFACE WAVE EFFECTS NEAR A STYROFOAM CYLINDER

At the request of General Dynamics/Fort Worth a study was undertaken to explain an unusual scattering effect observed when a sphere was mounted on a long Styrofoam cradle. The nature of this effect can be seen from Figure 2-10. The cradle was here a circular cylinder 6 inches in diameter and 43-1/2 inches in length, with ends at right angles to the axis, and was milled from a Dow Chemical Company buoyancy billet. To support a sphere in a stable manner, a saucer shaped depression was cut into the surface to a maximum depth of 1 inch. The diameter (at the surface) was approximately 3-1/2 inches and the lip was some 3 inches from one end of the cylinder. A metal sphere of diameter 3.935 inches was now placed in the hollow and the back scattering cross section measured as a function of the rotation angle θ of the entire assembly in the horizontal plane, where $\theta = 180$ degrees is the aspect at which the sphere was furthest from the transmitter. The results for horizontal polarization at 9.3 gigacycles are shown in Figure 2-10.

Apart from aspects within about 20 degrees of 180 degrees, the cross section is almost independent of aspect and differs by less than 1 db from that appropriate to the sphere alone. As θ increases beyond 160 degrees, however, the net return begins to oscillate with a period of approximately 7 degrees about a level which falls rapidly to a minimum some 16 db below the free space return from the sphere. This behavior appears to be independent of polarization and is similar to that previously found by General Dynamics/Fort Worth (Wolanski, 1963) using a larger sphere and a cradle of somewhat more complicated shape. On the other hand, when the sphere was raised 7 inches above the cradle, no reduction in the cross section near to $\theta = 180$ degrees was found.

It is obvious that these effects are of major importance in the design of target support pedestals, and an understanding of their orgin is therefore essential. Several possible mechanisms were examined and in the light of this study it was concluded that only an amplitude and/or phase disturbance, confined to the immediate vicinity of the surface and increasing with the length of Styrofoam over which the field has travelled could suffice to explain the observations. Direct measurement of the amplitude and phase of the field near to a Styrofoam cylinder have since confirmed the existence of a disturbance, and we shall here detail the results.

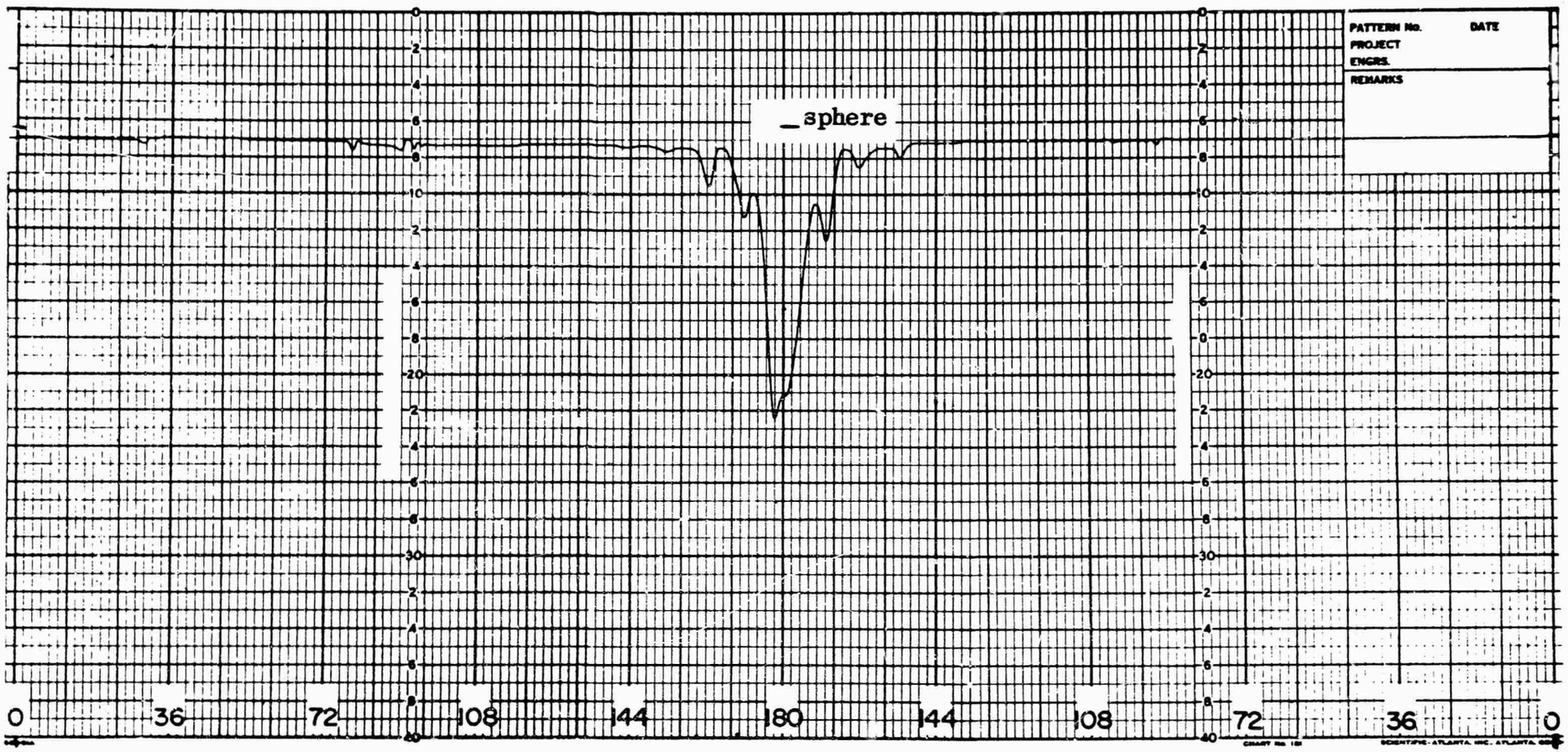

Fig. 2-10 CROSS SECTION OF STYROFOAM CYLINDER AND 3.935 IN. DIAMETER SPHERE 9.3 Gc, HORIZONTAL POLARIZATION

Method

The measurements discussed here were carried out with the Styrofoam cylinder described above. For the early ones the frequency was 9.2 gigacycles, and these were made before the saucer-shaped depression was cut into the surface. Subsequently, however, the frequency was increased to 9.3 gigacycles. This was used for all the work on the cut cylinder, and to minimize the effect of the depression on the near field measurements, the cylinder was placed on the support pedestal with the hollow on the side opposite to that being probed. The probe traverses were in a horizontal plane at several stations along the side of the cylinder. The illumination was at end-on incidence from a horn situated 15 feet (approximately) from the mid-point of the cylinder using vertical polarization.

A sketch showing a plan view of the experimental components is given in Figure 2-11. A receiving dipole, 1.51 cm long, was attached to a rigid, horizontal coaxial line 1/8 inch in diameter and 22 inches in length. The output was fed to one of the symmetrical arms of a hybrid tee through a section of flexible RG-9/U coaxial cable, and based on a few trial positions of the cable, it is estimated that flexing introduced no more than 5 degrees of phase shift.

The illuminating antenna was fed by a suitably-padded cavity-stabilized oscillator. Some of the energy was sampled, and passed through attenuators and a phase shifter to the other symmetrical arm of the hybrid tee, after which the sum of this signal and the one from the dipole was detected and fed to a superheterodyne receiver. The amplitude of the received signal at its highest was 50 to 60 db below that delivered to the illuminating antenna. The amplitude and phase were obtained by adjusting the attenuators and phase shifter in the symmetrical arm of the tee for a null at the receiver, and could be read directly from these devices.

All the hardware was shielded by a 2-inch thick barrier of hairflex. The operator of the equipment was likewise shielded, as was the wooden framework which supported the coaxial line feed from the dipole.

Procedure

In the initial experiment the probe was traversed in a radial direction at three selected stations along the length of the cylinder, corresponding roughly to the two ends and the mid-point. The actual distances d of these stations from the front end were

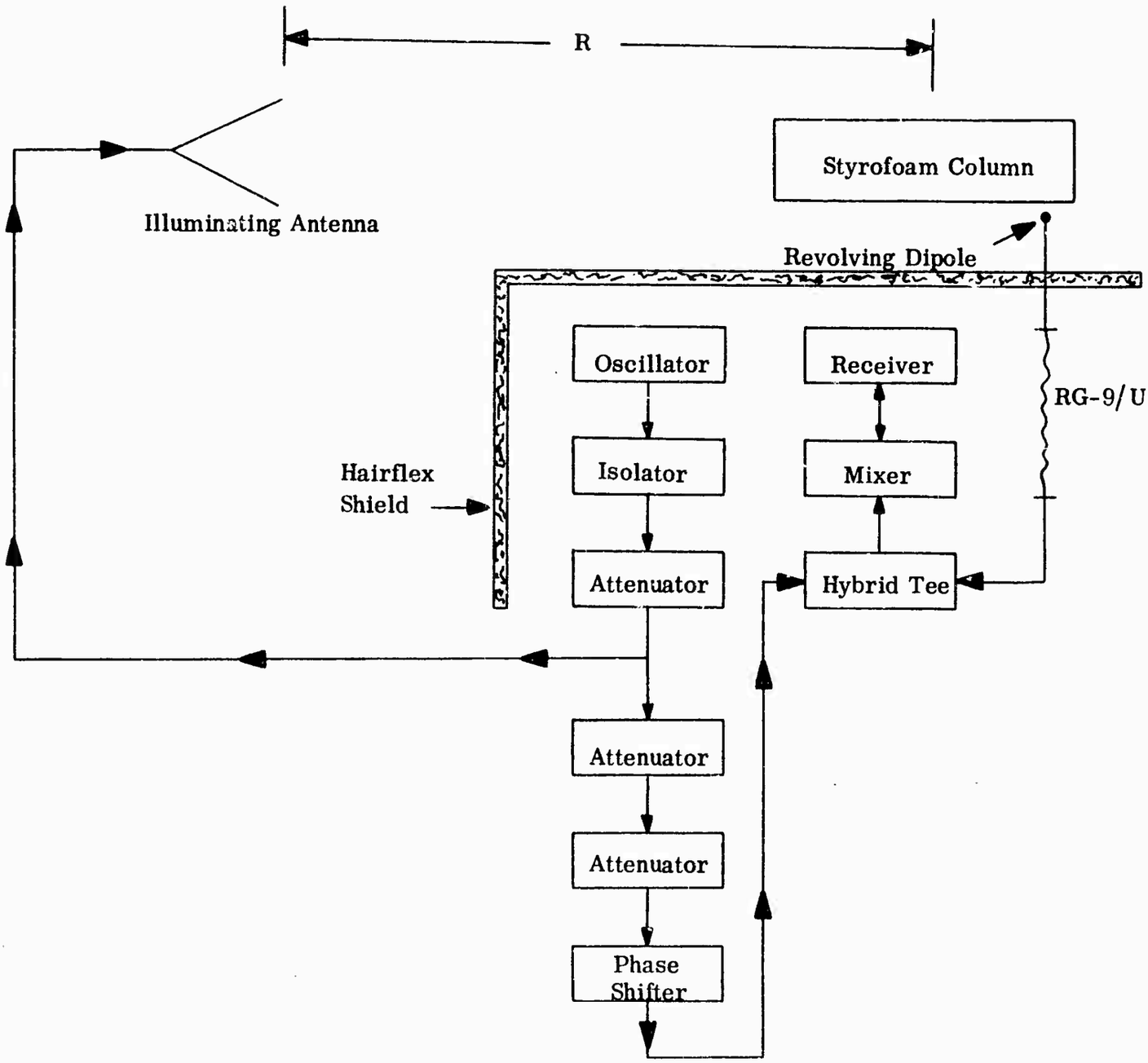

Fig. 2-11 EXPERIMENTAL SYSTEM

2, 22 and 42 inches, and at each location the field was measured at a variety of different radii starting at 1/8 inch above the surface (r = 3-1/8 inch, where r is the distance from the axis) and continuing out to r = 14-1/8 or 15-1/8 inch.

To provide some basis for comparison, most of the measurements were repeated without the cylinder in place, but since the main purpose of the work at this stage was to confirm the capability of the probe technique, no attempt was made to achieve common amplitude and phase calibration with and without the cylinder present. It was not possible, therefore, to deduce the amplitude and phase of the scattered field from a comparison of the total and incident field data without additional information, and in this connection we remark that a change of station of only 0.6 inch between the two cases would change the phase by 180 degrees. Nevertheless, the marked differences in the shape of the curves after the cylinder was introduced were sufficient to show the existence of a relatively large perturbation, and as this appeared to increase with distance from the front end of the cylinder additional measurements were made at two stations 13-1/4 and 21 inches beyond the cylinder. These will be discussed later.

At the conclusion of the above work, a depression was cut into the cylinder to support a metal sphere for the back scattering experiment, but the interesting and challenging nature of the near-field results demanded a renewal of this study. The frequency was now increased to 9.3 gigacycles, and to ensure accurate and uniform calibration, the following procedure was adopted. At each station, measurements were carried out with the cylinder present starting 1/8 inch above the surface and going out to the furthest desired distance. The cylinder was then removed with the probe left untouched, after which the incident field was sampled as the probe retraced its original path. To determine the extent to which such data was repeatable, the measurements at one station were reinforced with incident field values taken as the probe was moved out again to its maximum distance. The average amplitude discrepancy was a mere 0.04 db, and though the phase differences were somewhat larger, averaging 3 degrees, this was mainly due to a single 15 degree change at one point.

Results

Incident and total field data at the middle station for which d = 22 inches is presented in Figures 2-12 and 2-13 respectively, and the analogous results for a far station (d = 41-1/2 inches) are given in Figures 2-14 and 2-15. Since the amplitude and phase

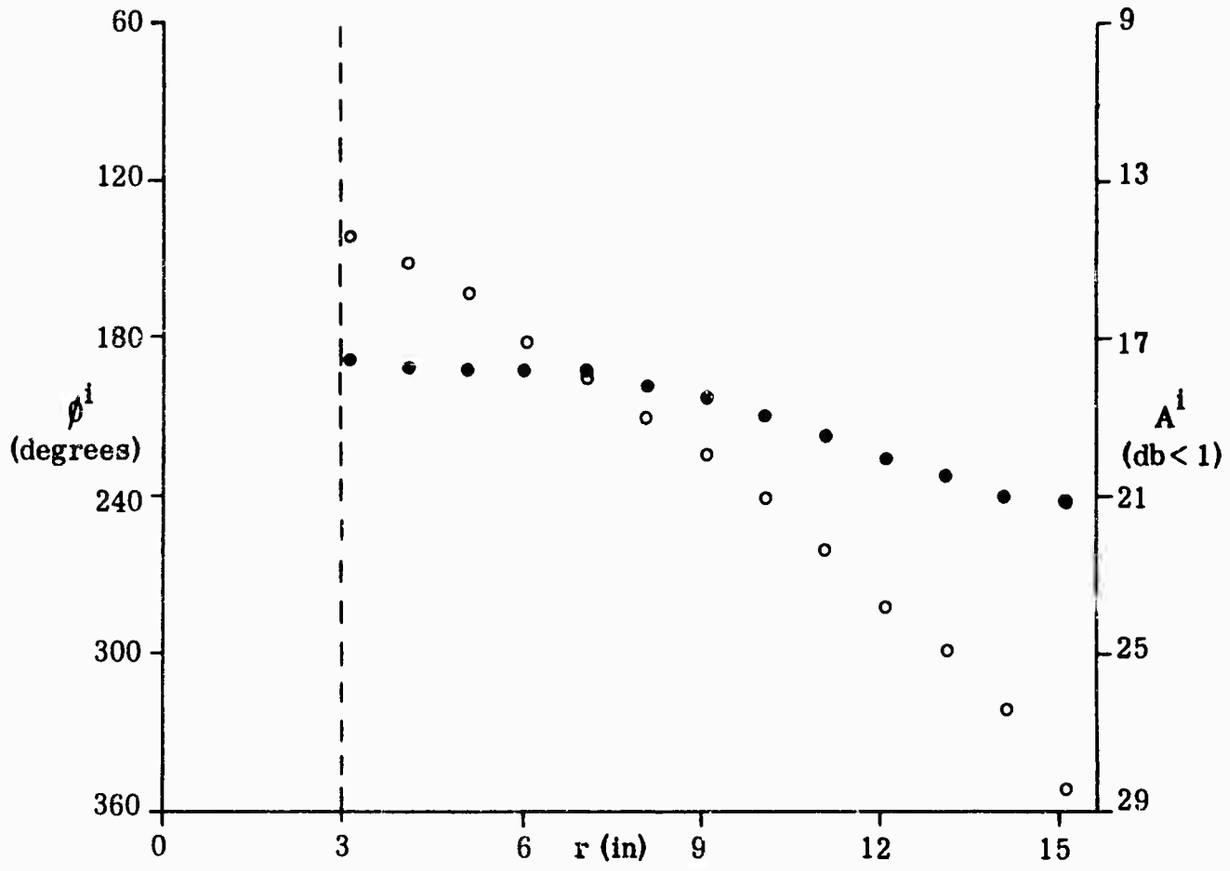

Fig. 2-12 AMPLITUDE (•) AND PHASE (o) OF INCIDENT FIELD FOR d = 22 IN.

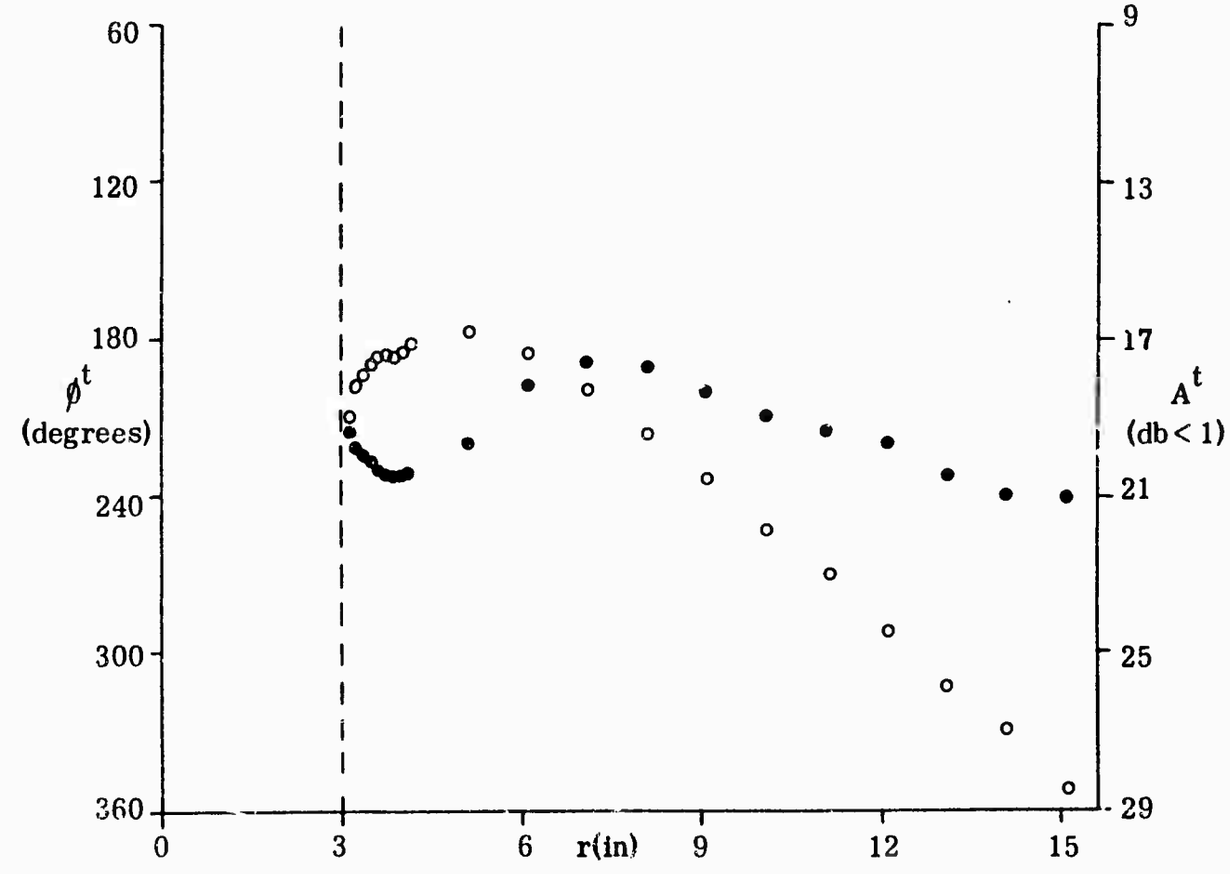

Fig. 2-13 AMPLITUDE (•) AND PHASE (o) OF TOTAL FIELD FOR d = 22 IN.

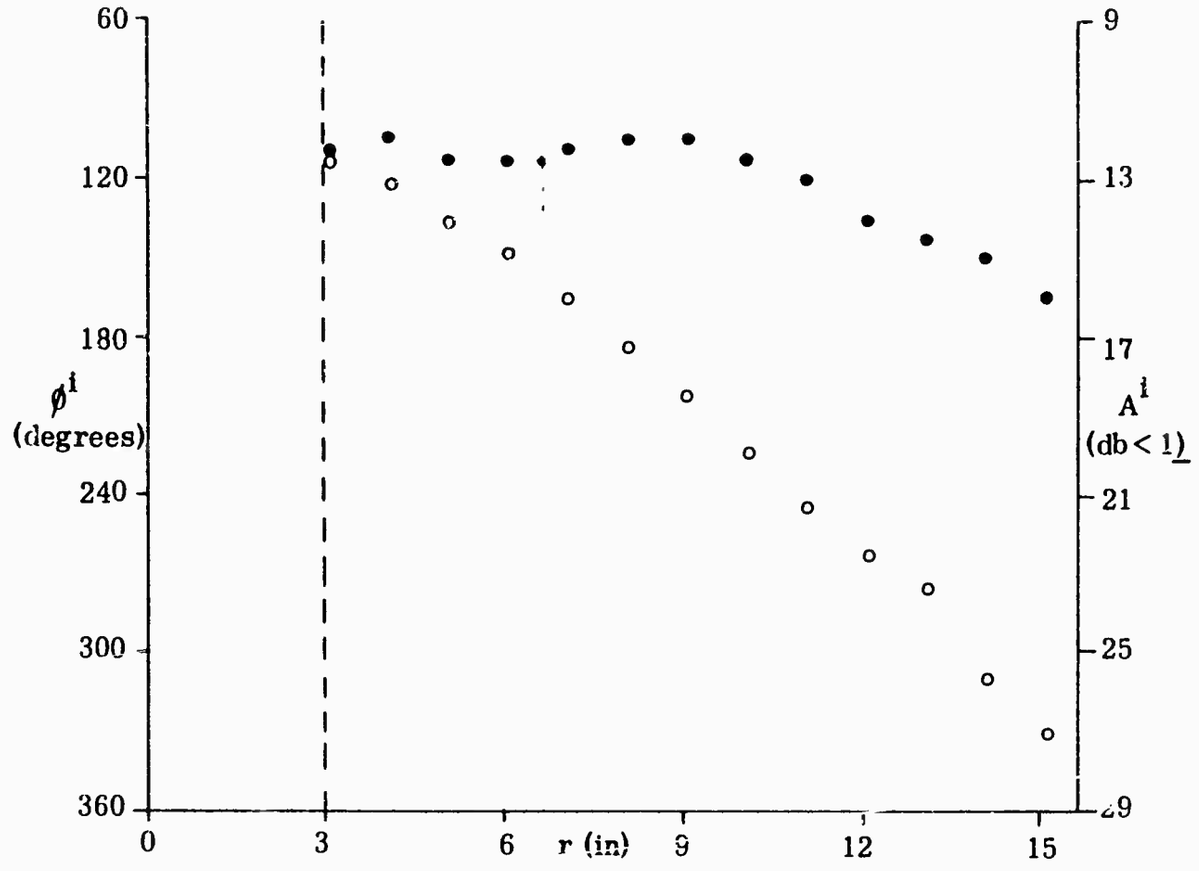

Fig. 2-14 AMPLITUDE (•) AND PHASE (o) OF INCIDENT FIELD FOR d = 41-1/2 IN.

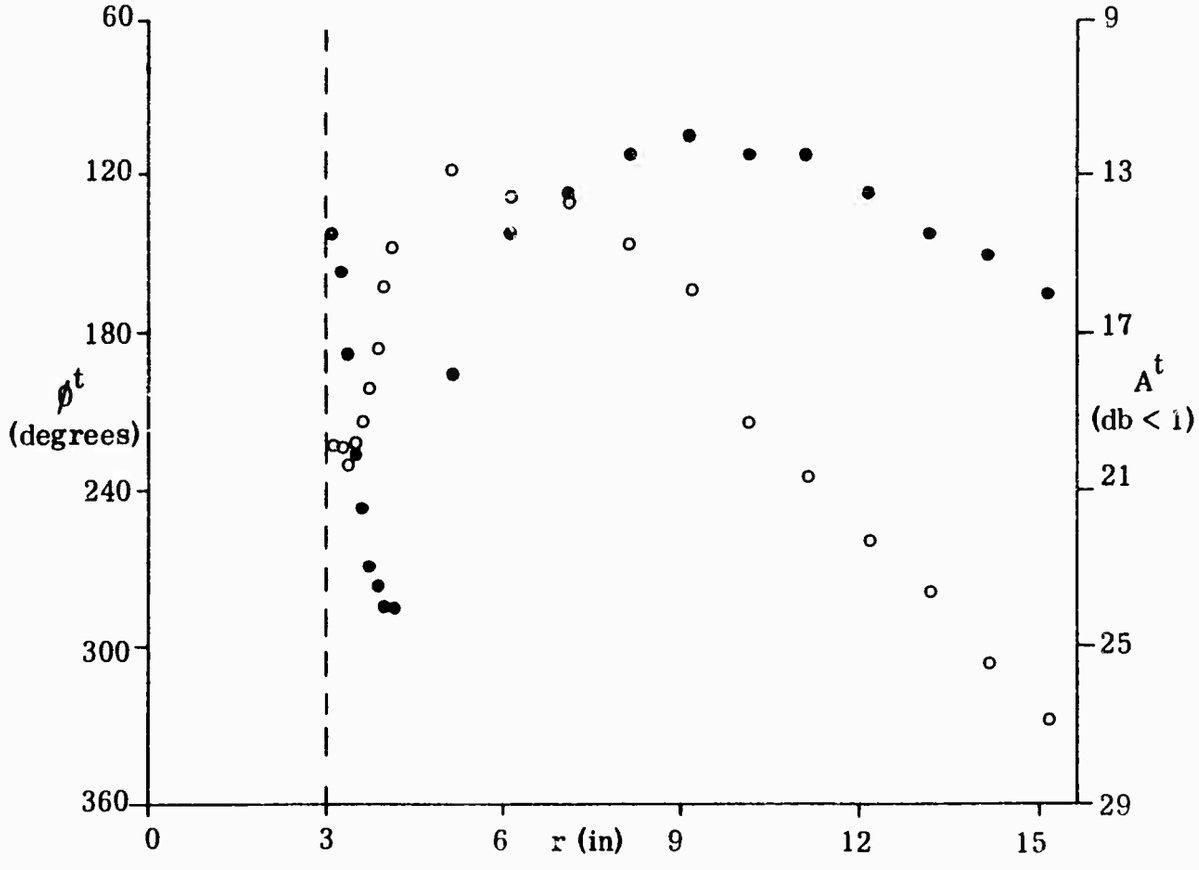

Fig. 2-15 AMPLITUDE (•) AND PHASE (o) OF TOTAL FIELD FOR d = 41-1/2 IN.

scales are now the same for both fields, the graphs can be compared directly and, if required, the scattered field deduced.

Taking first the incident field measurements at the two stations, the general trends of the amplitude and phase curves are reasonably consistent with a planar intersection of a spherical wave pattern originating some 15 to 17 feet away. What small variations there are, are almost certainly due to the support pedestal and/or room reflections, and we observe that the amplitude seems to vary a little more at the far station (behind the pedestal) than it does at the middle station where the pedestal is located.

The effect of introducing the cylinder can be seen by comparing Figures 2-12 and 2-13, 2-14 and 2-15. For d = 22 inches the regular decrease in phase as the probe approaches the surface is arrested some 2 inches away and thereafter the phase increases rapidly. This turnover is accompanied by a dip in the amplitude curve which is apparent even out to a distance of 3 inches from the surface, but is centered about 1 to 1-1/2 inches away. Such perturbations are even more apparent at the far station. The phase of the total field changes by over 100 degrees within the first two inches from the surface and there is some evidence of a levelling of the curve as the probe makes its nearest approach. We remark in passing that later measurements of the field with a cylinder 57-1/4 inches long (probe station 50 inches from the front) have shown that the phase does indeed remain constant very close to the surface. The radial extent of this platform increases with d, confining the phase swing to a smaller and smaller radial span.

Perhaps more striking is the amplitude behavior when d = 41-1/2 inches. The dip observed in Figure 2-13 is accentuated in Figure 2-15. Its depth has increased to about 12 db and since the width is less, the position of the minimum amplitude can be located at almost precisely 1 inch above the surface. At distances less than this the amplitude increases, and has almost achieved the incident field value by the time the probe gets to 1/8 inch from the surface.

A comparison of the incident and total field data also shows that as r increases beyond the position of the minimum the two fields approach one another. At all the stations examined the differences were negligible for r greater than (about) 10 inches and consequently, whatever the true origin of the scattered field, its influence is restricted to the first few wavelengths from the surface. This is in accordance with the conclusion reached from

the experiment conducted by General Dynamics/Fort Worth in which the sphere was raised above the cradle, and suggests that the scattered field is some form of surface wave. It also enabled us to resurrect the earlier measurements of the near field by introducing a calibration based on the equality of the incident and total fields for $r > 10$ inches. Such calibration confirmed that the scattered field at the forward station (d = 2 inches) was insignificant, a fact which was otherwise obvious from the complete identity of the curves with and without the cylinder in place. It is therefore unnecessary to present the data.

At stations beyond the cylinder, however, the results are more interesting, and for d = 56-3/4 inches the incident and total field data is given in Figures 2-16 and 2-17, with the analogous results for d = 64-1/2 inches in Figures 2-18 and 2-19. Note that the frequency is here 9.2 gigacycles, and that the calibration has been based on the assumed equality of the fields for r = 11 and 12 inches. Bearing in mind that the measurements now go down to r = 0, the incident field values are similar to those found at stations along the cylinder. The total field, on the other hand, does show some differences. The phase decreases uniformly with r, changing rapidly for r between 6 and 4 inches, and tapering off as the probe enters into the shadow region. There is no longer the turnover characteristic of the measurements at d = 22 and 41-1/2 inches. The minima in the amplitude curves are deeper than before (about 15 db instead of 12) and occur at a somewhat greater radius, though the precise location is difficult to determine because of the radial separation of the probe positions. For r less than about 5 inches, the amplitude increases, rapidly at first but more slowly within the shadow, and achieves a value some 6 to 8 db greater than the incident field on the continuation of the axis. No important differences in behavior at d = 56-3/4 and 64-1/2 inches are apparent, and the most that can be detected from the total field data is a slight tendency for the radial distance of the minimum to increase with d.

Knowing the amplitude and phase of the incident and total fields, it is a trivial matter to deduce the scattered field. For the two stations along the length of the cylinder, the results normalized relative to the incident field values, are shown in Figures 2-20 and 2-21. The rapid and possibly exponential attenuation of the field in the radial direction is now obvious, and both the surface value and the rate of attenuation increase with d. For $r > 8$ inches the ratio of the incident and total field amplitudes is so close to unity that small errors in the measured data (primarily of phase) produce quite sizable effects on the scattered field values, and at least some of the behavior at r = 7

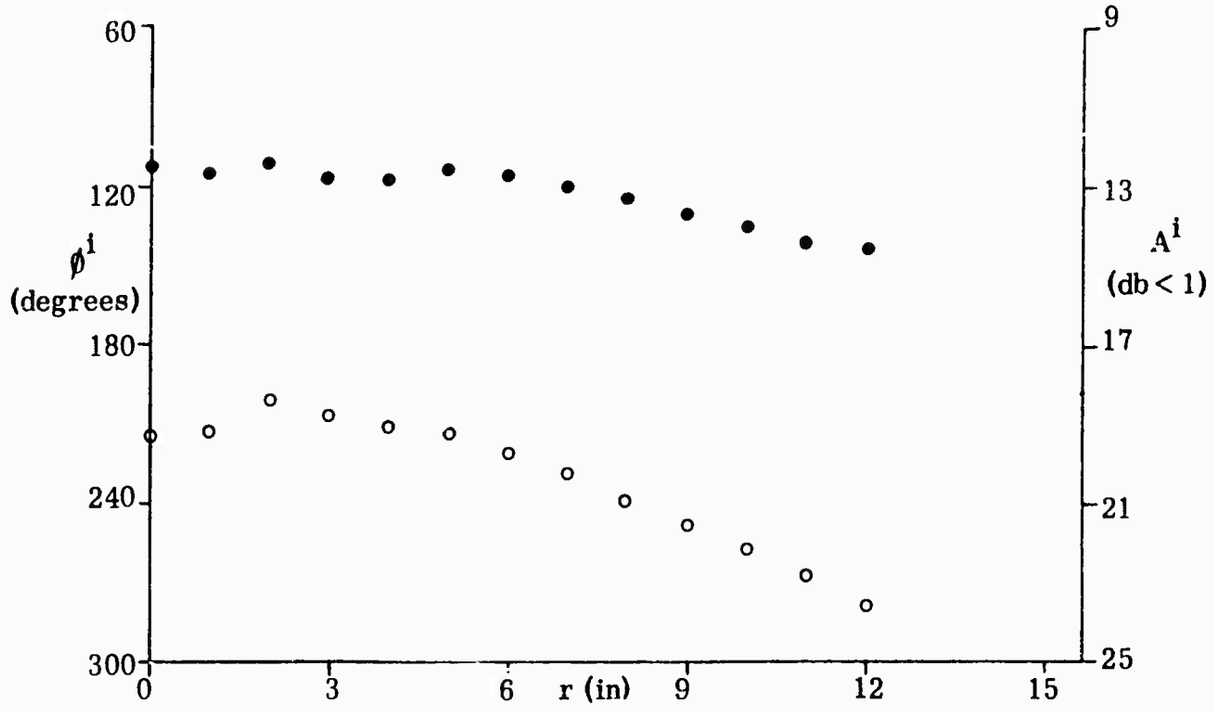

Fig. 2-16 AMPLITUDE (•) AND PHASE (o) OF INCIDENT FIELD FOR d = 56-3/4 IN.

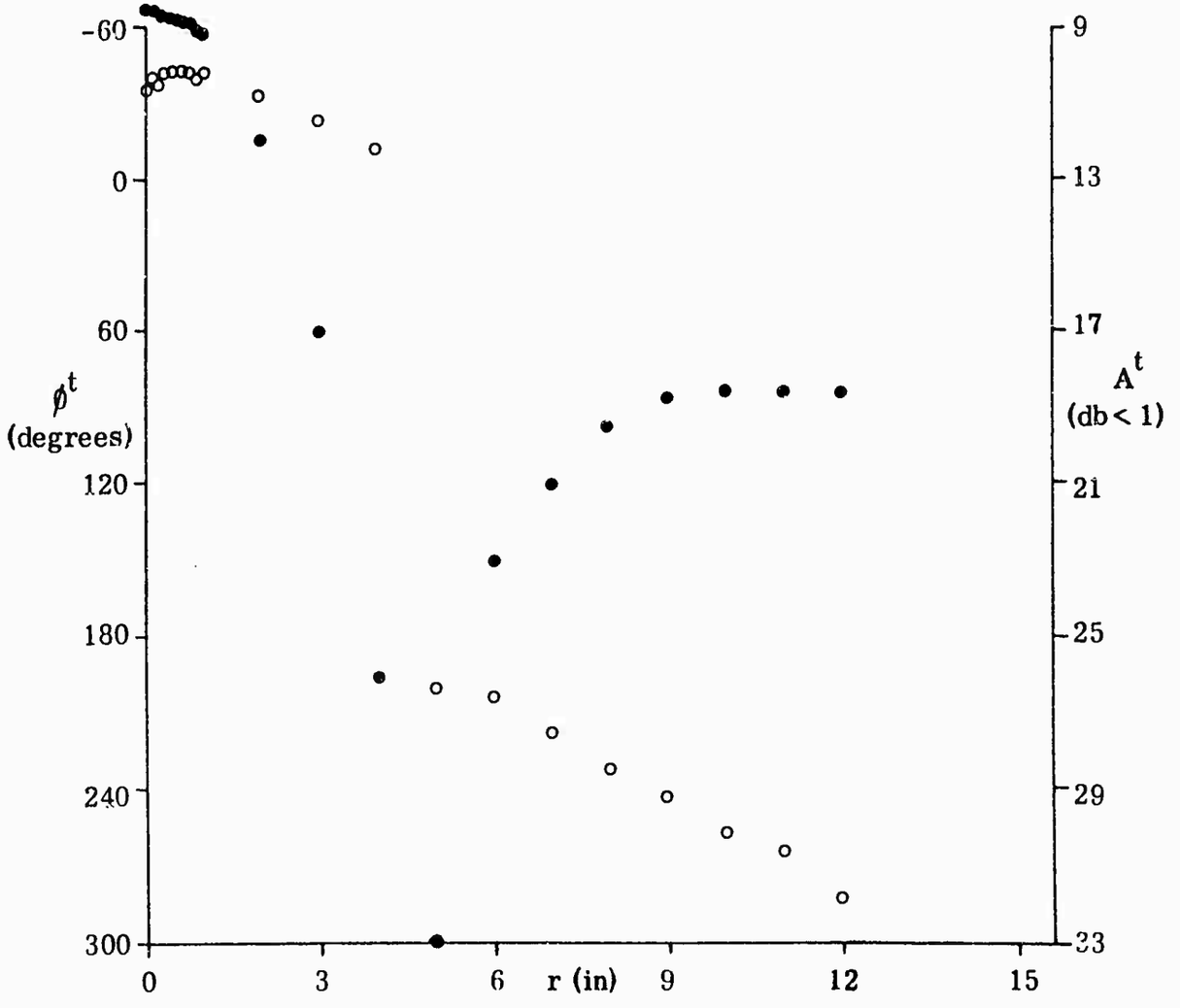

Fig. 2-17 AMPLITUDE (•) AND PHASE (o) OF TOTAL FIELD FOR d = 56-3/4 IN.

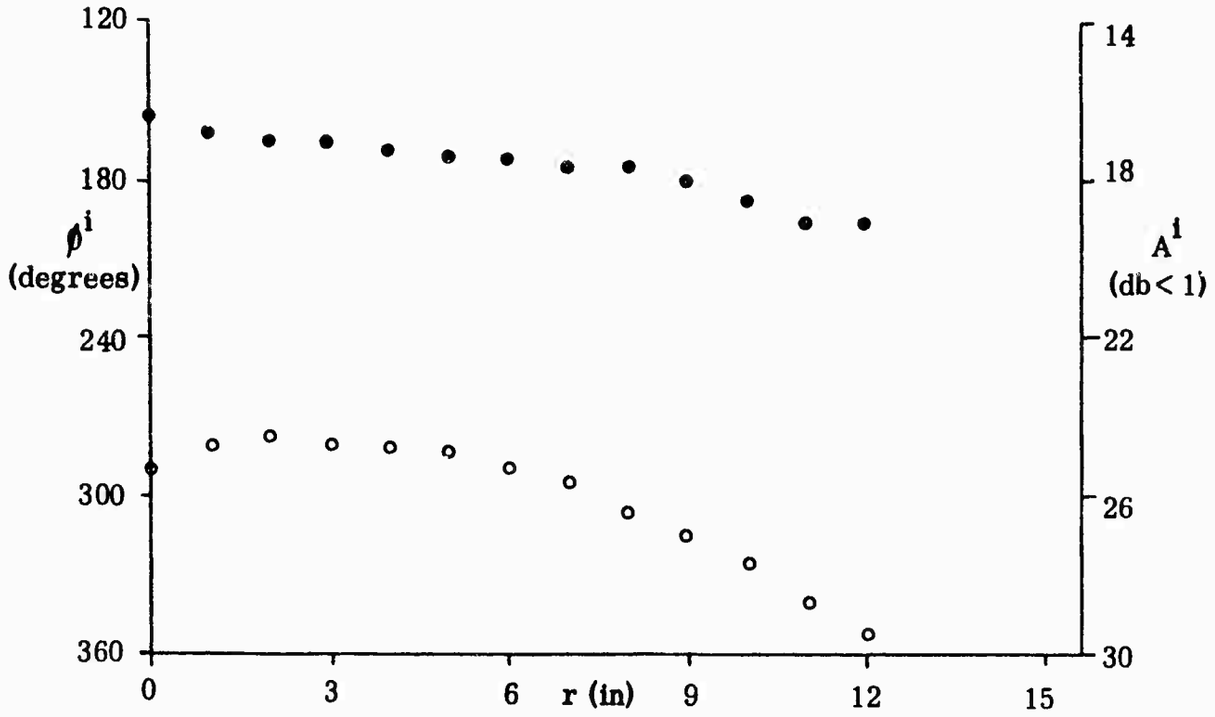

Fig. 2-18 AMPLITUDE (•) AND PHASE (o) OF INCIDENT FIELD FOR d = 64-1/2 IN.

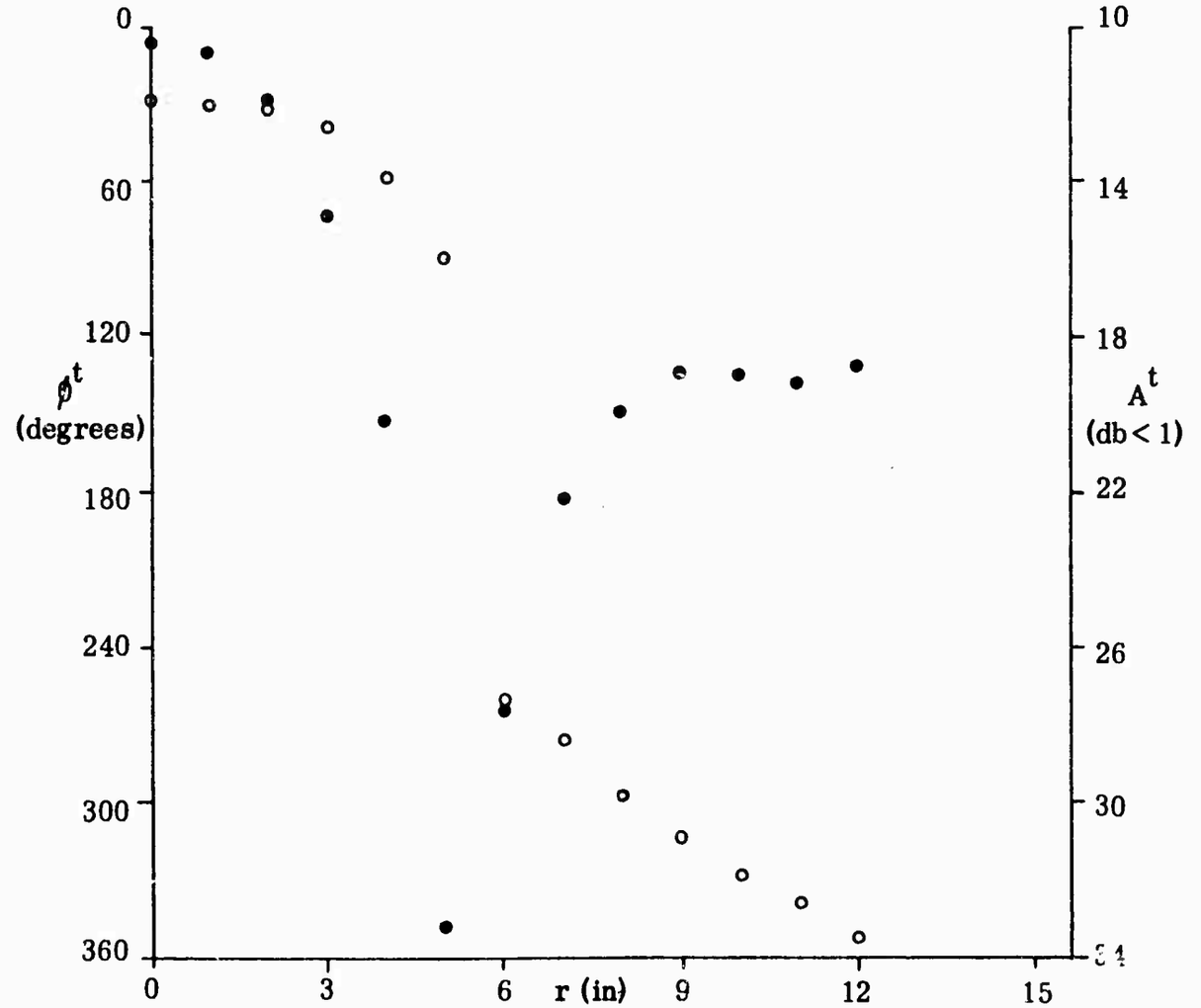

Fig. 2-19 AMPLITUDE (•) AND PHASE (o) OF TOTAL FIELD FOR d = 64-1/2 IN.

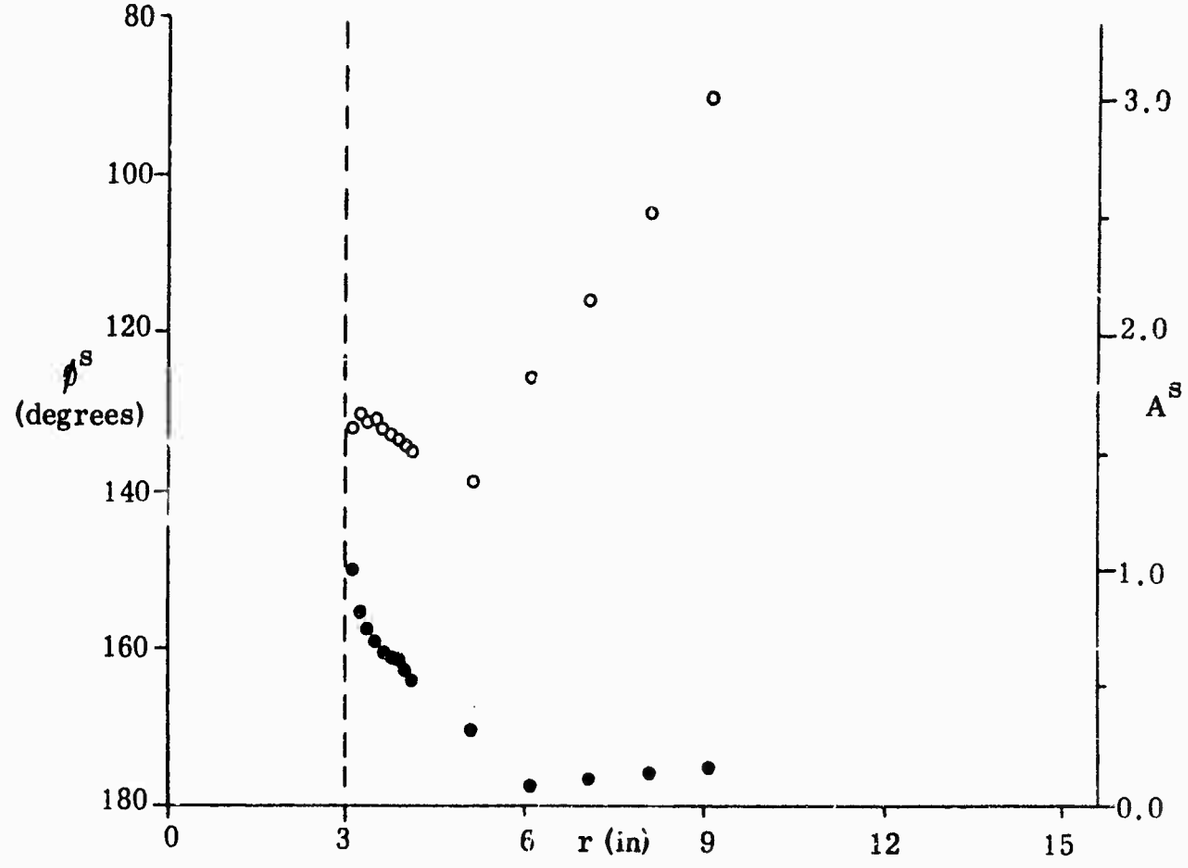

Fig. 2-20 RELATIVE AMPLITUDE (•) AND PHASE (∘) OF SCATTERED FIELD FOR d = 22 IN.

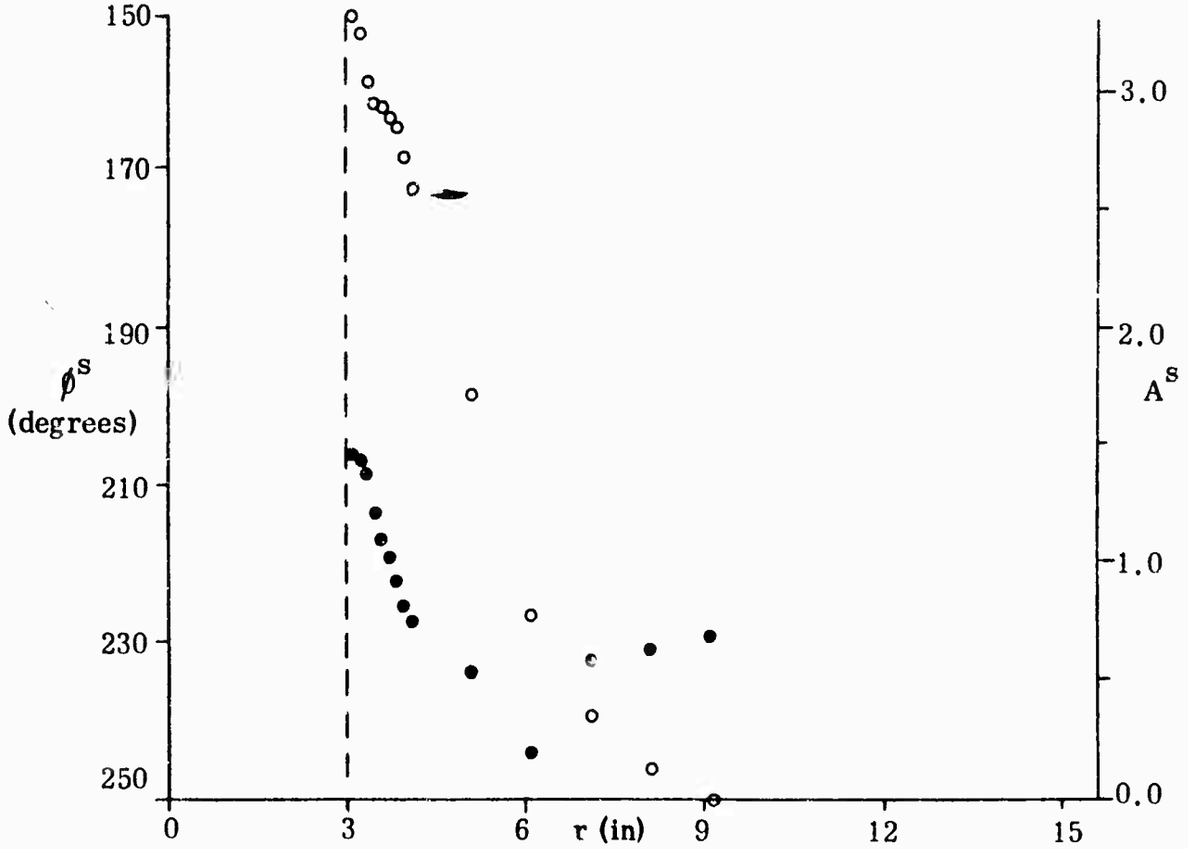

Fig. 2-21 RELATIVE AMPLITUDE (•) AND PHASE (∘) OF SCATTERED FIELD FOR d = 41-1/2 IN.

and 8 inches may also be attributable to this. Nevertheless, the startlingly different character of the phase curves at d = 22 and 41-1/2 inches is believed genuine. At the middle station, the phase remains constant for the first two inches, and then decreases slowly, whereas at the far station the phase increases almost uniformly out to the largest distance at which data is available. It may be pertinent that the difference in the phase velocities in Styrofoam and free space would create a phase lag of 115 degrees at the middle station and 218 degrees at the far one, and on this basis the results for d = 22 inches might be expected to resemble those for d = 52 inches rather than 41-1/2 inches. Measurements at d - 50 inches made with the longer cylinder have indeed shown that the scattered field phase is once again constant for the first inch or so, and then increases.

At the two stations beyond the cylinder the derived values for the scattered field are given in Figures 2-22 and 2-23. The results are quite similar. At the nearer station the amplitude decreases steadily from a (relative) value of 3.0 at r = 0 and is negligible for r > 10 inches. The phase, on the other hand, increases after an initial fall, but appears to decrease sharply beyond r = 9 inches. It is not known if this effect is real, although it does occur at the further station as well. The amplitudes here are fractionally less than for d = 56-3/4 inches, and show a slight increase as the probe moves away from r = 0. Outside the optical shadow of the cylinder both sets of curves are not unlike those of Figure 2-21 in general character, which suggests that the perturbation simply launches itself into space when the cylinder terminates.

Remarks

In an attempt to explain the above results, two different theoretical studies have been undertaken. Since the scattered field at any point is almost certainly affected by the progressive phase lag between a wave attempting to propagate down the cylinder and the incident field streaming past the outside, the simple problem of a source placed above a flat Styrofoam medium was considered (Memorandum No. 5849-509-M). This is analogous to the problem of propagation over a flat earth, but instead of the pole which is responsible for many features of the solution when the refractive index n is large and complex (the usual case), the dominant singularity for n almost real and near to unity is a branch point. As a consequence of this, the region where the diffraction effects are important is stretched out in directions parallel to the surface, and there the total field has a sinusoidal behavior, with maxima and minima whose magnitude and

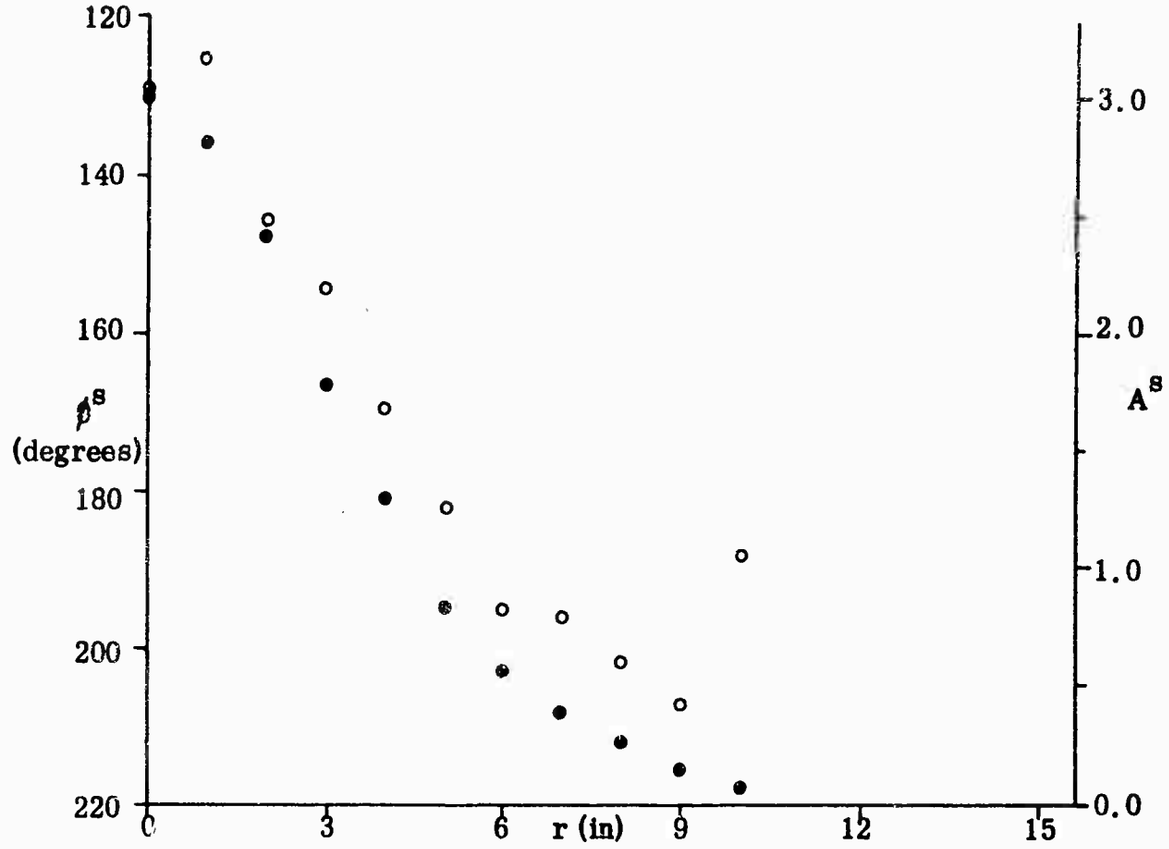

Fig. 2-22 RELATIVE AMPLITUDE (•) AND PHASE (○) OF SCATTERED FIELD FOR d = 56-3/4 IN.

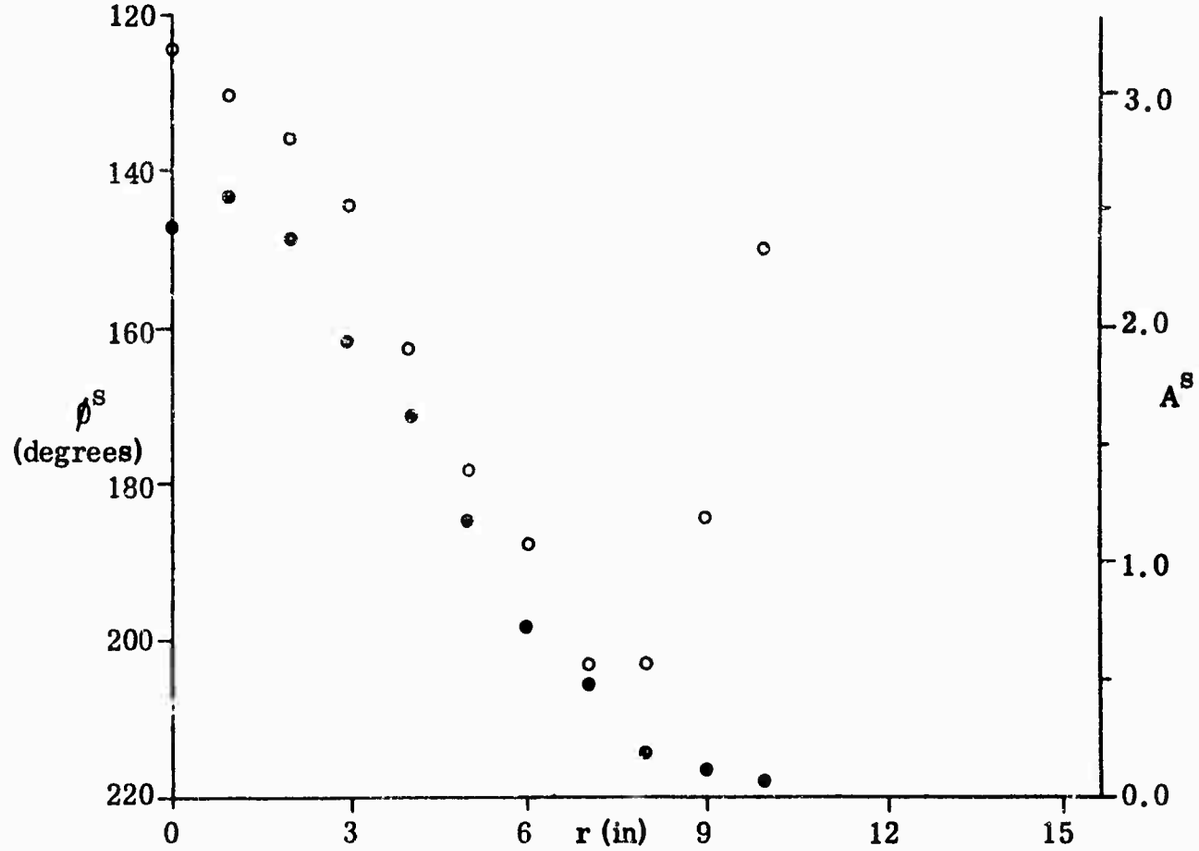

Fig. 2-23 RELATIVE AMPLITUDE (•) AND PHASE (○) OF SCATTERED FIELD FOR d = 64-1/2 IN.

position are determined by (n-1)d, where d is the horizontal distance from the surface.

Of more immediate application to the physical problem is an investigation of the surface or Goubau waves which could be supported by a cylinder of this size and material. This is currently in process[+], and it is hoped to model the experimental set-up by considering a Styrofoam cylinder of infinite length excited by a circumferential ring source. Until such time as more information is obtained about the scattered field either by analyses of this type or by more experimental work, it is premature to attempt a detailed interpretation of its influence of the far zone scattering pattern of an object placed on the cylinder, but it is clear that the magnitude of perturbation is quite sufficient to explain results such as those shown in Figure 2-10.

It is equally obvious that the existence of a large surface wave has an important bearing on the design of support pedestals for cross section measurements, and the cross section of the pedestal itself is not necessarily an indication of the effect that it will have. Since the intensity of the wave apparently increases with the length of the Styrofoam over which it has travelled, it is essential to keep to a minimum the diameter of the upper portion of the pedestal. The shaping of the upper surface, leading to an effective immersion of part of the target within the Styrofoam, should be as little as possible consistent with the required stability, and this is particularly vital for such bodies as the cone-sphere where a dominant contributor to the cross section is a surface wave. It may well be that for the measurement of heavy low-observable shapes, the design of a Styrofoam support with an acceptable surface field perturbation is more difficult than the construction of one with a small enough cross section.

[+]The analysis is being continued under a no-cost extension of the present contract through 15 June 1964.

SUMMARY

The gross physical features of cellular plastics have been described with emphasis on the more common and familiar foams. From a consideration of the load bearing capabilities and other physical properties the lower density foams are generally found to be the better materials for radar target supports.

In studying the scattering by cellular materials, most attention has been given to the return from the interior of the material since it is possible, theoretically at least to eliminate the coherent return from the exterior surfaces by shaping and/or cancellation. An expression has been developed for the incoherent scattering or "volume" contribution in terms of cell size, cell wall thickness, frequency and the relative permittivity of the basic foam material.

The experimental investigations included a series of back scatter measurements on a set of cellular plastic cylinders - this work being at the particular request of the sponsor. The data agreed well with the theoretical predictions, particularly in the periodicity of the return which was within 2 per cent.

In an effort to measure the "volume" return, back scattering data was obtained from a series of shaped foam blocks and ogives. The data from the shaped blocks gave useful information on the magnitude and source of the return but it did not provide clear information on the "volume" return since some surface wave contribution appeared to be present after the major specular returns were eliminated. The ogival shapes were selected with the thought that their nose-on return would be due to volume return only. An analysis of the measured return showed that here also surface wave effects were contributing. This study did provide, however, an upper bound for the incoherent contribution, varying from $8 \times 10^{-4} m^2$ per m^3 for Tyrilfoam down to $3 \times 10^{-4} m^2$ per m^3 for Thurane.

Attention was given also an anomalous behavior observed when a scatterer is placed very close to a foam-air interface. The study suggests that a surface wave is launched along the interface which can seriously change the field structure in the vicinity of the scatterer. Hence, in radar back scatter work, it is advisable to reduce the foam-target contact length as much as possible in the direction of illumination.

Although the study has not resulted in the discovery of an ideal target support - one that is both strong and invisible -

it has provided needed information on foam materials for target supports. We have presented information on the types of foams available, on their physical properties and their scattering return per unit volume. Finally we have shown that precautions are necessary when using foam target supports in order to prevent errors due to surface wave effects associated with foam-target interface.

REFERENCES

Albini, F. A. and E. R. Nagelberg (1962) J. Appl. Phys. 33, 1706-1713.

Baer, E. (1964) Engineering Design with Plastics, Reinhold Publishing Corp., New York.

Blore, W. E. (1964) IEEE Trans. PTGAP AP-12, pp. 237-238.

Cuming, W. R. and P. M. Andress (1958) "Plastics and Ceramic Foams for Electronic Applications," Electrical Manufacturing.

Hiatt, R. E., E. F. Knott and T. B. A. Senior, (1963) "A Study of VHF Absorbers and Anechoic Rooms" The University of Michigan Radiation Laboratory Report No. 5391-1-F.

Hodgman, C. D. (ed.) (1958) Handbook of Chemistry and Physics, 40th Edition, Chemical Rubber Publishing Co., Cleveland, Ohio.

McCann, H. (ed.) (1962) "Foamed Plastics" Modern Plastics Encyclopedia, Issue for 1963, 40, pp.395-396, Charles A. Breskin, Publisher, New York.

Mentzer, J. R. (1955) Scattering and Diffraction of Radio Waves, Pergamon Press, New York.

Myshkin, V. G. (1958) "On the Dependence of Dielectric Permeability of Foam Dielectrics on Their Density", Izvestia Vusov, Fizika, Siberian Physico-Technical Institute of the V. V. Kuibyshev State University of Tomsk.

Plonus, M. A. (1963) "Theoretical Investigations of Scattering from Plastic Foams," The University of Michigan Radiation Laboratory Report No. 5849-1-T.

Randolph, A. F. (ed.) (1960) Plastics Engineering Handbook, Reinhold Publishing Corp., New York.

Rhodes, D. R. (1953) "An Investigation of Pulsed Radar Systems for Model Measurements," The Ohio State University Antenna Laboratory Report No. 475-6.

Stengard, R. A. (1963) "Properties of Rigid Urethane Foams," bulletin published by E. I. duPont Nemours and Co.

Timoshenko, S. and G. H. MacCullough (1949) Elements of the Strength of Materials, Van Nostrand Co, Inc., New York.

Van de Hulst, H. C., (1957) Light Scattering by Small Particles, John Wiley and Sons Co., Inc., New York.

Wait, J. R. (1955) Can. J. Phys. 33, pp. 189-195.

Wolanski, H. S. (1963) Personal Communication to R. E. Hiatt, 26 September.

PUBLICATIONS UNDER THIS SUBCONTRACT

The following publications were prepared for General Dynamics/ Fort Worth by The University of Michigan in support of the subcontract (P/O No. 905616X):

M.A. Plonus, "Theoretical Scattering from Plastic Foams", submitted to Trans. IEEE-PTGAP, and published as Radiation Laboratory Report No. 5849-1-T, September, 1963.

T. B. A. Senior, "The Near Field of a Styrofoam Cylinder" and "Estimates of the 'Volume' Return from Styrofoam", to be presented at The Symposium on Radar Reflectivity Measurement", M.I.T. Lincoln Laboratory, June, 1964.

B. Memoranda

5849-501-M (E. F. Knott) Visit to Dow Chemical Company, Midland, Michigan

502-M (E. F. Knott) Data Accumulated on Styrofoam Blocks as of 19 July 1963.

503-M (M. A. Plonus) Mathematical Models for the Cell Structure of Plastic Foams.

504-M (E. F. Knott) Summary of Data for Styrofoam Blocks.

505-M (M. A. Plonus) Transparency of Glass.

506-M (R. E. Hiatt) Effect of Foam 'Cradle' on Cross Section of Conducting Target.

507-M (E. F. Knott) Summary of an Interview with Harold Borkin on Plastic Foams.

508-M (E. F. Knott) Summary of a Visit to DRTE in Ottawa.

509-M (T. B. A. Senior) Propagation over a Flat Styrofoam Earth.

510-M (T. B. A. Senior) Perturbations Produced by a Styrofoam Beam.

511-M (T. B. A. Senior) Measurements of the Back Scattering Cross section of Shaped Styrofoam Blocks.

512-M (E. F. Knott) Measurement of the Cross Section of Nine Styrofoam Cylinders.

513-M (E. F. Knott) Comparison of Six Rigid Plastic Foams.

SECTION 3

STYROFOAM SCATTERING INVESTIGATION

The basic task for General Dynamics/Fort Worth in the area of scattering by cellular plastic materials was to monitor and extend the work done by the Radiation Laboratory of The University of Michigan. The extension work was directed towards areas that had direct bearing on the target measurement capability of the RAT SCAT project. The scattering investigation was limited primarily to the study of right circular cylinders. Tests were implemented at The University of Michigan and the RAT SCAT Site to verify the theoretical cross section derived for right circular cylinders.

The theoretical scattering model discussed in Section 2 was the basic model used in the theoretical work done at General Dynamics/Fort Worth. Personnel at General Dynamics/Fort Worth modified the mathematical model developed by Plonus in order to more nearly predict the experimental data obtained in the anechoic chamber at The University of Michigan Radiation Laboratory and that obtained at the RAT SCAT Site.

As given by Plonus, the general form of the equation for coherent scattering is

$$\sigma_c = \sigma_i \left| \int_0^L n(r)\, e^{-2ikr}\, dr \right|^2 , \qquad (29)$$

where

σ_i = cross section of the individual particle (Rayleigh)

$n(r)$ = distribution function of the particles

r = length or distance into the particle system

L = total length of the particle system.

A more realistic representation than that described in equation 29 would include an "apparent" attenuation factor. This factor would take into account the attenuation and coupling as the wave propagates through the particle system. If this approach is taken, the equation takes the form of

$$\sigma_c = \sigma_i \left| \int_0^L n(r) e^{-2ikr} \, e^{-2\alpha r} \, dr \right|^2 = \sigma_i \left| \int_0^L n(r) e^{-2(\alpha + ik)r} \, dr \right|^2 , \quad (30)$$

where α represents an "apparent" attenuation constant. It is assumed that the density N/V, is constant throughout the material and that the distribution function n(r) is a function of shape only. Using the above representation, expressions which give the scattering from the Styrofoam blocks that were measured at The University of Michigan are derived. These blocks were fabricated in the three shapes shown in the sketch below.

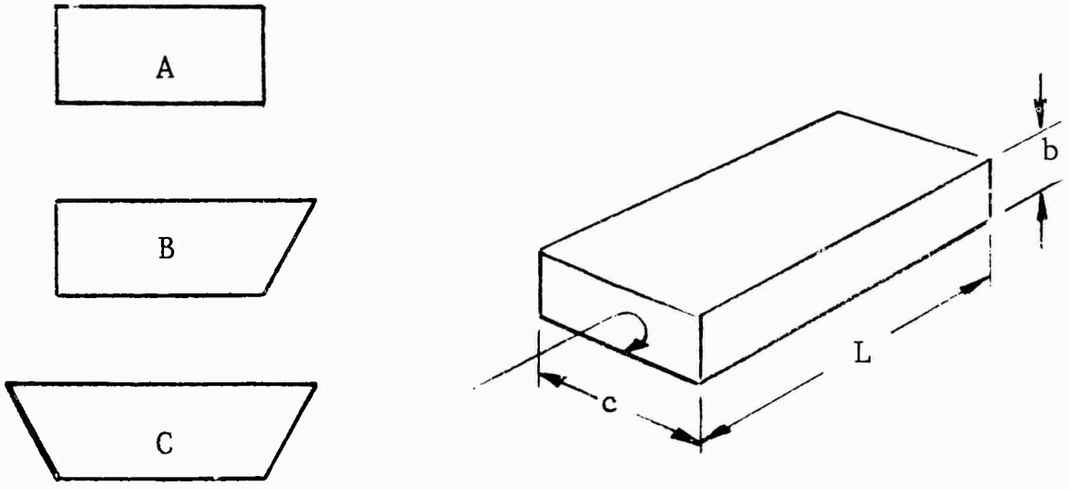

Shape C will be considered first since it can be seen by inspection to contain the other two shapes.

If shape C is divided into sections as shown below,

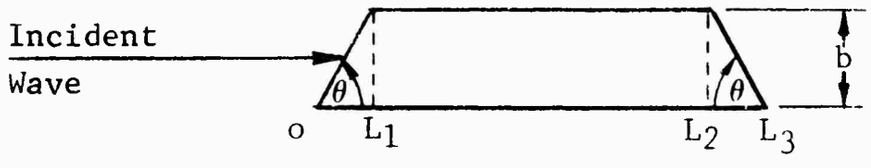

the distribution function for $r = 0$ to $r = L_1$ is

$$n_1(r) = c \frac{N}{V} r \tan\theta = \left(\frac{N}{V} c \tan\theta\right) r \quad , \tag{31}$$

where

$$\theta = \tan^{-1} \frac{b}{L_1} = \tan^{-1} \frac{b}{L_3 - L_2} \quad .$$

From $r = L_1$ to $r = L_2$

$$n(r) = \frac{N}{V} bc \tag{32}$$

and from $r = L_2$ to $r = L_3$

$$n(r) = c \frac{N}{V} \left(b - \left[r - L_2 \right] \tan\theta\right) . \tag{33}$$

By using equation 30,

$$\sigma = \sigma_i \frac{N^2}{V^2} \left| c \tan\theta \int_0^{L_1} r e^{-2(\alpha + ik)r} \, dr \right.$$

$$+ bc \int_{L_1}^{L_2} e^{-2(\alpha + ik)r} \, dr$$

$$\left. + c \int_{L_2}^{L_3} \left\{ b - \left[(r - L_2) \tan\theta \right] \right\} e^{-2(\alpha + ik)r} \, dr \right|^2 . \tag{34}$$

The three terms represent the corresponding sections of the Styrofoam block from left to right. The equation for the "squared-off" Styrofoam block, of length L, would then be

$$\sigma = \sigma_i \, b^2 c^2 \frac{N^2}{V^2} \left| \int_0^L e^{-2(\alpha + ik)r} \, dr \right|^2 \tag{35}$$

$$= \sigma_i \left(\frac{AN}{V}\right)^2 \left| \frac{1-e^{-2L(\alpha + ik)}}{2(\alpha + ik)} \right|^2 . \quad (36)$$

This equation represents the second term in equation 34.

To investigate how closely this expression agrees with the experimental data obtained at The University of Michigan, equation 36 can be put in the form

$$\sigma = B \left| 1-e^{-2L(\alpha + ik)} \right|^2 = B \left| \frac{e^{-2L}}{4} (\sinh L(\alpha+ik) \right|^2 . \quad (37)$$

If it is assumed that $\alpha << k$, the minimum occurs approximately at

$$Lk = N\pi \quad (38)$$

where N is equal to a positive integer.

To relate k to the free space wavelength recorded with the available data, the relative material constants $\epsilon' = \frac{\epsilon}{\epsilon_o}$ and $\mu' = \frac{\mu}{\mu_o}$ are used.

These material constants are related to the velocity of light, C, by

$$C = \sqrt{\frac{\epsilon'\mu'}{\epsilon\mu}} . \quad (39)$$

By using equations 38 and 39, K can be written as

$$K^2 = \frac{\epsilon'\mu'w2}{C^2} . \quad (40)$$

Since C can also be written as $C = \lambda f$ where λ = free space wave length, equation 40 may be written as

$$k = \sqrt{\epsilon'\mu'} \quad \frac{2\pi}{\lambda} . \quad (41)$$

For Styrofoam, $\mu' = 1$; hence equation 13 becomes

$$k = \sqrt{\epsilon'} \quad \frac{2\pi}{\lambda} . \quad (42)$$

By using equations 42 and 38, the relationship for evaluating the dielectric constant is given by

$$N = \sqrt{\epsilon'} \quad \frac{2L}{\lambda} \quad . \tag{43}$$

Using the relationship expressed in equation 43, along with the data presented in Table II of The University of Michigan report No. 5849-504-M (RAT SCAT Progress Report No. 15), yields the calculated values for ϵ' shown in Figure 3-1.

To obtain a value for the attenuation factor α , equation 36 may be written as

$$\sigma = A \lambda^2 \epsilon^{-2\alpha L} \left| \text{Sinh } L(\alpha + ik) \right|^2 . \tag{44}$$

Evaluation of 44 at two distinct frequencies to eliminate the constant A gives

$$\frac{\sigma_1}{\sigma_2} = \frac{\lambda^2_1}{\lambda^2_2} \left| \frac{\text{Sinh } L(\alpha + ik_1)}{\text{Sinh } L(\alpha + ik_2)} \right|^2 . \tag{45}$$

Expanding the Sinh(x + iy) into functions of real arguments gives

$$\frac{\sigma_1}{\sigma_2} = \frac{\lambda^2_1}{\lambda^2_2} \left| \frac{\text{Sinh } L\alpha \text{ Cos } k_1L + i \cosh L\alpha \text{ Sin } k_1 L}{\text{Sinh } L\alpha \text{ Cos } k_2L + i \cosh L\alpha \text{ Sin } k_2 L} \right|^2 . \tag{46}$$

If k_1L is chosen to equal $N\pi$, then $\sin k_1L = 0$. Likewise if $k_2L = \frac{N'\pi}{2}$, where N is odd, then $\cos k_2L = 0$, and equation 46 can be reduced to

$$\frac{\sigma_1}{\sigma_2} = \left(\frac{\lambda_1}{\lambda_2}\right)^2 (L\alpha)^2 . \tag{47}$$

In equation 47, the approximations $\sinh \alpha L \cong \alpha L$ and $\cosh \alpha L \cong 1$ were used. Table 3-1 contains the results of checking this relationship against the experimental data presented in The University of Michigan Report No. 5849-504-M.

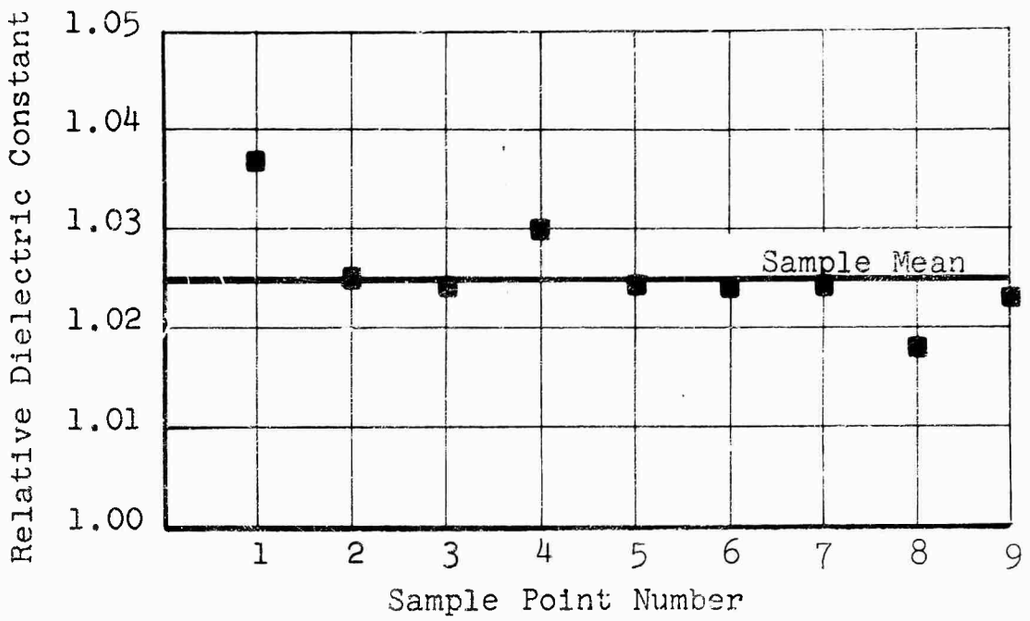

Fig. 3-1 CALCULATED DIELECTRIC CONSTANT FOR STYROFOAM

TABLE 3-1

ATTENUATION CONSTANT DATA

L (inches)	f (kmc)	$\lambda^2\sigma$ (db m^4)	α (nepers/meter)
33	9.39	-60.67	
33	9.49	-49.82	0.338
30	9.415	-50.2	
30	9.52	-63.33	0.334

The attenuation constant, α , may be related to the loss tangent (tan δ) as follows:

$$\epsilon_c = \epsilon\left(1 - i\ \frac{\sigma}{W\epsilon}\right) = \epsilon\ (1 - i \tan\delta)\ , \qquad (48)$$

where

ϵ_c = complex permittivity

σ = conductivity.

By using ϵ_c in place of ϵ in equation 42, k can be written as

$$k = \frac{2\pi\sqrt{\epsilon}}{\lambda}\quad (1 - i\ \frac{\tan\delta}{2}\ ) \qquad (49)$$

since tan δ is very small, i.e., $\tan\delta << 1$. To relate equation 49 to the attenuation constant α of equation 35, k is multiplied by i to give

$$ik = \frac{2\pi\ \sqrt{\epsilon'}}{\lambda}\quad \frac{\tan\delta}{2}\ + \frac{i\ 2\pi\sqrt{\epsilon}}{\lambda}\ . \qquad (50)$$

Solving equation 50 for α yields

$$\alpha = \frac{\pi\sqrt{\epsilon'}}{\lambda}\ \tan\delta\ . \qquad (51)$$

Hence the loss tangent is related to α by

$$\tan\delta = \frac{\alpha\lambda}{\pi\sqrt{\epsilon'}}\ . \qquad (52)$$

The loss tangent calculated for $\lambda = 3.2 \times 10^{-2}$ meter is

$$\tan\delta = \frac{.336(3.2)10^{-2}}{\pi\sqrt{\epsilon}} = 0.0035 . \qquad (53)$$

The model developed for the square Styrofoam blocks can be extended to the circular Styrofoam column by using the appropriate cell distribution function. For a right circular column with a uniform per-unit-volume cell structure, the distribution function is given by

$$n(r) = \frac{N}{V}\ 2L\sqrt{a^2 - r^2}\ , \qquad (54)$$

where

N = Total number of cells in the column

V = volume of column

a = radius of column

L = length of column .

The reasoning used for the previous case can be applied to the case of the monostatic cross section i.e.,

$$\sigma = 4\ \sigma_i\ (\frac{NL}{V})^2 \left| \int_{-a}^{a} \sqrt{a^2 - r^2}\ e^{-2(\alpha + ik)r}\ dr \right|^2 . \qquad (55)$$

In equation 55, the origin is taken at the center of the column in order to obtain compatibility with the cell distribution function of equation 54. To evaluate equation 55, integration by parts can be performed to give

$$\sigma = 4\ \sigma_i (\frac{NL}{V})^2 \left| \frac{1}{2(\alpha+ik)} \int_{-a}^{a} \frac{1}{\sqrt{a^2 - r^2}}\ e^{-2(\alpha+ik)r}\ dr \right|^2 . \qquad (56)$$

In equation 56, if the transformation $\frac{r}{a} = \cos\theta$ and $Z = 2(k-i\alpha)a$ is used, then σ becomes

$$\sigma = \sigma_i \left[\frac{NLa}{V|\alpha+ik|}\right]^2 \left| \int_{\pi}^{o} \cos\theta\ e^{-iZ\cos\theta}\ d\theta \right|^2 . \qquad (57)$$

The integral in equation 57 is related to the Bessel function $J_1(Z)$, as indicated in equation 58,

$$\sigma = \sigma_i \left[\frac{NLa}{V|\alpha + ik|}\right]^{-2} \left| i\pi \, J_1(\xi) \right|^2 . \qquad (58)$$

To evaluate equation 58 for the case of $\frac{4\pi a}{\lambda} >> 1$ and $\frac{4\pi a}{\lambda} >> \alpha a$, the asymptotic expansion of $J_1(\xi)$ can be used to give

$$\sigma \simeq \sigma_1 \left(\frac{NL}{V}\right)^2 \frac{\lambda^3 a}{8\pi^2} \left| \cosh\left[2\alpha a - i\left(\frac{4\pi a}{\lambda} - \frac{3\pi}{4}\right)\right] \right|^2 . \qquad (59)$$

From equation 59, it is observed that the cross section of the right circular column has the same type of "sinusoidal" dependance as that observed in the square block. This result seems reasonable at the higher frequencies $\left(\frac{4\pi a}{\lambda} >> 1\right)$ since the front and rear specular regions should provide the main contributions. If, as shown in the square block case, σ_i is replaced by the Rayleigh cross section of the thin spherical shell, the cross section can be written as

$$\sigma = \frac{2\pi L^2 a}{\lambda} \left[\frac{N2\pi t(a')^2(\epsilon_s - 1)^2}{V}\right]^2 \left| \cosh\left[2\alpha a - i\left(\frac{4\pi a}{\lambda} - \frac{3\pi}{4}\right)\right] \right|^2 . \qquad (60)$$

From equation 60, it is observed that the cross section varies in a manner similar to the optics case for the perfectly conducting right circular cylinder. The main functional modification is the oscillitory term caused by the phasing between the front and rear surfaces.

It was deemed worthwhile to design an experiment specifically for the purpose of gathering data to check the derived expressions for the cylindrical Styrofoam column.

Accordingly, The University of Michigan was requested to undertake the Styrofoam cylinder measurement program described in Section 2. The results of this measurement program were published in The University of Michigan Radiation Laboratory memo 5849-512-M. The data from that memo is herein reproduced verbatim as Figures 3-3 through 3-11.

Correction factors were applied to the cross section data obtained from cylinders 15 and 20 inches long in order to compensate for the curvature of the field used for the measurements. These correction factors were based on the field probe data supplied by The University of Michigan (Figure 3-12) and on

the assumption that the broadside cross sections of the cylinders were proportional to the square of the cylinder length.

The correction factors obtained for the 15-inch and 20-inch cylinders are 1.0 dbsm and 1.65 dbsm, respectively, for the 9.3-gigacycle field probe region, and 0.65 and 1.2 dbsm, respectively for the 8.5-gigacycle region. By using these correction factors, it is noted that the measured cross section varies in proportion to the square of the cylinder length as indicated by equation 60. If it is assumed that $\alpha = 0$, the minimum points obtained from equation 60, in terms of the column diameter D, free space wave length λ_o, and relative dielectric constant ϵ_s are as follows:

$$\frac{\sqrt{\epsilon_s} D}{\lambda_o} = \frac{5}{8} + \frac{N}{2}, \quad N = 0, 1, 2, \ldots \tag{61}$$

By using the minima points of the data in Figures 3-3 through 3-11 and a relative dielectric constant of 1.037, a constant of 5/8 is obtained to within 5 percent accuracy. Hence, the portion of equation 60 relating to the periodic nature of σ appears to be in excellent agreement with experimental data.

A recent paper by W. E. Blore, The Radar Cross Section of Polyfoam Towers, General Motors Defense Research Laboratories, supports the form of equation 60 both theoretically and experimentally. Although the diameter of the set of cylinders used in the experiment did not vary over a wide range, the measured data was in excellent agreement with Equation 60. In Reference 1 additional experimental verification of the dependence of cross section, σ, on column radius, a, is given.

Equation 61 is presently being used at the RAT SCAT facility in the design and/or selection of circular column supports in order to obtain a minimum cross section for vertical columns. An aid to column design is presented in Figure 3-2. In Figure 3-2, the column diameter normalized to its "electrical" diameter is plotted versus frequency as a function of the parameter N on the basis of the relationship of Equation 61. A set of column diameters which can be used to minimize the broadside cross section is given in Figure 3-2 for each operating frequency between 0.4 and 12 gigacycles.

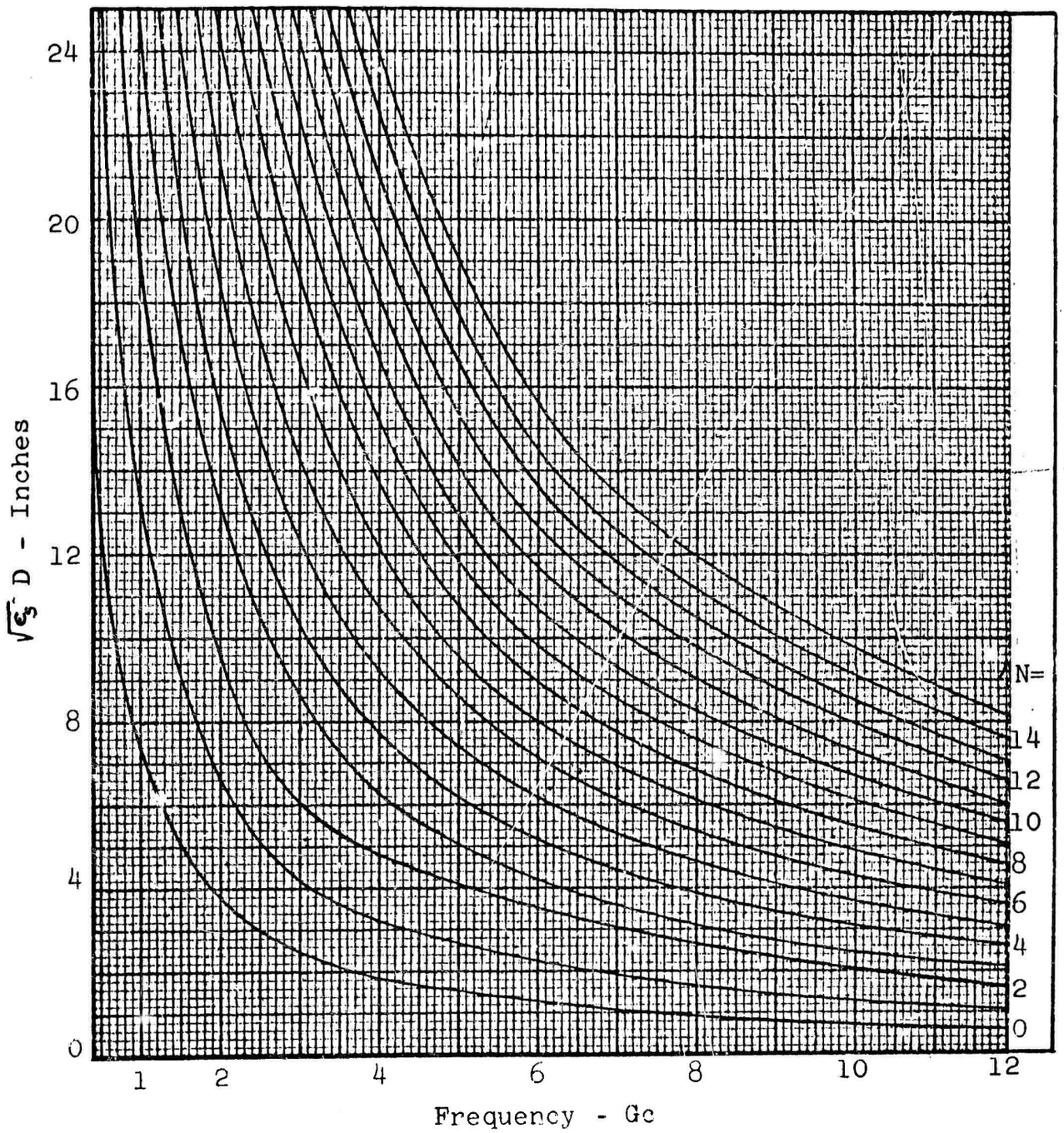

Fig. 3-2 COLUMN DIAMETER VERSUS FREQUENCY FOR MINIMUM BROADSIDE CROSS SECTION OF A PLASTIC FOAM CYLINDER

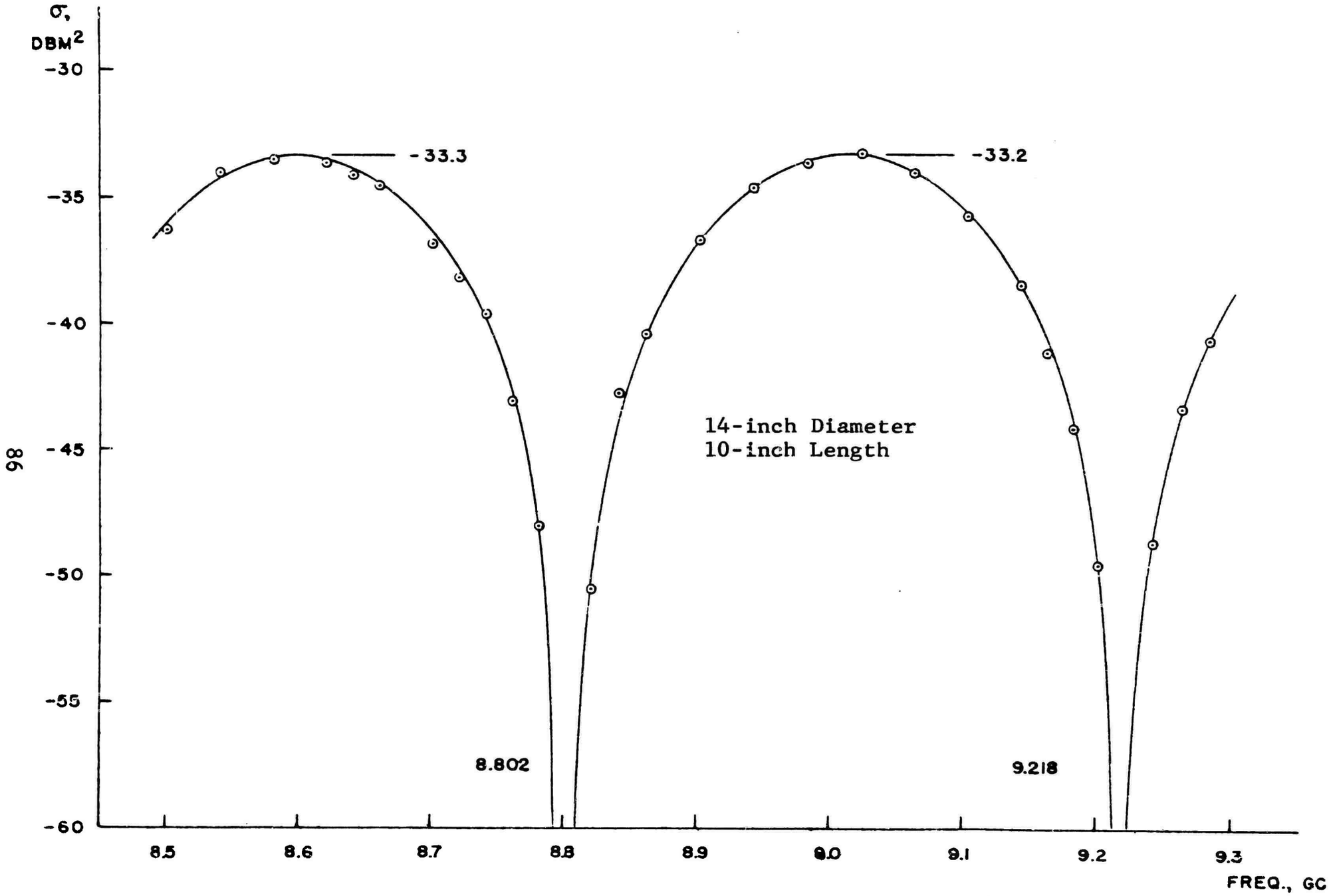

Fig. 3-3 CROSS SECTION VS. FREQUENCY OF 14" DIAMETER, 10" LONG STYROFOAM CYLINDER

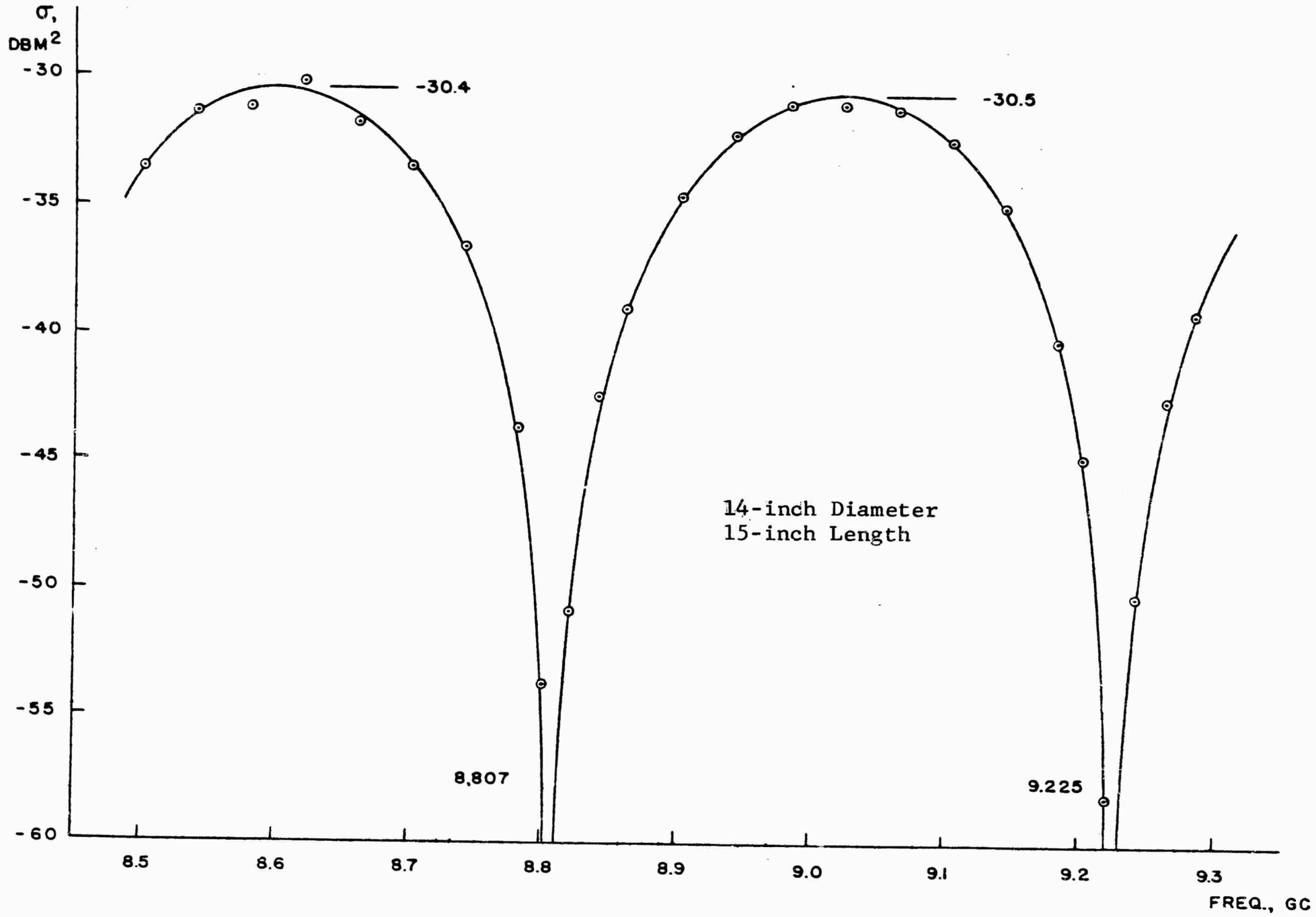

Fig. 3-4 CROSS SECTION VS. FREQUENCY OF 14" DIAMETER, 15" LONG STYROFOAM CYLINDER

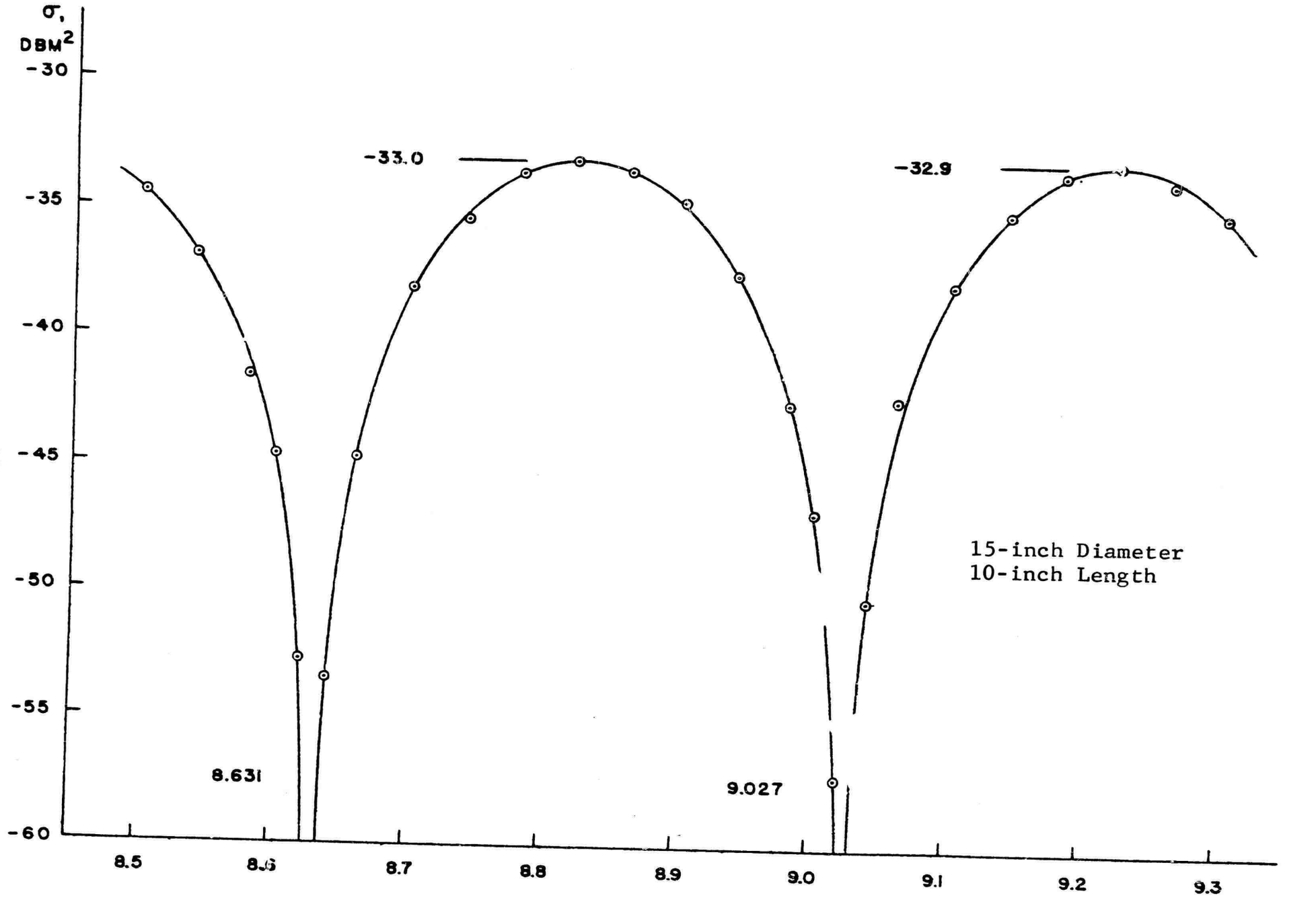

Fig. 3-6 CROSS SECTION VS. FREQUENCY OF 15" DIAMETER [illegible]

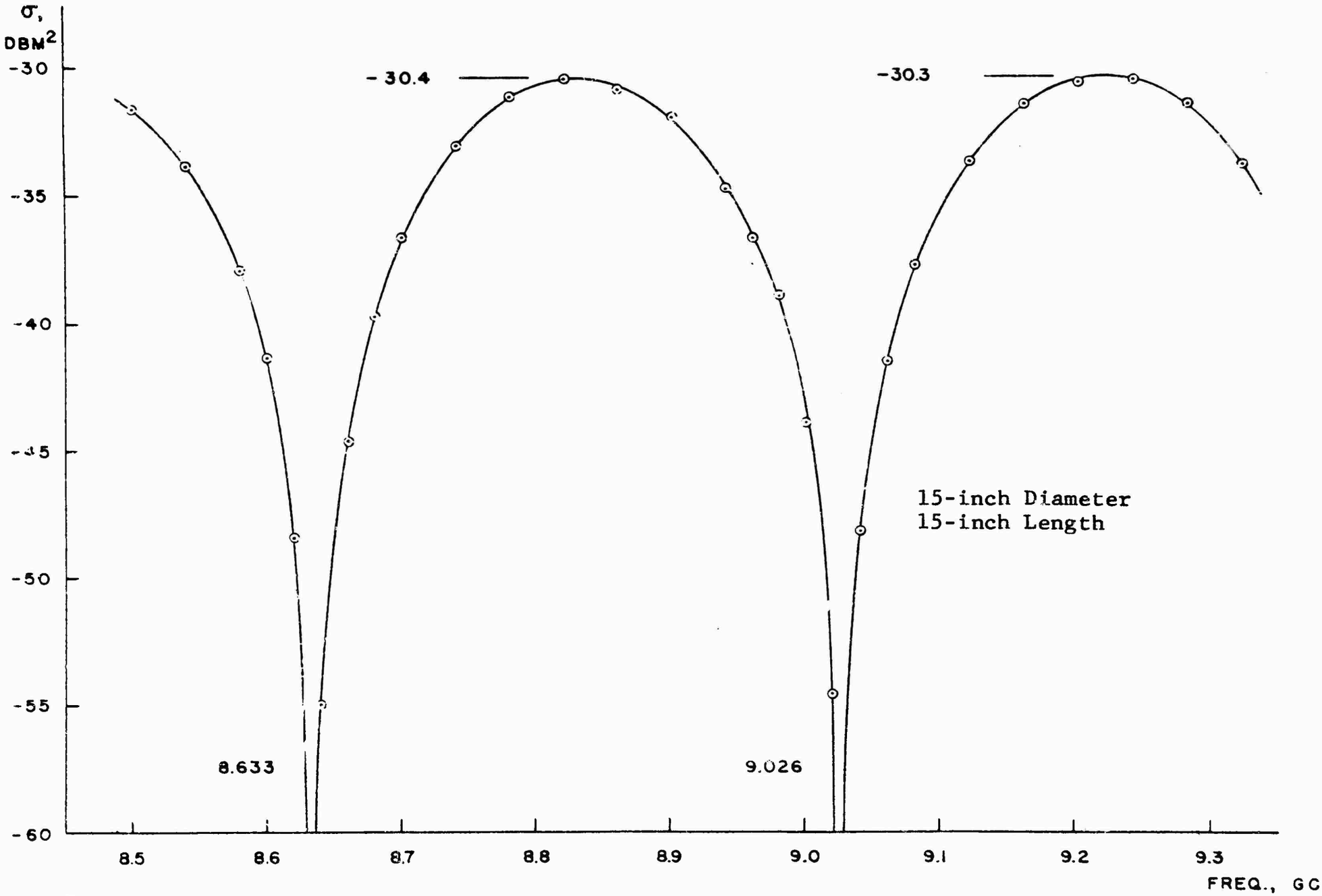

Fig. 3-7 CROSS SECTION VS. FREQUENCY OF 15" DIAMETER, 15" LONG STYROFOAM CYLINDER

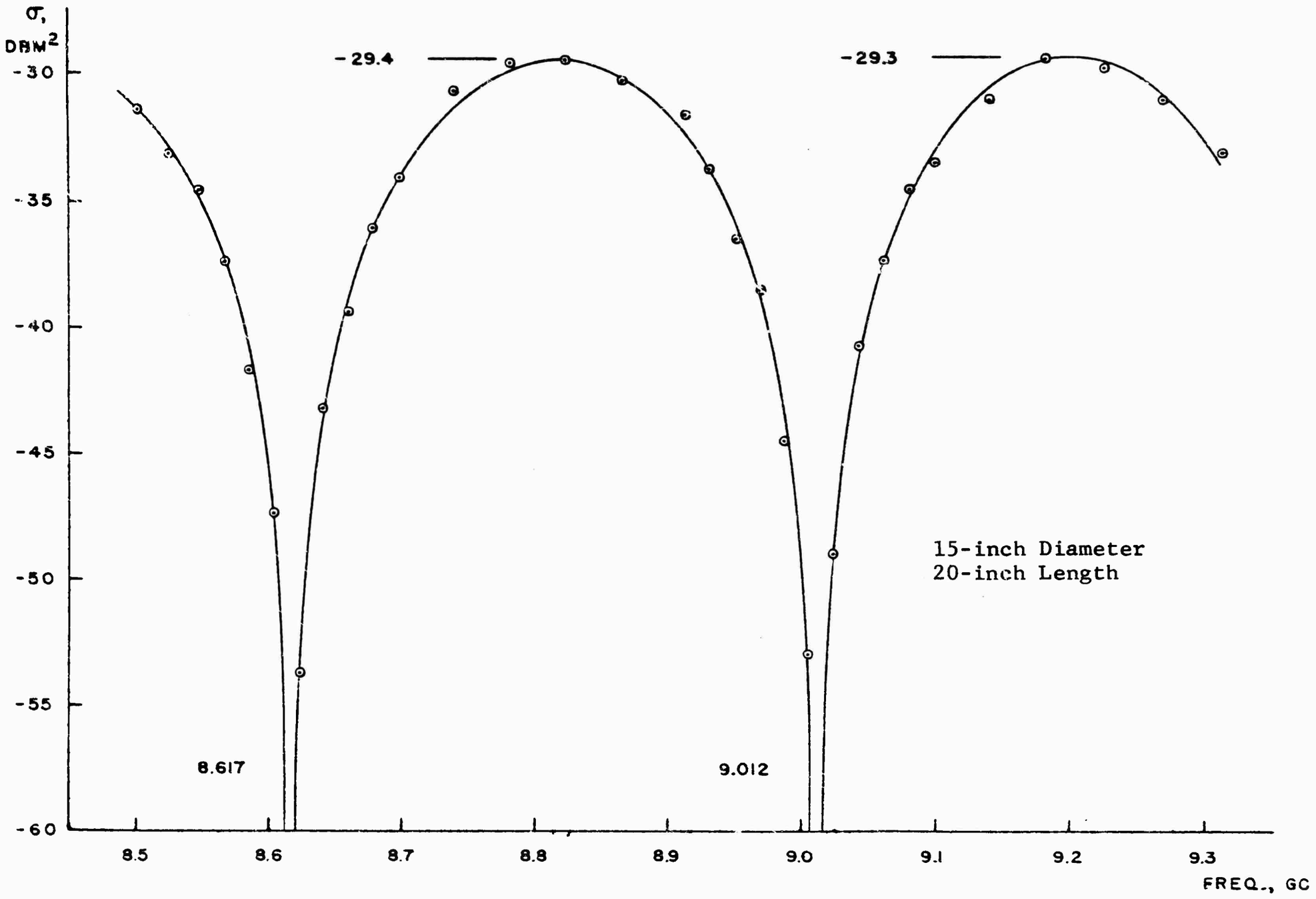

Fig. 3-8 CROSS SECTION VS. FREQUENCY OF 15" DIAMETER, 20" LONG STYROFOAM CYLINDER

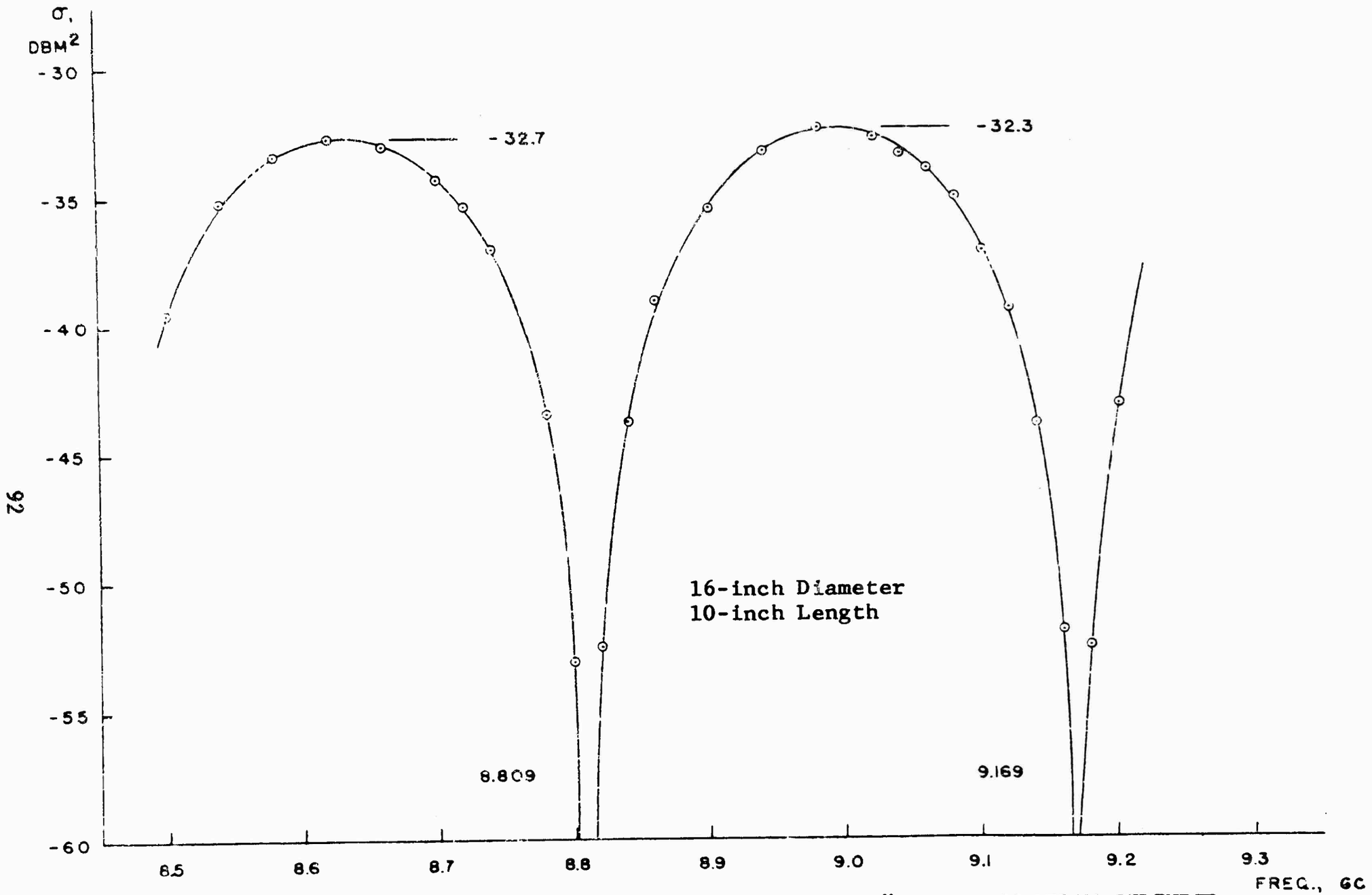

Fig. 3-9 CROSS SECTION VS. FREQUENCY OF 16" DIAMETER, 10" LONG STYROFOAM CYLINDER

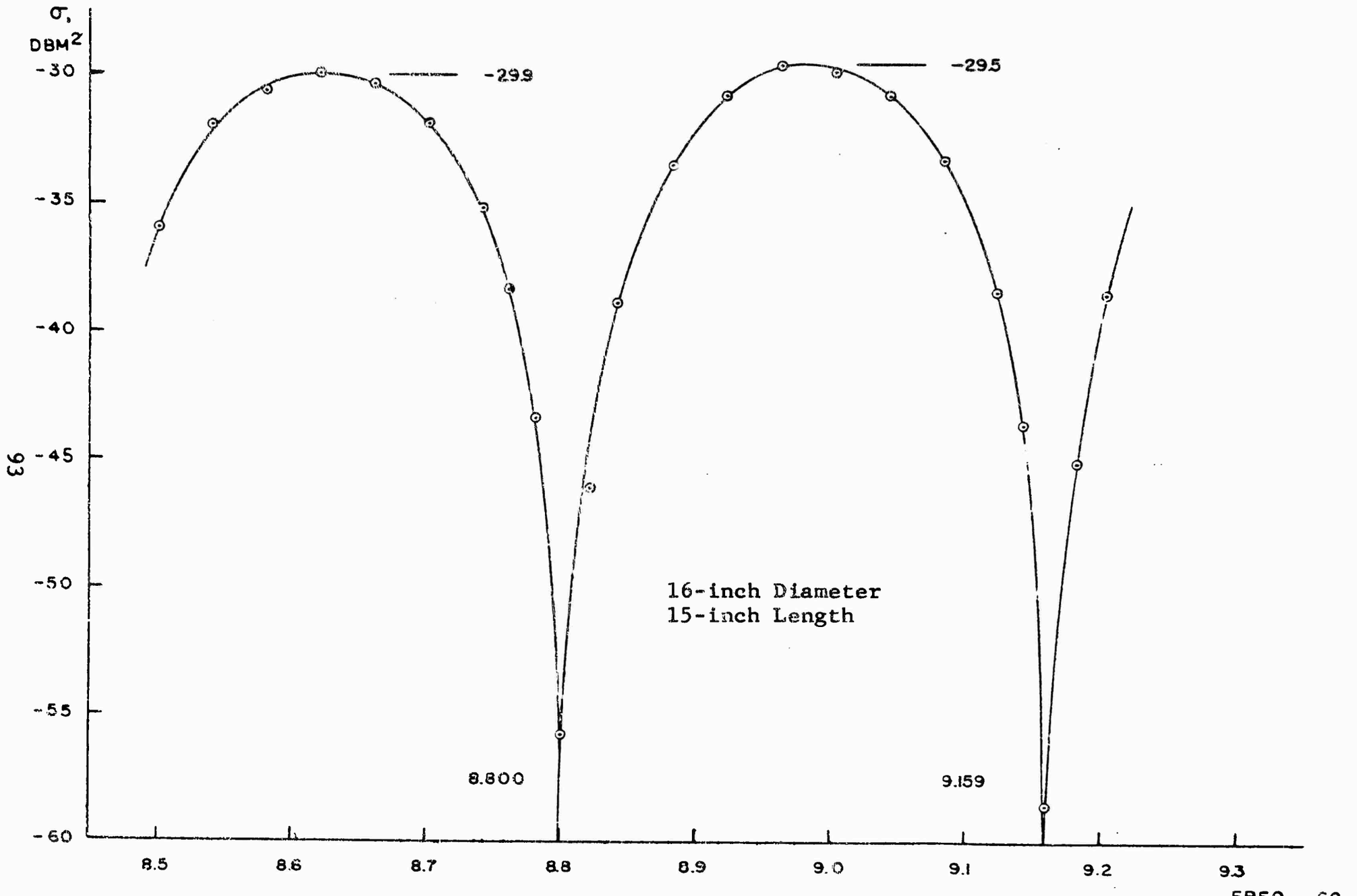

Fig. 3-10 CROSS SECTION VS. FREQUENCY OF 16" DIAMETER, 15" LONG STYROFOAM CYLINDER

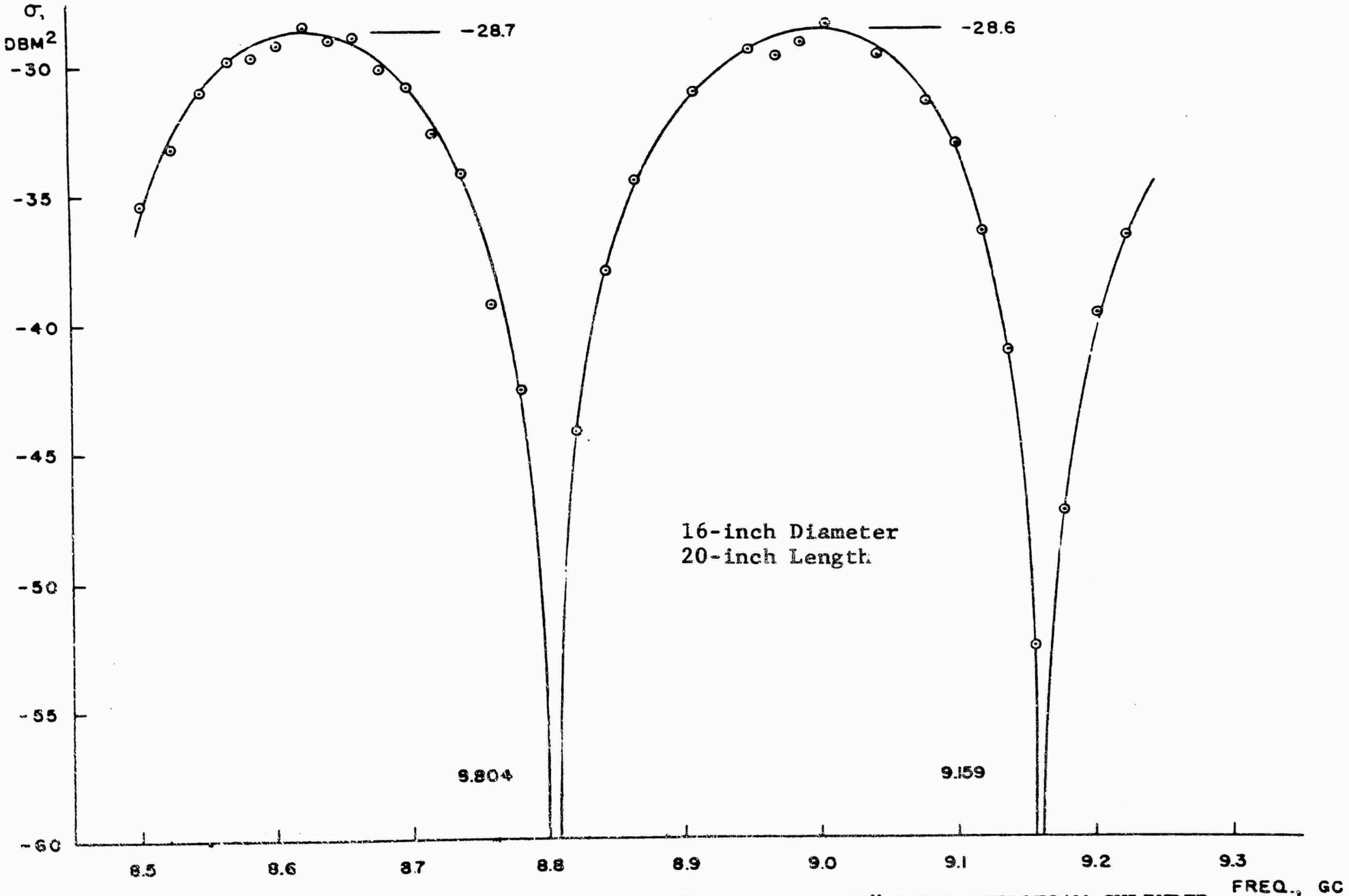

Fig. 3-11 CROSS SECTION VS. FREQUENCY OF 16" DIAMETER, 20" LONG STYROFOAM CYLINDER

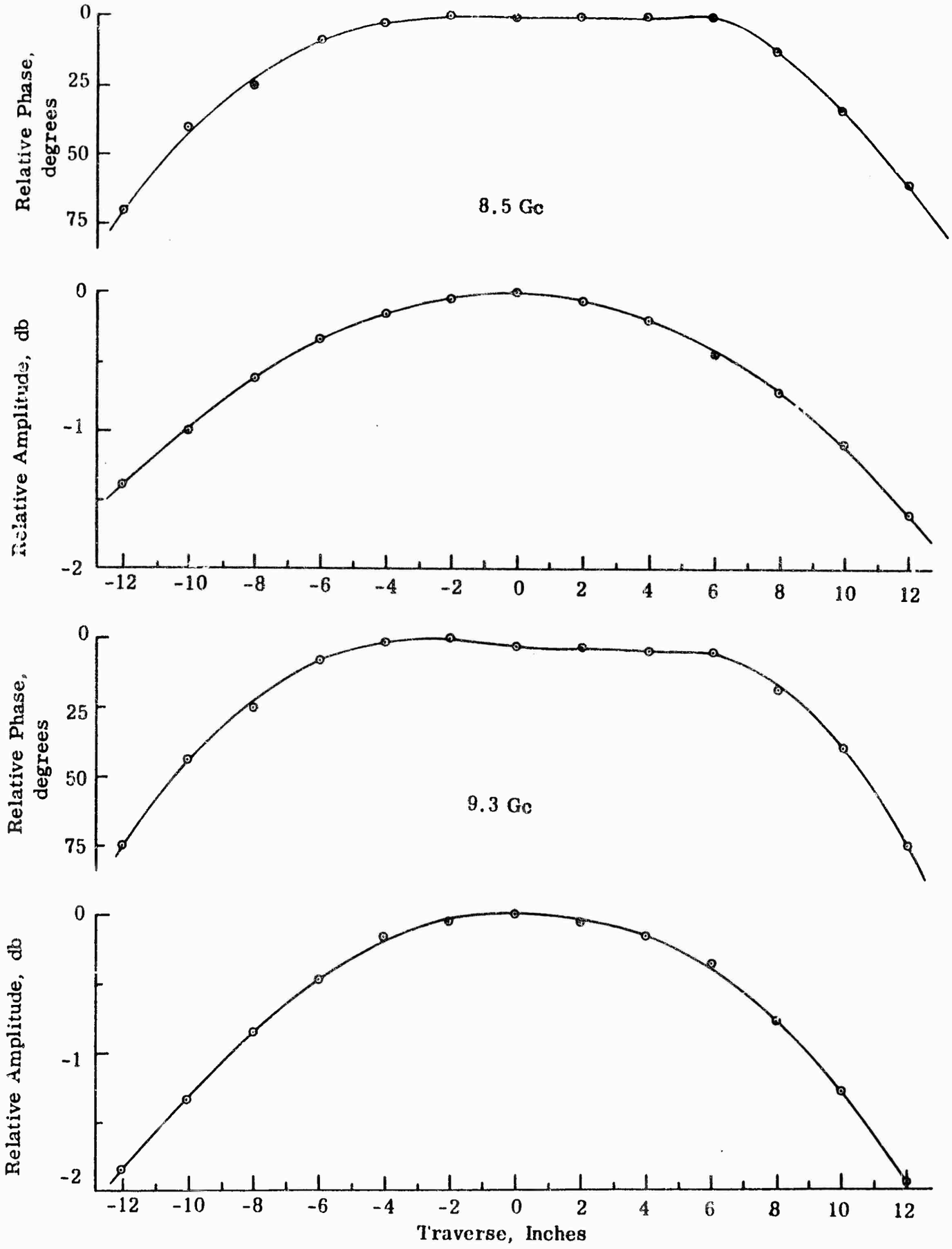

Fig. 3-12 PHASE AND AMPLITUDE OF INCIDENT FIELD AT RANGE = 226 INCHES

Typical values of target support cross sections measured at the RAT SCAT facility using the D/λ criteria given in Figure 3-2 are illustrated in Figures 3-13 through 3-16. The cross section patterns were obtained using a cylindrical Styrofoam column approximately 16 inches in diameter, 10 feet in length. A Styrofoam column of this size is capable of supporting 1000 pounds. The cross sections shown are for the case of vertical polarization since horizontal polarization produces returns 2 to 5 db less than in the vertical case. The four cross section patterns were obtained at frequencies in Bands 4 through 7 (L through X band). The data presented in Figures 3-13 through 3-16 indicate the dependence of the minimum cross section on D/λ . This lower bound value was discussed in Section 2 in terms of an "incoherent" return and in Section 3 in terms of apparent loss tangent. Adopting the loss tangent point of view, the variation with frequency of the minimum cross section in the measured data presented in Figures 3-13 through 3-16 is predicted quite accurately. Using equation 60 and assuming low loss material it is easy to show that the minimum cross section of a circular column varies proportional to $(D/\lambda)^3$. This being the case, the difference between the cross section levels in Figures 3-13 through 3-16 should follow the theoretical curve presented in Figure 3-17. The variation in mean values of measured data is also presented in Figure 3-17 for comparison. It can be seen that based upon the measured data a cubic dependence of the minimum cross section on λ appears to be a much better choice than a fourth power variation predicted by the incoherent theory discussed in Section 2. Figure 3-17 can be used to rapidly estimate the cross section reduction (increase) which may be obtained by decreasing (increasing) the column diameter and/or operating at a lower (higher) frequency given a fixed length circular column. For example, assume a minimum cross section of σ_1 was measured when operating at a frequency of f_1 and using a column size D_1. Then for the same length column with diameter D_2 operating at a minimum point with frequency f_2 the cross section reduction (increase) to be expected is given by the ordinate in Figure 3-17 determined by the abcissa value corresponding to the ratio f_2D_2/f_1D_1 (or inverse).

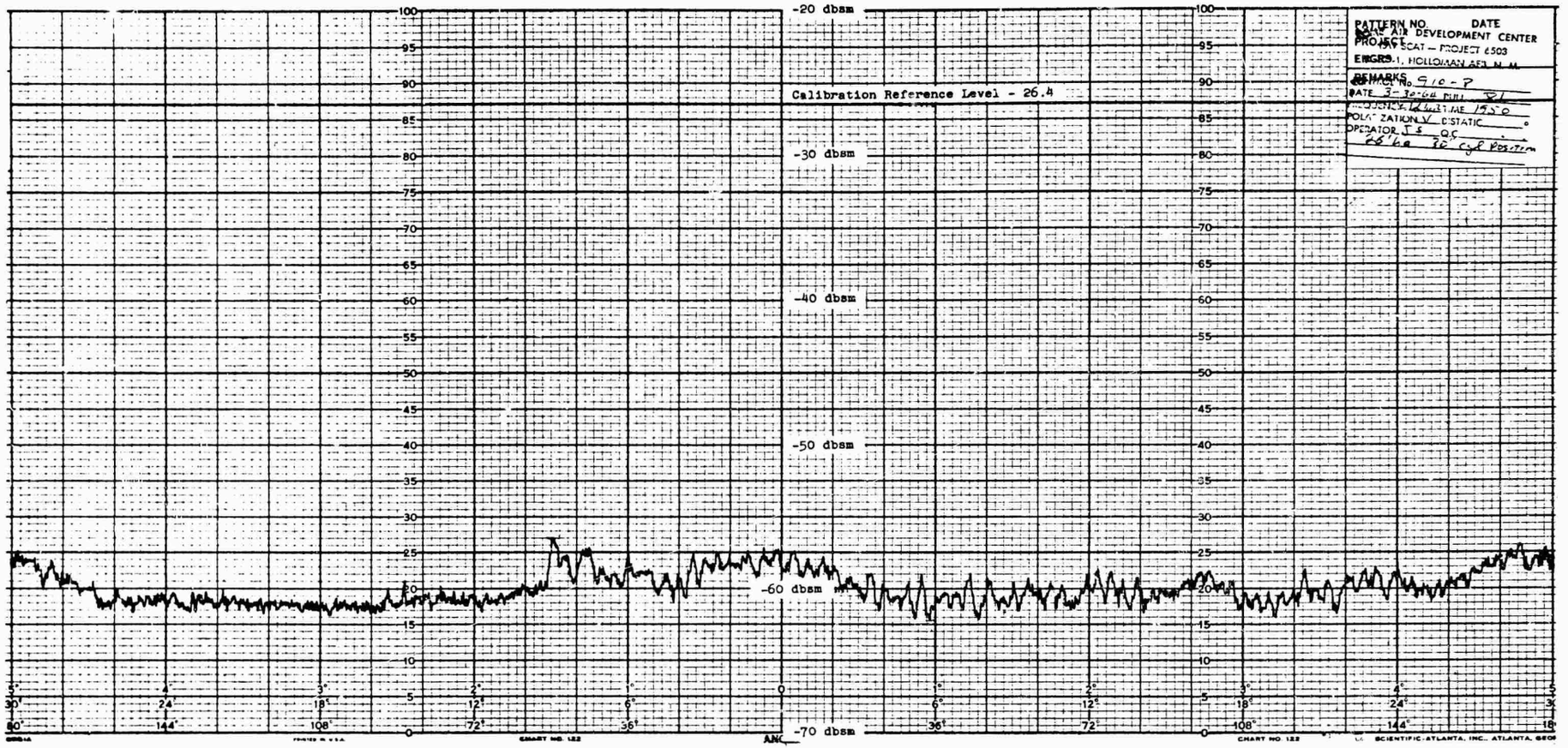

Fig. 3-13 CROSS SECTION RETURN FOR TUNED 15 INCH DIAMETER STYROFOAM COLUMN MEASURED AT L BAND

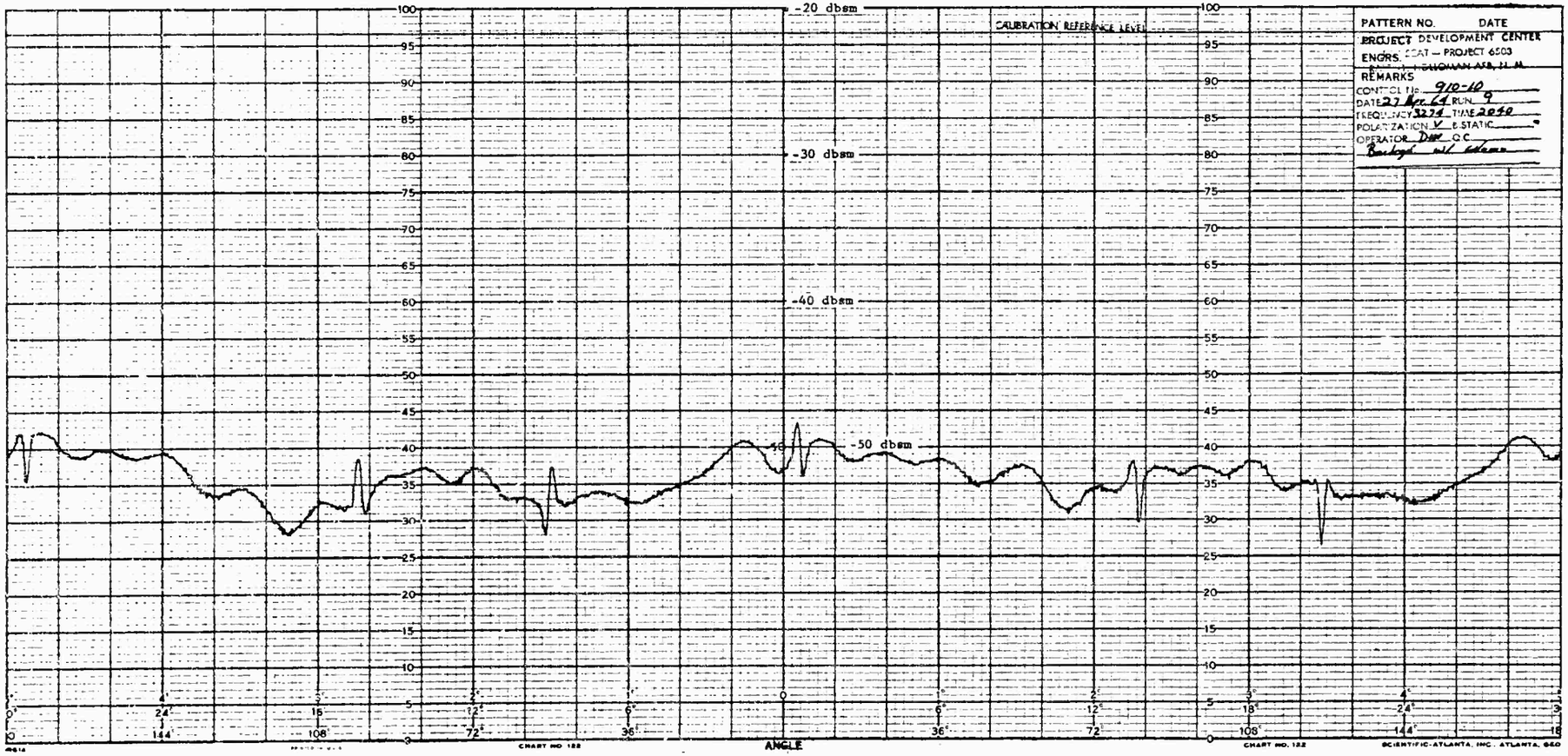

Fig. 3-14 CROSS SECTION RETURN FOR TUNED 16 INCH DIAMETER STYROFOAM COLUMN MEASURED AT S BAND

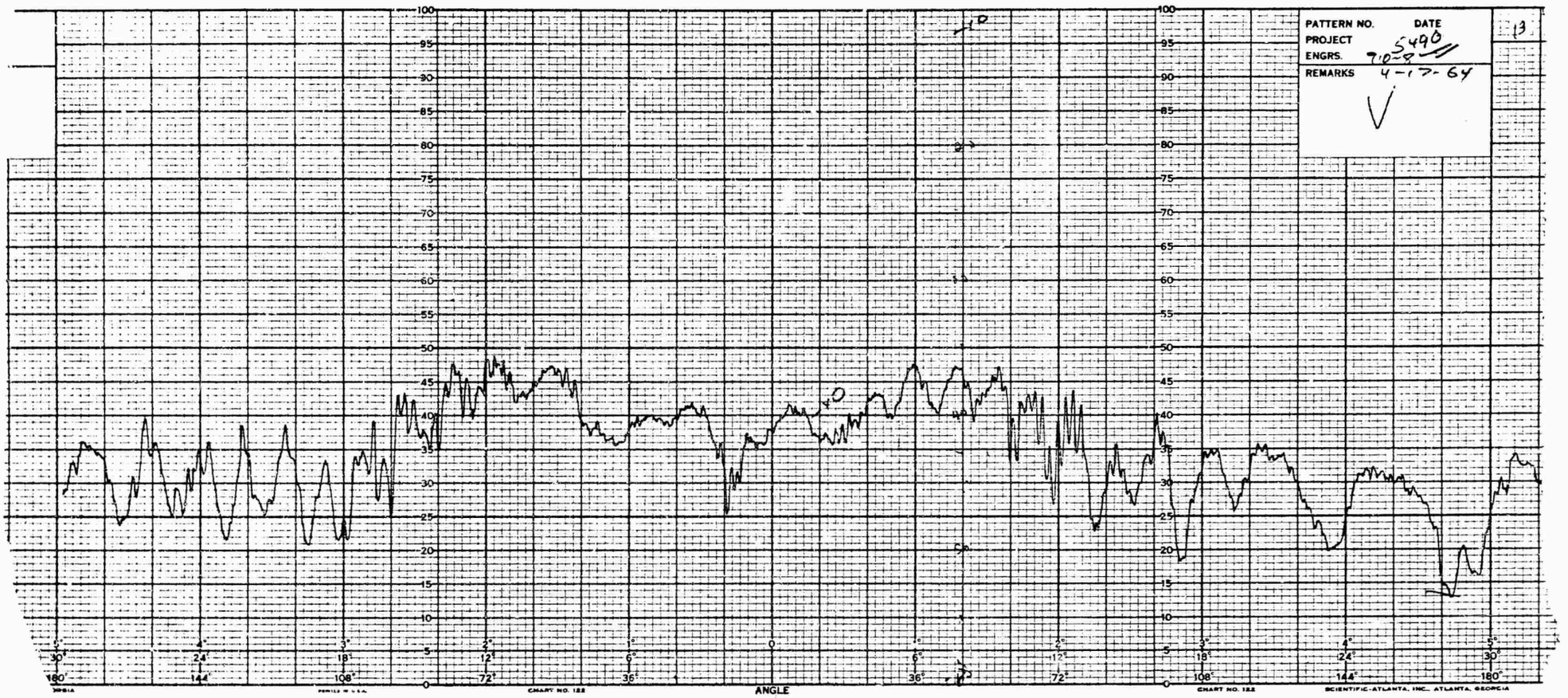

Fig. 3-15 CROSS SECTION RETURN FOR 16 INCH DIAMETER STYROFOAM COLUMN MEASURED AT C BAND

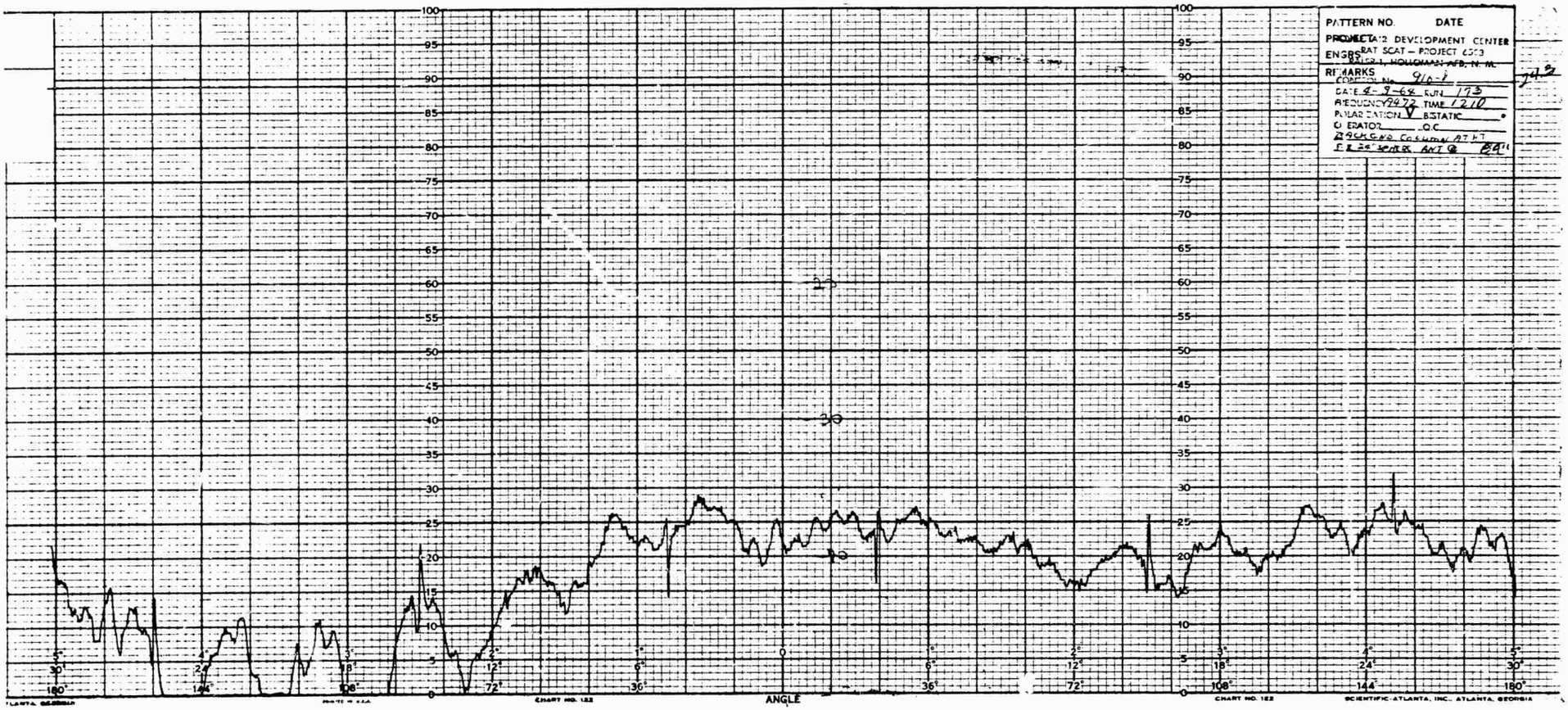

Fig. 3-16 CROSS SECTION RETURN FOR 16 INCH DIAMETER STYROFOAM COLUMN MEASURED AT X BAND

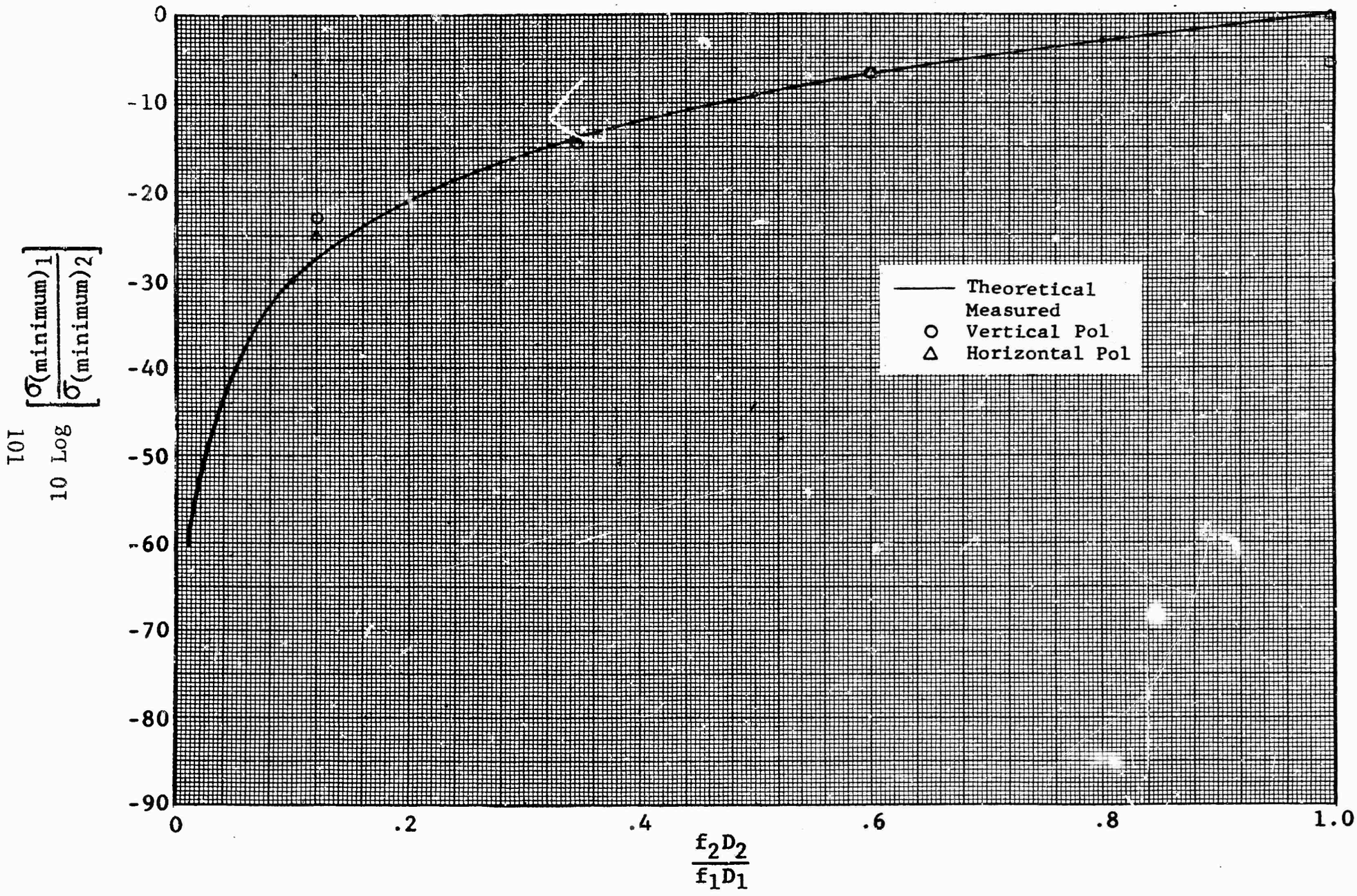

Fig. 3-17 CIRCULAR COLUMN TARGET SUPPORT MINIMUM CROSS SECTION VARIATION AS A FUNCTION OF DIAMETER AND FREQUENCY

SECTION 4

STRUCTURAL INVESTIGATION OF STYROFOAM COLUMNS

At the start of the program, an investigation of the structural limitations of Styrofoam for use as target supports was initiated. An analysis of the Styrofoam column was undertaken, supported by structural test data taken at the General Dynamics/Fort Worth Structural Test Laboratory.

The theoretical basis used in the analysis was the Euler criteria for column maximum allowable average intensity of stress. Using this criteria the ultimate average intensity of stress for three different column configurations is:

1. Column with both ends pinned, or rounded, and free to pivot

$$f = \pi^2 E\left(\frac{r}{L}\right)^2 \text{ psi} \tag{62}$$

2. Column with both ends fixed

$$f = 4\pi^2 E \left(\frac{r}{L}\right)^2 \text{ psi} \tag{63}$$

3. Column with one end fixed and one end rounded, or pinned

$$f = \frac{9}{4} \pi^2 E \left(\frac{r}{L}\right)^2 \text{ psi} \tag{64}$$

where

E = modulus of elasticity (psi)

r = least radius of gyration (inches)

L = column length (inches).

These formulas describe the conditions for long slender columns, wherein column bending and instability constitute the structural failure rather than pure compression.

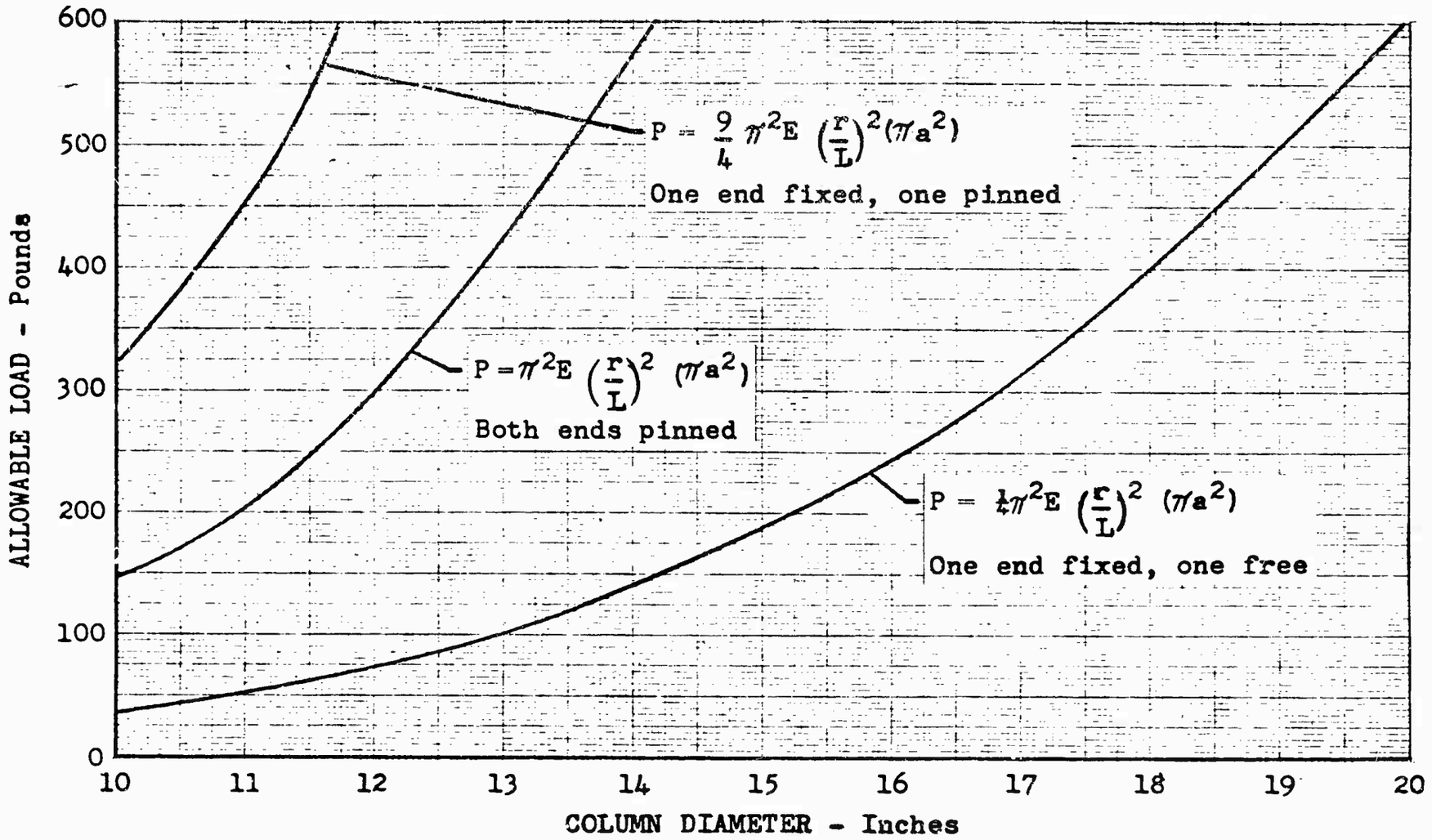

Fig. 4-1 10-FT. STYROFOAM COLUMN ALLOWABLE LOADS

For columns of low $\frac{L}{r}$ (thick columns) the Euler equation is no longer the governing factor in determining ultimate load. It is necessary to approximate the complex transition from the Euler criterion to pure compressive failure. A straight line approximation has been chosen for simplicity and is represented by the equation

$$f_c = 10 \left[1 - \left(\frac{L}{54r} \right) \right] . \qquad (66)$$

The two equations are plotted in Figure 4-2 for values of L/r from 0 to 48. The Euler curve and the straight line intersect tangentially at L/r = 36, approximately. For values of L/r below 36, the straight line formula is used. Above L/r = 36, the Euler formula is applied.

Tests have been performed on four Styrofoam specimens by the General Dynamics/Fort Worth Structural Test Section to determine the characteristics of the material under axial compression. A description of the specimens is presented in Figure 4-3. The test data are shown in Table 4-1. It will be noted that these points lie well above the maximum allowable stress plotted for their respective $\frac{L}{r}$; consequently, the curves are shown to be conservative.

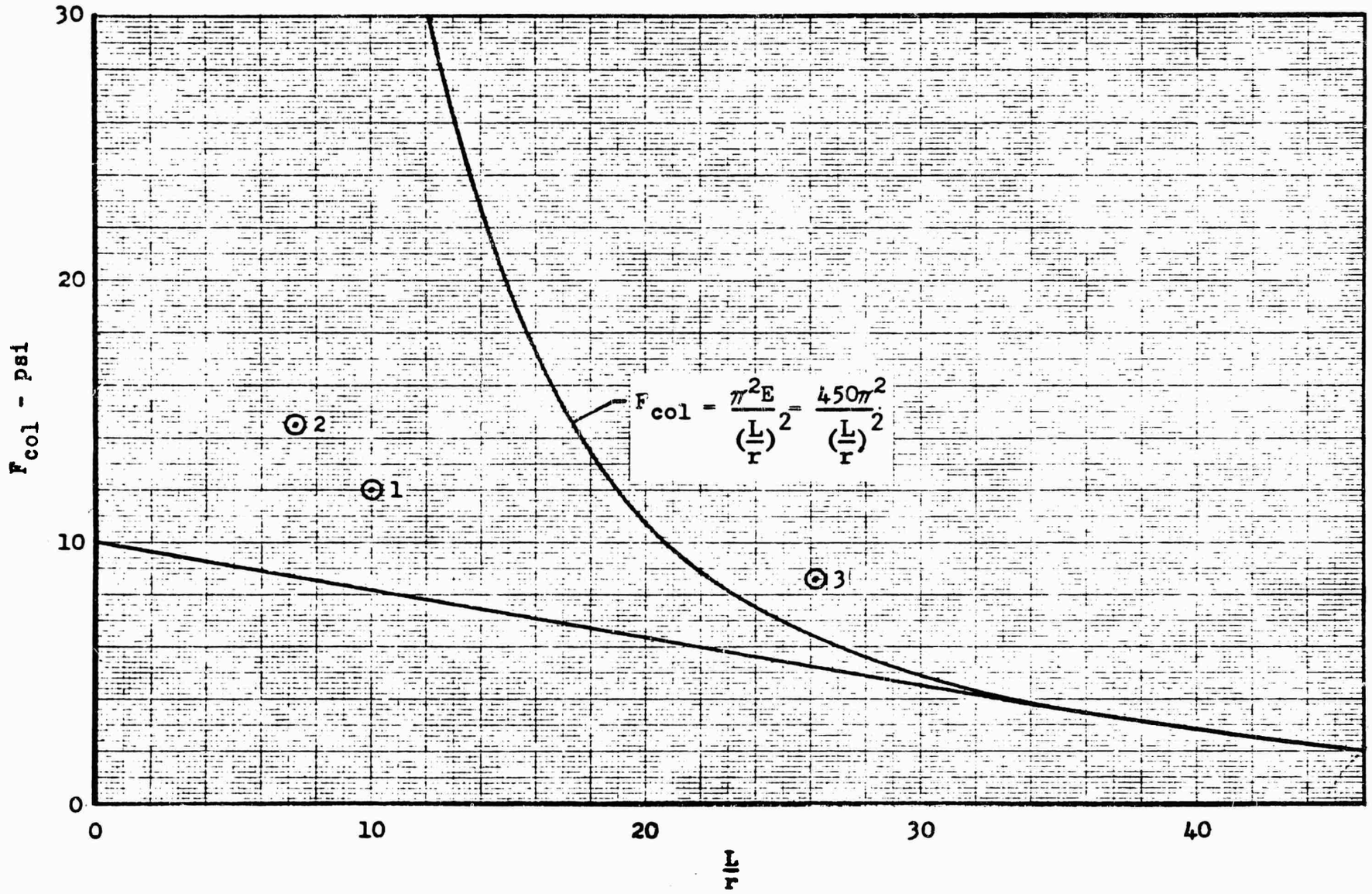

Fig. 4-2 COLUMN ALLOWABLE LOAD CURVES FOR STYROFOAM

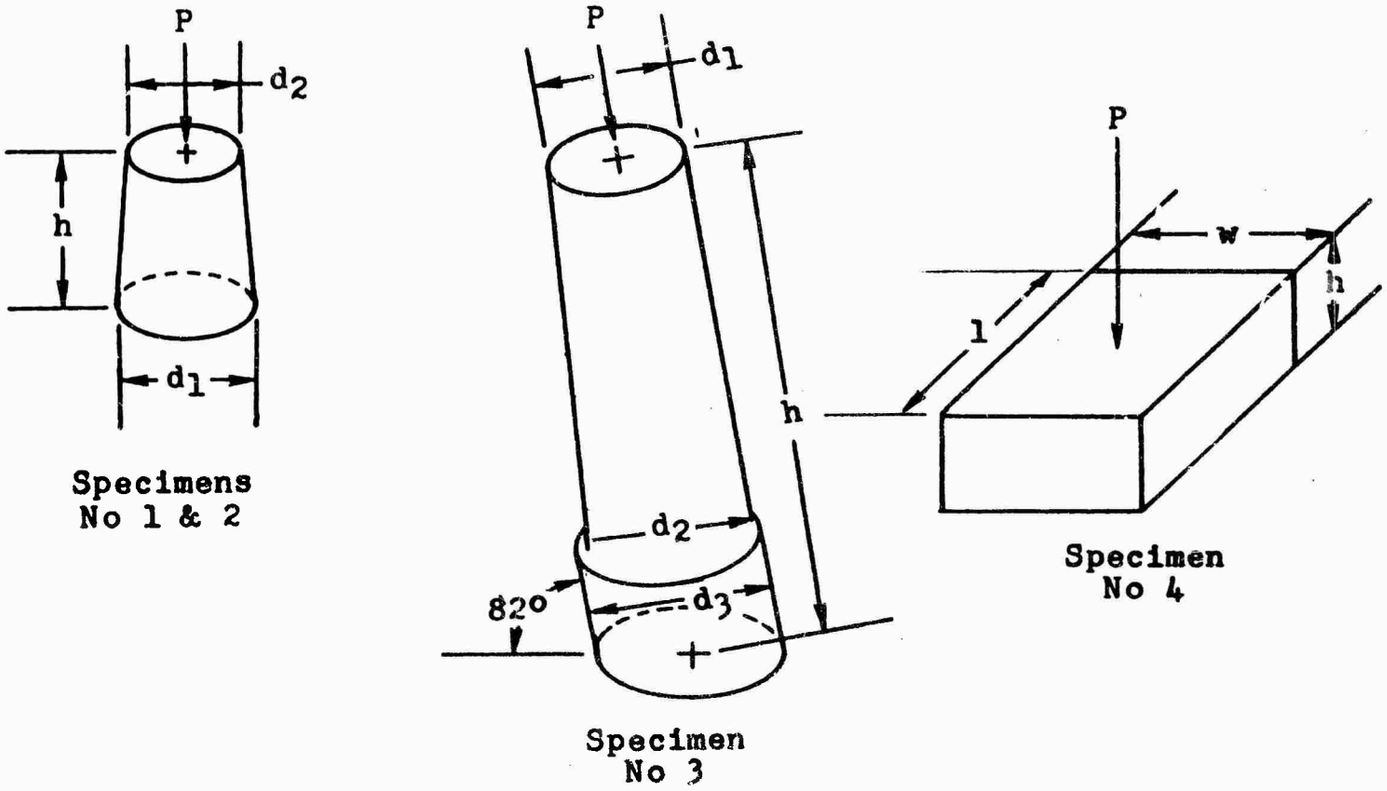

Fig. 4-3 DESCRIPTION OF STYROFOAM TEST SPECIMENS

Table 4-1 STYROFOAM STRUCTURAL TEST RESULTS

SPECIMEN NO.	DIMENSIONS(in) d_1	d_2	h	VOL (ft^3)	DENSITY ($\#/ft^3$)	MAX LOAD (lbs)	MAX STRESS (psi)	d_3 (in)
1	17.87	16.66	43.0	5.80	1.68	2780	11.9	
2	19.44	18.10	33.97	5.43	1.62	4000	14.5	
3	15.00	16.75	103.5		1.58	1700	8.64	19.62

SPECIMEN NO.	DIMENSIONS(in) h	w	l	VOL (ft^3)	DENSITY ($\#/ft^3$)	MAX LOAD (lbs)	MAX STRESS (psi)
4	5.06	10.72	12.19	.382	1.94	5700	43.6

SECTION 5

STYROFOAM BONDING INVESTIGATION

It was anticipated, early in the program, that target supports and/or saddles might be required in configurations that could not be fabricated in one piece from a standard Styrofoam rough billet. These would have to be fabricated by bonding two or more pieces of Styrofoam together. There were already many bonding materials and techniques available to produce bonds of sufficient strength for this purpose. However, all of them had one failing for this application in that they all produced heavy solid surfaces at the bonded interfaces that produce high radar backscatter. It was, therefore, decided to attempt to develop a new bonding technique that would produce bonds of sufficient strength, without the penalty of high radar cross section.

The basic approach that was adopted was to try to find a relatively slow acting solvent that would soften a Styrofoam surface upon application, without collapsing the cell structure. Two such "softened" surfaces could then be joined together to form a bond. A list of solvents that dissolve polystyrene is presented in Table 5-1. These solvents are listed in order of boiling point temperatures.

After a certain amount of experimentation, one solvent was selected as being most suitable. This solvent was Xylene, a commercial solvent of the class known as xylols. The specific compound is 1,2-dimethylbenzene. Using suitable techniques for applying the solvent, bonds have been obtained that have good mechanical strength and that appear to have fairly normal cell structure at the bond. Two bonding processes have been developed which have thus far proven to give uniform and repeatable results, even when large surfaces are being bonded together. The basic difference between the two procedures is in the techniques for applying the solvent to the surfaces. Two basic problems encountered while evolving the procedures were; (1) applying the solvent to the surface evenly and in the correct amount and (2) providing for evaporation of the solvent after the surfaces have been mated.

The first technique utilizes a single layer (sheet thickness) of clean cheesecloth saturated with Xylene. The cheese cloth is allowed to become nearly dry, and is then placed on the surface to be bonded. Very little experience is required to

Table 5-1 SOLVENT CEMENTS FOR POLYSTYRENE[+]

Solvent	Boiling Point (°C)	Tensile Strength of Joint (psi)
Fast drying		
methylene chloride	39.8	1800
carbon tetrachloride	76.5	1350
ethyl acetate	76.7	1500
benzol	80.1	———
methyl ethyl ketone	79.6	1600
ethylene dichloride	83.5	1800
trichloroethylene	87.1	1800
Medium drying		
toluol	110.6	1700
perchlorethylene	121.2	1700
ethyl benzene	136.2	1650
xylols	138.4 - 144.4	
p-diethyl benzol	183.7	1400
Slow drying		
amylbenzol	202.1	1300
2-ethylnaphthalene	251	1300

[+]From Plastic Engineering Handbook (1960) Randolf, A. F. (ed) Reinhold Publishing Corp., New York.

judge the necessary evaporation. The corresponding surface of the second piece to be bonded is then mated, and pressure of 0.1 to 0.25 pounds per square inch is applied and maintained. Several inches of cheesecloth material must be exposed on all sides of the bonded area to allow the solvent to evaporate completely. The cheese cloth, of course, remains embedded in the Styrofoam. One hour of setting time is sufficient to insure a good bond; after which time, the excess cheese cloth is trimmed away.

The second technique consists of using a saturated pad to wipe the Xylene lightly onto the surfaces to be bonded. Again, little experience is needed to judge how "lightly" the solvent must be wiped onto the surfaces. Where large surfaces are to be bonded together, special provision must be made to allow the solvent to evaporate from the bonded joint. This is done by lightly scoring the surfaces with parallel lines spaced at 1/2- to 3/4-inch intervals prior to application of the solvent. When this technique is used, a setting time of approximately three hours is required.

Of the two techniques, the one which leaves the cheese cloth embedded in the Styrofoam has produced the stronger and more uniformly repeatable bonded joints.

Tests were conducted in the General Dynamics/Fort Worth anechoic chamber to deterimne the effect of such bonded joints on the radar cross section of Styrofoam. Five samples were used, each in the form of a right circular cylinder, approximately ten inches in diameter and twenty-one inches long. Each cylinder was mounted as shown in Figure 5-1 and rotated through 360 degrees azimuth as its cross section was recorded at 8.0 gigacycles. Four of the samples were then cut in the middle, parallel to the ends, and bonded back together. Samples 4 and 5 were bonded by using the embedded cheesecloth process. Samples 2 and 3 were bonded by use of the other technique. Sample No. 1 was not cut and bonded after the initial measurement.

One measurement was then made of each sample at each of four frequencies: 8.0, 5.0, 3.03 and 1.5 gigacycles. Vertical polarization was used. A typical plot of radar cross section is shown in Figure 5-2. The scale range for the figure is 50 db. Although the amount of data taken was limited by economic considerations, it appears that some useful conclusions can be drawn from a comparison of the "end-on" cross section and the width of the pattern lobes of the "end-on" return. These data are presented in Tables 5-2 and 5-3, respectively.

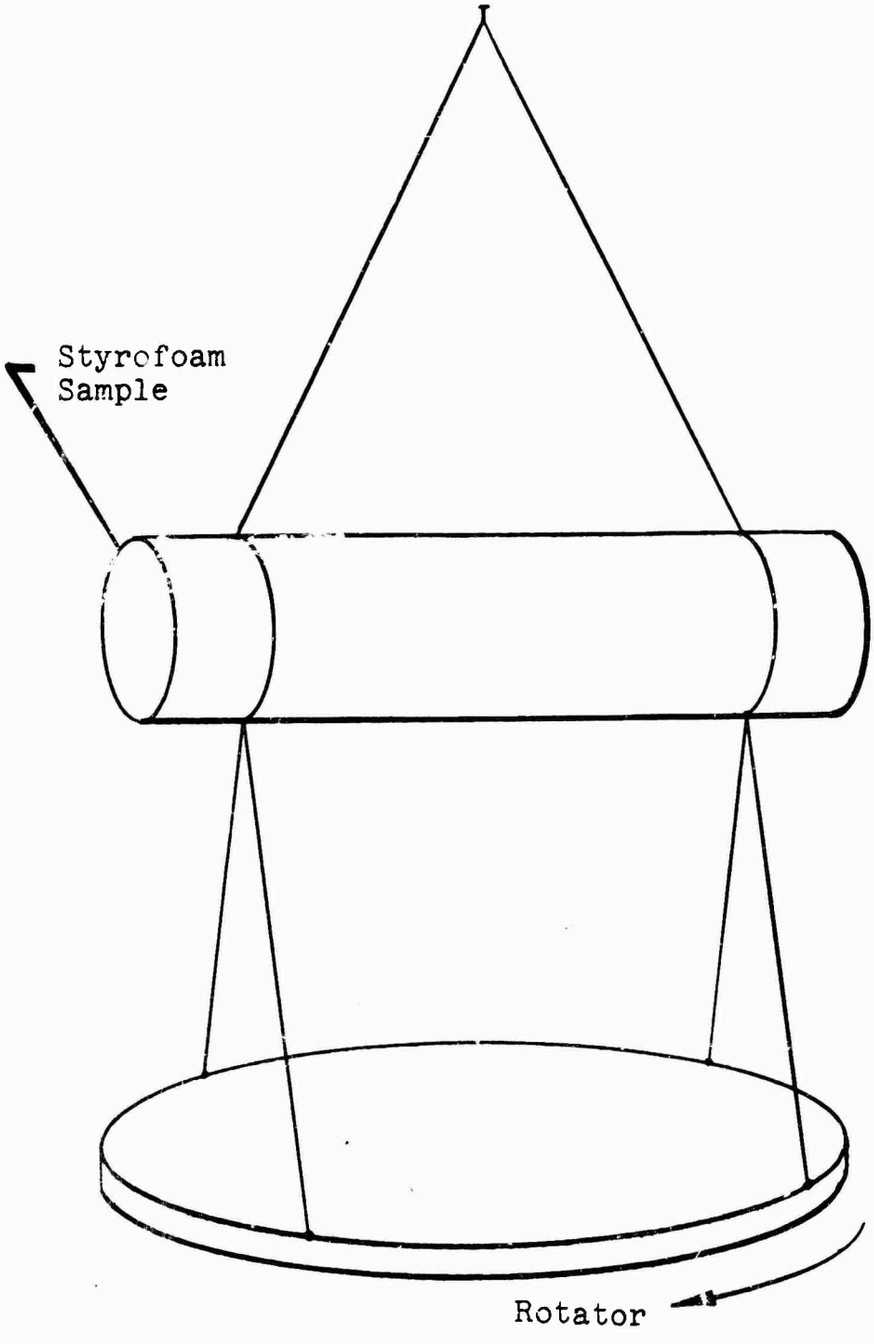

Fig. 5-1 MOUNTING TECHNIQUE FOR BONDED STYROFOAM SAMPLES

Table 5-2 BONDED STYROFOAM CYLINDER CROSS SECTION

Sample	Frequency Gc	End-on Radar Cross Section (dbsm) 1.5	3.03	5.0	8.0	8.0 (unbonded)
1		-46.5	-33.5	-34.5	-25	-25.5
		-46.5	-33	-34	-25	-25.5
2		-47	-30	-30	-22.5	-25.5
		-48.7	-33	-30	-20.5	-30.5
3		-46.5	-32	-28	-23	-25.5
		-48.5	-31	-28	-23.5	-23
4		-45.5	-31.5	-33	-29.5	-26
		-46.5	-32	-31.5	-24	-26
5		-45.5	-33.5	-35	-27	-27
		-46.5	-34.5	-37	-25	-27

Table 5-3 BONDED STYROFOAM CYLINDER LOBE WIDTH

Lobe Width (Θ) @ - 20 db pk (degrees)

Sample \ Frequency Gc	1.5	3.03	5.0	8.0	8.0 (unbonded)
1	50	60 (30)	Not	20	20
	50	42 (25)	Readable	20	20
2	40	40	30	20	25
	30	30	35	20	30
3	40	30	20	20	30
	30	30	30	20	20
4	45	30	35	25	25
	40	30	35	20	25
5	45	30	25	20	25
	35	45	30	20	20

SECTION 6

AIR INFLATED TARGET SUPPORT INVESTIGATION

A part of the work statement for Contract AF30(602)-2831 was the study of air inflated target supports for possible use at the RAT SCAT Site. This study was initiated at General Dynamics/Fort Worth and progressed through a preliminary structural analysis of this type of target support and an estimate of its potential utility before it was cancelled by AF directive. A parallel and independent effort by General Dynamics/Fort Worth personnel at the RAT SCAT Site included the specification and purchase of a trial air bag target support. The results of both efforts are included herein.

The structural analysis of the air inflated target support is based on that of the pressurized thin-walled cylinder. The primary structural load on a pressurized thin-walled cylinder is the tangential of "hoop" stress, S_t, illustrated in Figure 6-1.

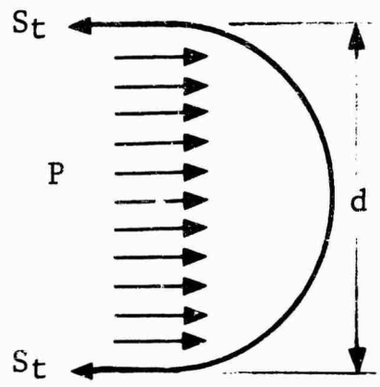

Fig. 6-1 TANGENTIAL STRESS DIAGRAM

The magnitude of this stress is given by

$$S_t = \frac{Pd}{2t} \quad , \text{ lbs/in}^2 \, , \tag{67}$$

where

P = inflation pressure, lbs/in^2

d = diameter, inches

t = wall thickness, inches.

In the case of the air-inflated target support, this stress must be related to fabric strength, usually specified in lbs/in. This can be interpreted as the amount of tension a one inch wide strip of material can withstand. This eliminates the "thickness" term in equation 67, which then reduces to

$$S_t = \frac{Pd}{2} \quad , \text{ lbs/in.} \tag{68}$$

A seventeen foot (204 inches) diameter cylinder, inflated to three psi would have to withstand a tangential stress of 306 lbs per inch. There are many fabrics commercially available that are capable of withstanding this stress.

Another structural consideration is that of the lifting force on the target support. Under pressure, the bottom of the target support tends to balloon out and approach an hemispherical shape. This will exert an upward force on the target support that is equal to the inflation pressure multiplied by the area on contact with the rotator table. This area may approach 30,000 square inches and will impose severe stresses on the tie-down points on the target support and on the rotator.

The most attractive shape for an air-inflated target support from the standpoint of structural stability, is the truncated cone, or some variation thereof. The shapes deemed most worth of consideration are shown in Figure 6-2.

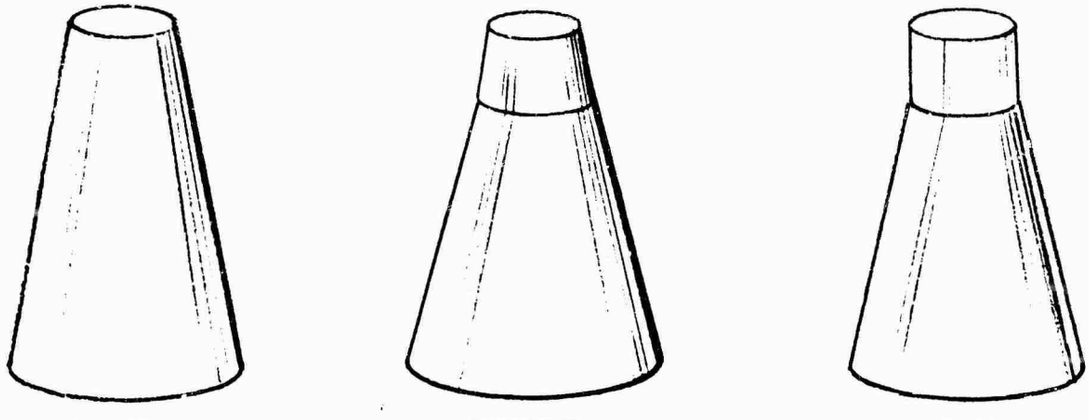

SIMPLE TRUNCATED CONE | DOUBLE TRUNCATED CONE | CONE CYLINDER COMBINATION

Fig. 6-2 PROJECTED SHAPES FOR AIR BAG TARGET SUPPORTS

The more complex shapes may offer slightly reduced cross section due to the reduction in material near the center of

the beam. However, it is expected that the simple conical shape will be most practical in the overall consideration of cost, load bearing capacity and cross section. It should be noted that the axial symmetry of all three shapes is amenable to the use of cancellation techniques for the reduction of background.

This type of support offers two operational advantages that are readily apparent. One is that it can be fabricated in a wide range of heights permitting target elevations as high as thirty feet. This would be very useful for low frequencies, where the nearest pit must be used and it is desired to keep the antenna as low as possible to reduce reflection from the pit. Another advantage is the ease of raising and lowering the target by inflating and deflating the airbag.

It is recognized that the top of this support will tend to balloon out into a hemispherical shape, which may pose mounting problems for certain types of targets. This can be overcome by properly designed Styrofoam saddles, which will provide the necessary stability and attitude control.

It is anticipated that this type of target support will offer lowest cross section at the lower frequencies, that is, 1000 mc and below.

The air inflated target support contracted for by General Dynamics/Fort Worth personnel at the RAT SCAT Site was designed and built by Commercial Sales Corp. of El Paso, Texas, at a cost of approximately $1200. It is in the shape of a truncated cone, 16 feet in diameter at the bottom, 30 feet high, and 3 feet in diameter at the top. It is fabricated from neoprene coated nylon, and the seams are sewn, rather than bonded.

This target support has been inflated to a pressure of 0.25 psi at RAT SCAT, which it withstood very well. It proved to be very stable, moving less than six inches in a forty knot wind. The support has been used to elevate a 150 lb. target and has a theoretical capacity at that inflation pressure of 250 lbs.

The system was calibrated at 425 mc with a 24-inch sphere atop the target support. The 500 ft range was used. After calibration, the sphere was removed, and background measured with the target support in place. Background was below -22 dbsm through 360 degrees rotation at horizontal polarization, and below -31 dbsm at vertical polarization. The widest variation in background was approximately 5 db at vertical polarization.

It is believed that this variation would be reduced if the wind were calm. The variation at horizontal polarization was less than 2 db. This degree of stability indicates that this type of support is compatible with background cancellation techniques.

DOCUMENT CONTROL DATA - R&D

(Security classification of title, body of abstract and indexing annotation must be entered when the overall report is classified)

1. ORIGINATING ACTIVITY (Corporate author)
GENERAL DYNAMICS/FORT WORTH
P. O. Box 748
Fort Worth, Texas 76101

2a. REPORT SECURITY CLASSIFICATION
UNCLASSIFIED

2b. GROUP
NA

3. REPORT TITLE
Radar Cross Section Target Supports - Plastic Materials

4. DESCRIPTIVE NOTES (Type of report and inclusive dates)
Final

5. AUTHOR(S) (Last name, first name, initial)
C. H. Smith
C. C. Freeny
E. F. Knott } Section 2 (The University of Michigan)
T. B. A. Senior)

6. REPORT DATE	7a. TOTAL NO. OF PAGES	7b. NO. OF REFS
June 1964	128	17

9a. CONTRACT OR GRANT NO.	9e. ORIGINATOR'S REPORT NUMBER(S)
AF30(602)-2831	RADC-TDR-64-381
b. PROJECT NO. 6503	9b. OTHER REPORT NO(S) (Any other numbers that may be assigned this report)
c.	GD/FW Report No. FZE-222-6
d.	

10. AVAILABILITY/LIMITATION NOTICES
Qualified requesters may obtain copies of this report from DDC.

11. SUPPLEMENTARY NOTES	12. SPONSORING MILITARY ACTIVITY
None	RADC (EMASP) Griffiss AFB NY 13442

13. ABSTRACT The results of studies by The University of Michigan Radiation Laboratory and General Dynamics/Fort Worth into the scattering properties of cellular plastic materials are presented. A mathematical model for scattering from cellular plastics, developed by The University of Michigan and extended by General Dynamics/Fort Worth, to provide a method of determining the optimum low cross section target support for a given application is also presented. The results of investigations of field perturbations near a Styrofoam surface are described along with cross section measurements made at the RAT SCAT Site using theoretical minimum cross section formula for circular target supports. Structural considerations in the use of Styrofoam as target support material are discussed. Methods for achieving low cross section bonds between pieces of Styrofoam are also discussed.

The results of a limited study of the feasibility of air inflated structures as target supports at the RAT SCAT Site are also presented.

This is Report No. 6 of a series of eight RAT SCAT Research and Development reports.

DD FORM 1 JAN 64 1473

KEY WORDS	LINK A		LINK B		LINK C	
	ROLE	WT	ROLE	WT	ROLE	WT
Scattering Properties of Cellular Plastic Materials						
Radar Cross Section Measurements With Styrofoam Supports						

INSTRUCTIONS

1. ORIGINATING ACTIVITY: Enter the name and address of the contractor, subcontractor, grantee, Department of Defense activity or other organization *(corporate author)* issuing the report.

2*a*. REPORT SECURITY CLASSIFICATION: Enter the overall security classification of the report. Indicate whether "Restricted Data" is included. Marking is to be in accordance with appropriate security regulations.

2*b*. GROUP: Automatic downgrading is specified in DoD Directive 5200.10 and Armed Forces Industrial Manual. Enter the group number. Also, when applicable, show that optional markings have been used for Group 3 and Group 4 as authorized.

3. REPORT TITLE: Enter the complete report title in all capital letters. Titles in all cases should be unclassified. If a meaningful title cannot be selected without classification, show title classification in all capitals in parenthesis immediately following the title.

4. DESCRIPTIVE NOTES: If appropriate, enter the type of report, e.g., interim, progress, summary, annual, or final. Give the inclusive dates when a specific reporting period is covered.

5. AUTHOR(S): Enter the name(s) of author(s) as shown on or in the report. Enter last name, first name, middle initial. If military, show rank and branch of service. The name of the principal author is an absolute minimum requirement.

6. REPORT DATE: Enter the date of the report as day, month, year, or month, year. If more than one date appears on the report, use date of publication.

7*a*. TOTAL NUMBER OF PAGES: The total page count should follow normal pagination procedures, i.e., enter the number of pages containing information.

7*b*. NUMBER OF REFERENCES: Enter the total number of references cited in the report.

8*a*. CONTRACT OR GRANT NUMBER: If appropriate, enter the applicable number of the contract or grant under which the report was written.

8*b*, 8*c*, & 8*d*. PROJECT NUMBER: Enter the appropriate military department identification, such as project number, subproject number, system numbers, task number, etc.

9*a*. ORIGINATOR'S REPORT NUMBER(S): Enter the official report number by which the document will be identified and controlled by the originating activity. This number must be unique to this report.

9*b*. OTHER REPORT NUMBER(S): If the report has been assigned any other report numbers *(either by the originator or by the sponsor)*, also enter this number(s).

10. AVAILABILITY/LIMITATION NOTICES: Enter any limitations on further dissemination of the report, other than those imposed by security classification, using standard statements such as:

(1) "Qualified requesters may obtain copies of this report from DDC."

(2) "Foreign announcement and dissemination of this report by DDC is not authorized."

(3) "U. S. Government agencies may obtain copies of this report directly from DDC. Other qualified DDC users shall request through _____."

(4) "U. S. military agencies may obtain copies of this report directly from DDC. Other qualified users shall request through _____."

(5) "All distribution of this report is controlled. Qualified DDC users shall request through _____."

If the report has been furnished to the Office of Technical Services, Department of Commerce, for sale to the public, indicate this fact and enter the price, if known.

11. SUPPLEMENTARY NOTES: Use for additional explanatory notes.

12. SPONSORING MILITARY ACTIVITY: Enter the name of the departmental project office or laboratory sponsoring *(paying for)* the research and development. Include address.

13. ABSTRACT: Enter an abstract giving a brief and factual summary of the document indicative of the report, even though it may also appear elsewhere in the body of the technical report. If additional space is required, a continuation sheet shall be attached.

It is highly desirable that the abstract of classified reports be unclassified. Each paragraph of the abstract shall end with an indication of the military security classification of the information in the paragraph, represented as *(TS)*, *(S)*, *(C)*, or *(U)*

There is no limitation on the length of the abstract. However, the suggested length is from 150 to 225 words.

14. KEY WORDS: Key words are technically meaningful terms or short phrases that characterize a report and may be used as index entries for cataloging the report. Key words must be selected so that no security classification is required. Identifiers, such as equipment model designation, trade name, military project code name, geographic location, may be used as key words but will be followed by an indication of technical context. The assignment of links, rules, and weights is optional.